

# Slow Drive of Many-Body Localized Systems

Thesis by  
Evgeny Mozgunov

In Partial Fulfillment of the Requirements  
for the Degree of  
Doctor of Philosophy

The logo for the California Institute of Technology (Caltech), featuring the word "Caltech" in a bold, orange, sans-serif font.

CALIFORNIA INSTITUTE OF TECHNOLOGY  
Pasadena, California

2017  
Defended May 26th, 2017

© 2017

Evgeny Mozgunov

Some rights reserved. This thesis is distributed under a Creative Commons  
Attribution-NonCommercial-ShareAlike License

## ABSTRACT

We investigate a many-body localized 1d spin chain with a Hamiltonian consisting of classical disordered Ising and a small transversal field. An existing perturbative diagonalization by Imbrie is simplified and reinterpreted in order to prove the anticipated form of the Lieb-Robinson bound and the area law in an eigenstate. We also show how to approximately reduce Imbrie's unitary to a finite depth circuit. The concept of resonances in Imbrie's work can be given a physical meaning as an avoided crossing of levels as functions of a magnetic field. For a slow drive of this field, we discuss the proofs of validity for an efficient classical simulation of such disordered systems, both isolated and in contact with the environment. Our results are applicable to Floquet systems and describe an unexpected mechanism of heating up over long times. We also revisit noisy quantum adiabatic annealers like the D-wave machine and find a nontrivial physics that can possibly be observed in them.

<p style="text-align: center;"><b>Executive summary:</b></p> <p style="text-align: center;">A simplified description of the circuit constructed by Imbrie for a many-body localized 1d system.</p> <p style="text-align: center;">Similarities of Imbrie circuit and Quasi-Adiabatic evolution, but unlikely that Imbrie circuit can replace it for <math>&gt;1d</math>.</p> <p style="text-align: center;">Lieb-Robinson bound and a bound on entanglement entropy for Imbrie circuit.</p> <p style="text-align: center;">A new level statistics tool that can be used to identify MBL: level slopes.</p>	<p style="text-align: center;">(pedagogical)</p> <p style="text-align: center;">(new, negative)</p> <p style="text-align: center;">(known)</p> <p style="text-align: center;">(new)</p> <p style="text-align: center;">(new, useful)</p>
<p style="text-align: center;">Correspondence between resonances in Imbrie circuit and avoided crossings of levels w.r.t. a parameter.</p> <p style="text-align: center;">Poly-time simulation of a closed system drive.</p> <p style="text-align: center;">Poly-time estimate of deviations from a Gibbs state of a driven open system.</p>	<p style="text-align: center;">(new)</p> <p style="text-align: center;">(new)</p> <p style="text-align: center;">(new, testable)</p>
<p style="text-align: center;">Testable predictions about runs of a D-wave machine.</p> <p style="text-align: center;">D-wave does not provide an advantage for the study of MBL.</p> <p style="text-align: center;">However that inspires data analysis techniques for D-wave, proposals for an adjustment of the protocol to suit our goal, and a new tool for approximate simulation of quantum dynamics.</p>	<p style="text-align: center;">(new, testable)</p> <p style="text-align: center;">(new, negative)</p> <p style="text-align: center;">(new)</p> <p style="text-align: center;">(new)</p> <p style="text-align: center;">(new, useful)</p>

## PUBLISHED CONTENT AND CONTRIBUTIONS

David Gosset, Evgeny Mozgunov (2016). “Local gap threshold for frustration-free spin systems”. In: *Journal of Mathematical Physics* 57.9. URL: <http://aip.scitation.org/doi/abs/10.1063/1.4962337>.

E.M. participated in the conception of the project, solved and analyzed the 2d case, and participated in the writing of the manuscript.

Mozgunov, Evgeny (2016). “Local Master Equation for Small Temperatures”. In: *arXiv:1611.04188*. URL: <https://arxiv.org/abs/1611.04188>.

E.M. started the project independently, as it was a necessary tool for the work presented here.

# TABLE OF CONTENTS

Abstract . . . . .	iii
Executive summary . . . . .	iv
Published Content and Contributions . . . . .	v
Table of Contents . . . . .	vi
List of Illustrations . . . . .	vii
Nomenclature . . . . .	x
Chapter I: Introduction . . . . .	1
Chapter II: Imbrie's construction . . . . .	6
Chapter III: Properties of Imbrie circuit . . . . .	13
Chapter IV: Along the adiabatic path . . . . .	18
Chapter V: Slopes . . . . .	21
5.1 Time-averaging of Hamiltonian terms . . . . .	29
Chapter VI: Crossings . . . . .	33
6.1 Identification of crossings . . . . .	39
6.2 Resonance densities . . . . .	41
Chapter VII: Slow drive . . . . .	45
7.1 Finite velocity perturbation theory . . . . .	49
7.2 Floquet . . . . .	55
Chapter VIII: D-wave . . . . .	61
8.1 Failure of the collection of $(\delta E, n_r)$ data . . . . .	63
8.2 Prediction about distribution deviating from Gibbs . . . . .	69
8.3 Distributions as slopes, small systems . . . . .	73
8.4 Distributions too thin to sample . . . . .	78
Chapter IX: Generalization to other systems . . . . .	80
9.1 Efficient simulation of big systems via master equation . . . . .	80
Bibliography . . . . .	82
Appendix A: Transfer matrices . . . . .	86
Appendix B: Proofs of properties of Imbrie Circuit . . . . .	90
B.1 Telescopic sum for Imbrie circuit . . . . .	90
B.2 Circuit approximation . . . . .	97
B.3 Area law . . . . .	99
B.4 LRB . . . . .	101
Appendix C: Interpretation of Imbrie's proof . . . . .	104
C.1 Bound on generators . . . . .	104
C.2 Effective Hamiltonian of an avoided crossing . . . . .	108
C.3 Level repulsion is generic . . . . .	113

## LIST OF ILLUSTRATIONS

<i>Number</i>	<i>Page</i>
2.1 The circuit diagonalizing the system. . . . .	7
2.2 Circuit diagonalizing the system with no resonances; the terms of the generators are shown as blue dots . . . . .	9
3.1 First way to conjugate a local operator. . . . .	14
3.2 Second way to conjugate a local operator. . . . .	14
3.3 Entropy across the cut in the system with no resonances . . . . .	15
3.4 Entropy across the cut, generic. . . . .	15
3.5 Dynamics as in LRB. . . . .	17
4.1 Levels along the protocol . . . . .	18
4.2 For system sizes $n = 7$ to 20 ensemble-averaged gap approaches $1/n$ scaling. One can extend the data to bigger system sizes in poly-time, as outlined in appendix A. . . . .	19
4.3 For system sizes $n = 1$ to 9 the smallest gap of avoided crossing that ground state encounters is expected to be $e^{-n}$ — not observed for small systems. (B. Altshuler, Krovi, and Roland, 2010) presents a poly-time procedure for collection of this data for big systems sizes, assuming MBL. . . . .	20
5.1 Level repulsion parameter $r$ along the protocol, averaged over disorder. We see that it detects the extended phase, but does not distinguish between the systems close to disordered $H_z$ and non-disordered $H_x$ . . . . .	22
5.2 An illustration of smart level labels used to determine slopes at big $ds$ . . . . .	23
5.3 The quantities $R(s, ds)$ , $R(s, ds)/S(s, ds)$ , $S(s, ds)$ are plotted along the protocol. Step $ds_1$ is in blue, step $ds_2$ with smart overlap labels is in gold . . . . .	24
5.4 The quantity $D(s)$ is in blue, $S(s)$ in gold . . . . .	25
5.5 The quantity $D(s)$ for different realizations of disorder . . . . .	26
5.6 The quantity $D(s)$ for different system sizes . . . . .	26
5.7 The quantity $D(s, ds_2)/80ds_2$ for different step sizes: $1/w = 1/80ds_2 = 4, 1, 0.5, 0.5$ for blue, red and two yellow lines correspondingly. Here $L = 6$ . . . . .	28

5.8	The level repulsion parameter $r$ for the full Hamiltonian $H$ , calculated in the mid 20% of levels where the MBL breaks down the fastest. System sizes $L = 12, 10, 8, 6$ in blue, gold, green and red, respectively.	28
5.9	The level repulsion parameter $r$ for time-averaged mid-chain Hamiltonian $H'_a$ . System sizes $L = 6, 8, 10$ in blue, gold and green correspondingly.	29
6.1	One can identify resonances as places where the state is flipped to approximately orthogonal	40
6.2	In the midband large gaps are obscured by multi-crossing.	40
6.3	Resonances vs. level number	41
6.4	The histogram of frequencies $1/\Delta s_r(n_r)$ collected in the last $[7/8, 1]$ of $s$ (left) and in the middle $[4/8, 5/8]$ of $s$ . Blue line is a theoretical prediction. The system size $L = 6$ , we average over 15 disorder realizations	42
6.5	Total density of resonances plotted along the protocol	43
6.6	Median of $\delta E$ with resonance size for length- $1/8$ intervals of $s$ along the protocol, from $[4/8, 5/8]$ in blue to $[7/8, 1]$ in red. The theoretical fit (purple) with $\gamma_{eff} = 1/8$ is plotted to guide the eye	43
6.7	Resonance density with size. Extended in gold, MBL in blue. We see that large ( $\sim L$ ) resonances are always present in the extended system	44
7.1	The peaks in $X(\gamma = 0.1, r = 1, T)$	57
7.2	The peaks in $X(\gamma = 0.1, r, T = 6)$ (blue) and $X(\gamma = 0.1, r, T = 1)$ (gold)	57
7.3	Saturation of $\text{Av.}X(\gamma = 0.1, T)$ . The narrow peaks lead to a numerical noise.	58
7.4	Enhancement $\text{Av.}X(\gamma, T = 500)/\gamma$ in the limit of long times	58
7.5	The jump in $\text{Av.}X(\gamma, T)/\gamma$ for $L = 10$ system	59
7.6	The values of $\text{Av.}X(\gamma, T)/k$ before and after the jump. An integer $k$ is chosen to approximately match the small $\gamma$ slope.	60
8.1	Phase diagram (a) is expected for our spin chain. Mobility edge (b) and a fully extended phase (c) is shown for comparison.	68
8.2	The Hamiltonian rescaling procedure used to determine slopes involved in <i>frequency</i> of resonances. Steps (a) and (b) are averaging, then at step (c,d) the transformation is found and applied to original slopes	74

8.3	The data processing procedure where end populations are interpreted as points along the evolution of the level, and then they are collapsed to $s^* = 0.98$ and used to determine a first approximation to slopes. . . . .	75
9.1	Layout of pathes for a 2d system . . . . .	81
B.1	We see how the right-hand side is always bigger for $Z = 1.6$ . . . . .	94

## NOMENCLATURE

- Conductance.** A number quantifying how well the system transports one of the following conserved quantities: charge, heat, magnetization.
- Conserved quantity.** A physical observable that doesn't change with time in the system.
- Diagonalize.** An operation that reduces a general Hamiltonian operator to its diagonal form, with energies on diagonal.
- Disordered.** A model where local energies (local terms in the Hamiltonian) differ from place to place.
- Finite-depth local circuit.** A sequence of quantum operations on spins such that each operation is local, and each spin is involved in finitely many (less than depth) operations.
- Local.** A property of an observable (operator) that it is supported (can be measured) in a fixed-size neighborhood of some point. Sometimes also a sum of such operators, as in Local Hamiltonian.
- Localization.** A property that a particle remains near its starting point (as defined originally by Anderson). The term Many-body Localization (MBL) is an overarching term that includes both Anderson localization of free particles and the same phenomenon for interacting particles or spins. Zero interaction case (or z-basis Hamiltonian for spins) is considered trivial. The term MBL is used only if localization persists after turning on interactions.
- Many-body.** A term in physics that refers to either a system of many particles, or many spins sitting fixed on the lattice and interacting.
- Spins.** Quantum mechanical objects that have a discrete set of states, usually two.
- z-basis Hamiltonian for spins.** A special case of a system of spins that has a classical description: each combination of discrete states is associated with a number - energy (Hamiltonian). The states are said to be in z-basis. This is in contrast to quantum mechanical systems where energy is an operator acting on states. As an operator, z-basis Hamiltonian is a diagonal matrix, while the general Hamiltonian is not.

*Chapter 1*

## INTRODUCTION

**Literature** The central concept of this work is Many-Body Localization (MBL) - a property of quantum-mechanical many-body systems. The original work (Anderson, 1958) posed a question whether the MBL can exist and as a way to solve it studied the localization of a single particle. The distinction between the MBL and the Anderson localization is not strict: a state of an  $L$ -spin system can be represented by a position of a single particle in an  $L$ -dimensional hypercube (Thouless, 1977). The first MBL system with a mathematical solution converging in a realistic range of parameters (such as the interaction strength, lattice connectivity and temperature) was presented by (Basko, Aleiner, and B.L. Altshuler, 2006). The system they considered contained interacting 2d electrons in a strongly disordered material (grains of metal with a weak tunneling between them). They have proved zero conductance at finite temperature as an experimental manifestation of MBL. The idea was universal enough to be applicable to other many-body systems. The simplification to spin chains soon followed: strongly disordered spin chains have been claimed to possess MBL, which manifested in rich mathematical structure including zero conductance. The intuition for said mathematical structure was pioneered by conjectures of local conserved quantities (Oganesyan and Huse, 2007; Serbyn, Papić, and Abanin, 2013) and finite depth local circuits (Bauer and Nayak, 2013). The latter conjectured that an MBL spin chain Hamiltonian could be diagonalized by such circuit, at least approximately. It culminated in an exact construction by (Imbrie, 2016): a proof that a certain disordered spin chain can be solved exactly if we extend our notion of finite depth local circuits slightly. We will use that construction to obtain a better understanding of MBL phase.

The previous work on MBL conjectured results for:

- **Lieb-Robinson bound** (Lieb and Robinson, 1972). A dynamical property that characterizes the spread of correlations with time in a given system. Hamza, Sims, and Stolz, 2012 showed that effective speed of light (Lieb-Robinson velocity) in systems reduced to Anderson localization is zero. A proof for a certain definition of MBL can be found in (Kim, Chandran, and Abanin, 2014).

- **Entanglement.** A static property defined for a bipartition of the system that quantifies how much of the purity of each part is missing. A numerical study of entanglement in small MBL systems was performed by (Bauer and Nayak, 2013), and one of the open questions in that work is an explanation of outlier entanglement logarithmic in system size. We address it in this work.
- **Entanglement growth.** A dynamic property that describes how fast the entanglement grows after a quench (instantaneous change in the Hamiltonian). Bardarson, Pollmann, and Moore, 2012 found logarithmic growth with time numerically, while Kim, Chandran, and Abanin, 2014 presented a mathematical proof.
- **Closed system.** A system isolated from an environment.
- **Floquet.** A closed system with a Hamiltonian that is not constant, but depends on time periodically. Ponte et al., 2015 and Abanin, Roeck, and Huvneers, 2016 investigated such an evolution of the MBL system numerically and concluded that the system remains localized and cold (retains some memory of the initial condition) up to infinite times.
- **Open system.** A part of a bigger closed system, where the rest is considered to be the environment. A study of how the MBL is destroyed in the presence of the environment can be found in (Medvedyeva, Prosen, and Žnidarič, 2016). The model studied here is very similar, but the presence of MBL shows up in the nonequilibrium effects.
- **Adiabatic protocol** A process in a closed system where the Hamiltonian is varied slowly. B. Altshuler, Krovi, and Roland, 2010 showed that MBL is a major obstacle for useful computational applications of such a protocol. (Khemani and S. L. Sondhi, 2015) studied nonlocal rearrangements in the slow drive of Anderson localization, a work which we generalize here to the MBL systems.

**Our contribution** All of these results we revisit and build upon here. The motivation for these developments can be explained as follows: MBL is a special property that greatly simplifies the underlying physics. Therefore some generally intractable dynamical problems become accessible. For instance, we provide an insight into mathematical conditions that are required for Floquet MBL to have local memory of the initial state up to infinite times (Ponte et al., 2015; Rehn et al., 2016; Abanin,

Roeck, and Huveneers, 2016), and describe the short time (first few periods of the drive) with more detail than is usually found in literature. These results are presented in Chapter VII. For LRB and entanglement, see Chapter III and Appendices. We also provide a new (to the best of our knowledge) indicator of an MBL phase in Chapter V.

As another example, consider a D-wave machine (Dickson et al., 2013), which takes a spin system  $z$ -Hamiltonian as an input, runs an adiabatic protocol (from a uniform field along  $x$  to our input Hamiltonian) and returns a state measured in  $z$ -basis as an output. It is believed to be described by open system dynamics. Big system sizes with disorder on a D-wave machine are expected to be hard to simulate classically. Some insights into closed system adiabatic protocol were given in (B. Altshuler, Krovi, and Roland, 2010). In particular, they established the expected scaling of the minimal gap (the difference of energies between the two lowest energy states) encountered in the protocol, and presented perturbative tools that allow such estimates for big system sizes of generic MBL systems. We investigate similar questions in Chapters IV and VI. For an open system (which is the case in D-wave), the environment makes this approach irrelevant. We show that in the specific case of 1d chains (as well as other rapidly mixing systems, those that reach thermal equilibrium quickly when in contact with the environment) some features of the output can be predicted up to big system sizes. These predictions may shed some light on potential new applications of the D-wave machine for detection and characterization of MBL phases. In particular, we propose a set of data analysis tools that has never been applied to D-wave data before. One can think of it as a simulate-and-compare tool. So far no direct simulations for big system sizes have been carried out. We propose a way to do it in Chapter VIII.

**Topological motivation** As an aside, we comment on another reason to study MBL systems. In (Bauer and Nayak, 2013), there was a proposal of a disordered Toric code. (Bravyi and Koenig, 2012) considered a disordered Majorana chain. Both are quantum memories based on the theory of topological phases. But the classification of those phases was developed without consideration for disorder, with an exception of the periodic table (Kitaev, 2009). We will give a short and very partial account of the state of affairs in the theory of topological phases, and how disorder can come in.

Let us start with a concept of quasi-adiabatic continuation (QAC, Matthew B.

Hastings and Michalakis, 2015) that gives one a unitary to build a ground state of a gapped (with the gap of order 1) perturbed system from the unperturbed one. The benefit w.r.t. using the adiabatic protocol is that an error remains exactly zero without taking the protocol time  $T \rightarrow \infty$  limit. The generator of the evolution has exponential (suppressed faster than any power of interaction range, to be precise) tails — that is, it's approximately local. Cutting off those tails and making a Trotter approximation would lead to an error similar to the one of adiabatic protocol (error is linear in the number of qubits). However it boasts an extra exponential suppression in terms of the gap and the QAC parameter  $\alpha$  that allows one to optimize for a much better performance.

Will the QAC work for the MBL system? No, because it doesn't handle levels closer than the gap correctly. Imbrie's construction can be thought of as a working alternative, as it also takes eigenstates of the unperturbed (z-basis) Hamiltonian and prepares the true eigenstates with zero error.

Let's consider the following problem (motivation will come later). Start with a Hamiltonian  $H = \sum_i Z_i$  — a trivial gapped Hamiltonian (here  $Z_i$  is a Pauli-z matrix  $\text{diag}(1, -1)$  on spin  $i$ ). Without symmetry restrictions, it is connected to any bosonic symmetry-protected topological phase, which is just a set of spin Hamiltonians with a representative given in (Chen et al., 2012) and the accompanying work. Connection is defined as a path  $H(s)$  that's gapped in the bulk. General gapped Hamiltonians are believed to be well represented by this theory, however nobody has rigorously explored how connected they are. It is hard to make the phrase "gapped in the bulk" in the definition rigorous. But at least, if spins are laid out on a sphere, bulk is everything, so  $H(s)$  is gapped in a conventional sense. Consider a sphere with an interpolation of Hamiltonians  $H(\theta/\pi)$  — such that at one pole the Hamiltonian is  $H(0)$  and at another  $H(1)$ . Let the interpolation affect every term according to the position of the center of its support. Will such a Hamiltonian be gapped?

For a subclass of frustration-free Hamiltonians (those where the ground state is also the ground state of every local term), questions like this are answered by Knabe's lemma (Knabe, 1988; Gosset and Mozgunov, 2016). For noninteracting frustrated Hamiltonians the answer is positive as well (unpublished supplement for Kitaev, 2009). For interacting frustrated ones, it is not clear. In the specific case of the continuous path above, it is possible to construct a different gapped Hamiltonian with approximately the same ground state, by using the quasiadiabatic evolution

with a position-dependent factor in front of the generators. The spectrum doesn't change as a quasiadiabatic evolution is a unitary, so the result is gapped. For a sufficiently big size of the sphere, the ground states of the two should be pretty close.

This is one problem that appears if one tries to build *topological classification of phases*. Of course, one need not go this route, but by the law of conservation of evil it has to get technical somewhere. In the existing work on classification of phases rigorous proofs like this have not been spelled out yet.

So here we propose a different approach. Instead of requiring the gap to be present in the family of Hamiltonians that we try to classify, we require them all to be MBL. The MBL gives one some benefits with such proofs; for instance, the frustration doesn't matter anymore, instead it's the level statistics in the thermodynamic limit that determines whether the Hamiltonian still belongs to the family. It is easy to just conjecture that the level statistics is favorable (no level attraction) in the continuous path construction above; in the end what we get by spatial interpolation is just another realization of disorder.

In this work we investigate the circuits involved in the MBL theory, and our results illustrate some of the challenges of the above approach. In particular, rigorous proofs for the MBL will all rely on some version of Imbrie's construction, unless one wishes to restrict one's attention to Hamiltonians made of commuting terms.

## Chapter 2

### IMBRIE'S CONSTRUCTION

Imbrie, 2016 presented a procedure to diagonalize the following Hamiltonian in the many-body localized regime (which is achieved in a range of parameters to be specified below):

$$H = \sum_i h_i \sigma_z^i + \sum_i J_i \sigma_z^i \sigma_z^{i+1} + \sum_i \gamma_i \sigma_x^i. \quad (2.1)$$

The system described by it is a chain of spin-1/2 degrees of freedom. All the coefficients of the Hamiltonian are disordered:  $J_i$ ,  $h_i$  and  $\gamma_i/\gamma$  are random numbers drawn independently from a distribution that can be quite general. The results apply for familiar distributions like uniform on an interval  $[-1, 1]$  or normal. The constant  $\gamma$  is a small parameter representing the scale of the offdiagonal terms.

The term many-body localization for this model should be understood as "each eigenstate is approximately a product state". Intuitively, we expect such structure at a sufficiently small  $\gamma$ . Indeed, the  $\gamma = 0$  Hamiltonian is diagonal in the  $z$ -basis. The existence of Imbrie's diagonalization procedure can be thought of as a precise way of saying "approximately a product state". Denote the diagonalization procedure by a unitary  $U$  such that  $U^\dagger H U = H_{diag}$ , where  $H$  is the Hamiltonian defined in Eq. (2.1) and  $H_{diag}$  is diagonal in the  $z$ -basis. Note that we put the  $\dagger$  the other way by convention, as the main role of  $U$  is to act on a Hamiltonian operator from the left. Such unitary always exists; what Imbrie shows is its local structure for a sufficiently small  $\gamma$ . We can represent such structure pictorially if we think of  $U$  as a quantum circuit acting on our spin chain (see Fig. 2.1). The first step of the circuit is:

$$U = e^{-A} \dots \quad (2.2)$$

Here  $A$  is a local generator:  $A = \sum_i A_i$ , such that each  $A_i$  acts on just a few neighboring spins. We absorb  $i$  into  $A$  such that  $iA$  is Hermitean and  $e^{-A}$  is unitary. The rotation  $e^{-A}$  is small in the sense that each  $\|A_i\|$  is small:

$$\|A_i\| < \chi \ll 1, \quad (2.3)$$

where the small number  $\chi$  is related to  $\gamma$ , and we use the operator norm  $\|A\| = \max|\lambda|$  where  $\lambda$ 's are eigenvalues of  $A$ . Then one can show that if  $|\pi\rangle$  is a product

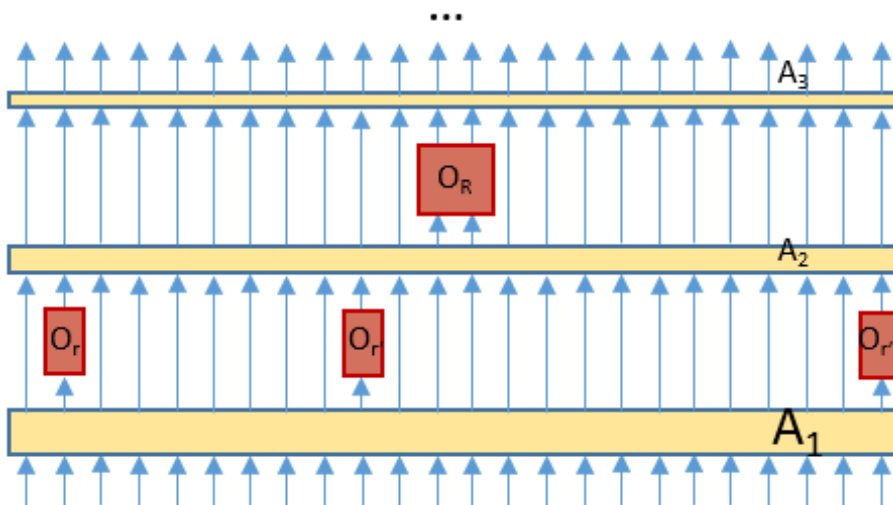


Figure 2.1: The circuit diagonalizing the system.

state,  $e^{-A}|\pi\rangle$  locally remains close to a product state as well. That's how each eigenstate will remain "approximately a product state" after this step.

On the next step of the diagonalization, eigenstates are allowed to deviate from product states in rare regions of the chain called the *resonant* regions. We denote them by an index  $r \in R$ , and the rotation required in each of them by  $O_r$ . The total rotation on this step will be given by  $O = \otimes_{r \in R} O_r$ :

$$U = e^{-A} O \dots \quad (2.4)$$

The resonant regions are very rare. The probability for a spin  $i$  to lie within one of them is bounded as

$$P(i \in R) < \epsilon \ll 1, \quad (2.5)$$

where  $\epsilon$  is another small parameter related to  $\gamma$ . We see that more than  $1 - \epsilon$  of all spins remain untouched by the operator  $O$  — it acts on them as 1. After the above two steps, the procedure repeats itself on the next scale (See Fig. 2.1):

$$U = e^{-A} O e^{-A'} O' \dots \quad (2.6)$$

The terms in  $A'$  are allowed to couple spins at longer distances than in  $A$ , and the resonances in  $O'$  are allowed to be bigger than in  $O$ . It turns out that when  $A$  and  $O$  are chosen optimally, the bounds on  $A'$  and  $O'$ , analogous to Ineq. (2.3, 2.5), can be made tighter. To make it precise, let's denote the length scales at steps  $k = 1, 2, 3..$  by  $L_k$ . Imbrie chooses an exponential sequence of scales for his proof:

$L_k \sim (L_1)^k$ , where  $L_1 \approx 2$ ,  $L_0 = 1$ . We now present the full set of conditions on the diagonalization procedure  $U$  (there are some differences from Imbrie, 2016, which we will discuss below):

$$U = e^{-A_1} O_1 e^{-A_2} O_2 \cdots = \prod_{k=0}^{\infty} e^{-A_k} O_k, \quad (2.7)$$

$$A_k = \sum_i A_{k,i}, \quad \text{supp} A_{k,i} < L_k, \quad \|A_{k,i}\| < \chi^{L_k-1}, \quad (2.8)$$

$$O_k = \otimes_{r \in R_k} O_r, \quad \text{supp} O_r = |r| \leq L_k, \quad P(i \in R_k) \leq \epsilon^{k^2} = \epsilon^{\ln^2 L_k / \ln^2 L_1}. \quad (2.9)$$

Here  $R_k$  is the set of resonances at the  $k$ 'th step. Note that technically the circuit is of infinite ( $\infty$ ) depth, but the rotations become smaller/more sparse as we go deeper in the circuit.

The parameter  $\chi$  that we will use for purely theoretical proofs is  $\chi = \gamma/\epsilon$  as it is the one that both produces a match with the explicit form of the first few orders of the circuit and gives correct results for correlation functions. We derive  $\chi \approx 4\gamma/\epsilon$  norm bound on  $A_{k,i}$  from the formalism developed by Imbrie in Appendix C. For more practical estimates for  $\gamma \approx 0.1$  we will use a notation  $\chi = \gamma_{eff}$ , to point out that it can get renormalized in a nontrivial way.

The range of applicability of Imbrie's result (the convergence radius of infinite product) is not to all the Hamiltonians defined above, only those with  $1 \gg \epsilon > \gamma^{1/20}$  that satisfy an extra assumption on the statistics of eigenvalues of  $H$ :

(*Assumption about level statistics*)  $U$  converges if for all  $L$  the block of size  $L$  of  $H$  has not too strong level attraction:

$$P(\min_{n \neq m} |E_n - E_m| < x) = \text{const} \cdot c^L x^a, \quad (2.10)$$

with  $a > 0$  and  $c$  some constant. We note that  $a = 1$  for the Poissonian statistics expected of MBL.

Next thing we note here is the  $\epsilon^{\ln^2 L_k}$  scaling of the density of resonances. It is an important quantity to test experimentally. In particular, it implies that the biggest resonance in the system of size  $L$  has size  $< e^{\sqrt{\ln L}}$  (essentially indistinguishable from  $\ln L$  for all numerical purposes).

The choice of which sites to include in resonant blocks at each step is made by comparing the energy differences between states connected by spin flips within the block of size  $L_k$  to an exponentially decreasing energy window  $\epsilon^{L_k}$ . If those

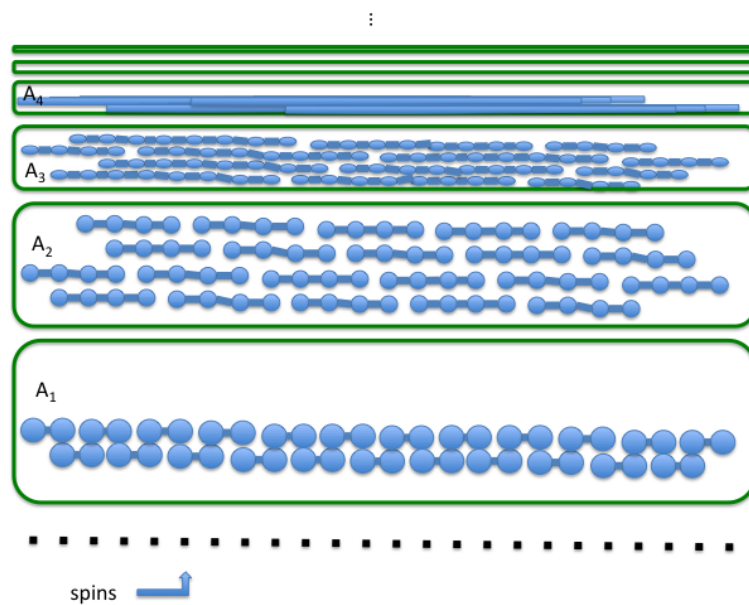
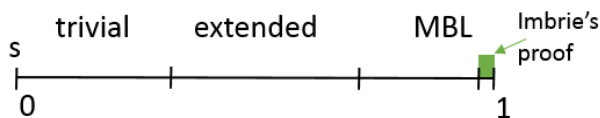


Figure 2.2: Circuit diagonalizing the system with no resonances; the terms of the generators are shown as blue dots

differences are below  $\epsilon^{L_k}$ , the perturbation theory fails and we expect the amplitudes of the eigenstates to be nonperturbative. We can think of  $\epsilon$  as a free parameter: we have a choice of how far to stretch what we call nonperturbative. In the (Imbrie, 2016) proof  $\epsilon$  is a scale that's chosen based on the perturbation strength  $\gamma$ . Specifically, for  $\epsilon = \gamma^{1/20} \ll 1$  the proof goes through. Note how small this makes the range of validity of the construction! A reasonable threshold is  $\epsilon < 0.5$ , so the Imbrie's proof works only for  $\gamma < 10^{-6}$ . That's why here we left  $\epsilon$  and  $\chi$  as parameters in the circuit, without specifying their dependence on  $\gamma$ . We believe that even though the proof stops working for  $\gamma > 10^{-6}$ , one can numerically check that the circuit still exists up to  $\gamma$  of order 0.1 with some parameters  $\epsilon$  and  $\gamma$ . We will measure those indirectly through numerics. The other phases will be explained in chapter 5.



In (Imbrie, 2016) the resonance density is presented at each step via two bounds on quantities called  $Q$  and  $P$ . Besides the structure of the circuit above, they contain extra information that will be useful for some of the estimates in this work. To explain it, we will need to delve deeper into the construction. A typical resonance

would appear at some step  $k_1$ , and is diagonalized by a nonperturbative rotation at a step  $k_2 \geq k_1$ , not necessarily equal to  $k_1$ .

The quantity that counts the number of resonances that appear (but are not necessarily diagonalized) at step  $k$  is described on pages 13-14 of (Imbrie, 2016) - it's  $P_{xy}^{(k)}$ . By definition, it is a probability for sites  $x$  and  $y$  to belong to the same resonant block appearing at step  $k$ . Imbrie proves a bound ((4.1) in Imbrie, 2016)

$$P_{xy}^{(k)} \leq (c\rho_1\epsilon^s)^{(|x-y|^{(k-1)} \vee L_k)/8}. \quad (2.11)$$

Here  $\vee$  means the maximum of the two.  $|x-y|^{(k-1)}$  differs from the ordinary distance  $|x-y|$  by a constant factor. We can deduce the bound on the density of step  $k$  resonant blocks by taking  $y = x$  in the above expression. We get

$$P^{(k)} \leq (C\epsilon)^{c'L_k}. \quad (2.12)$$

Note that  $c' < 1$ , because  $c' = s/8$ , where  $0 < s < 1$  is a constant parameter in a Holder-continuity type bound on the initial randomness. A weaker bound ( $Q^{(k)}$ ) is proven by Imbrie for the density of resonant blocks that are rotated at a step  $k$ . Above we used it in the description of the circuit. But  $P$  is also useful for us: to understand the physical meaning of resonances, we need to see how they appear.

Simply put, every resonant block corresponds to at least two eigenenergies  $E_j, E_{j+1}$  being close as  $|E_j - E_{j+1}| \leq \epsilon^{L_k}$ . The minimum distance between resonant levels  $E_j - E_{j+1}$  is approximately described by a difference of eigenvalues of a matrix

$$\begin{pmatrix} E_j^{(0)} & a\gamma^n \\ a\gamma^n & E_{j+1}^{(0)} \end{pmatrix}, \quad (2.13)$$

where  $E_j^{(0)}$  is the way the energy would go if the other level was not there, and  $n$  is the consecutive support of spins flipped in the resonance. We call the distance between the leftmost and the rightmost spin flip the consecutive support.  $a$  is an  $O(1)$  constant that we drop for scaling estimates. The eigenvalues of such matrix approximate  $E_j, E_{j+1}$  up to terms that are small in comparison to  $\gamma^n$ . The actual minimal distance is found at the crossing point to be  $2a\gamma^n$ . A careful proof of that requires using more details of Imbrie's construction and can be found in the Appendix C. We conjecture this statement  $\min\delta E < \gamma_{eff}^n$  to hold for some  $\gamma_{eff}$  in all of the MBL phase and check it with our numerics in Chapter 6.

Note that our splitting is  $< O(\gamma^{L_k})$ , so much smaller than the window  $\epsilon^{L_k}$ .

Let's quote the specific definition used by Imbrie for when the block is considered resonant. Looking at the equation (4.8) in Imbrie, 2016, we note two major adjustments of the above intuition:

1. The energy levels are taken not from the the final diagonal Hamiltonian, but from the diagonal elements that appear at the intermediate steps of the construction.
2. Even if the level splitting is big, there's an extra opportunity for a block to be resonant if the numerator in the perturbation theory happens to be particularly big.

The second one only contributes extra resonances to the bound (2.12); what holds for all of them remains for more strictly defined ones. But the first adjustment above obfuscates the meaning of resonant blocks: does their presence mean anything in terms of the original system levels  $E_j, E_{j+1}$ ? In fact, in the first three paragraphs of the proof of Theorem 5.1 Imbrie, 2016, argues that the true level distance  $\Delta E^{def} = \Delta E + O(c\gamma/\epsilon)^{n/4}$ , where  $n$  is the number of spins involved in this particular potential resonance. Here Imbrie proceeds to show that since  $\gamma = \epsilon^{20} \ll \epsilon$ , the correction is much less than the separation scale  $\epsilon^n$ . Then Imbrie concludes that the bound (2.12) holds to the first order also for resonances defined in terms of final energy levels. There is a subtlety here: the idea of the proof with exponential smallness in  $n$  relies on the separation condition, which only holds for "small blocks" (resonances that appear in isolated clusters of size  $< L_k$ ). But the bound (2.12) is for all blocks that appear at a certain level of construction. Some of them are not separate from the other blocks at this step. One can potentially think of a chain reaction where a spin next to the block that is resonant becomes resonant, violates the  $\Delta E^{def} = \Delta E + O(c\gamma/\epsilon)^{n/4}$  of the next spin, which then becomes resonant and so on. Imbrie does not present an argument that would exclude that scenario (as he does not need it in the proof), but we expect that it can be done. We will only use the bound (2.12) as a qualitative explanation of numerics in Chapter 6. We summarize our interpretation below:

Consider a system of size  $L$ . Now assign to each eigenenergy  $E_j$  a corresponding (by  $U$  up till the appearance of a resonance) z-basis product state. Each energy eigenstate will have a number  $E_j$  and a string  $\sigma_j$  corresponding to it. Among the pairs of strings separated by a flip of spins in a block of size  $< L_k$ , the pairs of corresponding levels are either  $|E_j - E_i| < \epsilon^{L_k}$  or the other way. In the former case,

we call the block that needed to be flipped resonant. The density of such blocks is bounded as

$$P^{(k)} \leq (C\epsilon)^{c'L_k}. \quad (2.14)$$

*Chapter 3*

## PROPERTIES OF IMBRIE CIRCUIT

The easiest way to formulate the results of this paper is to state them for the case with no resonances (also shown on fig. 2.2)

$$U = e^{-A_1} e^{-A_2} \dots = \prod_{k=0}^{\infty} e^{-A_k}. \quad (3.1)$$

The presence of resonances is a low-probability event, so typically the simplest form of results hold. Here we only discuss the effect of resonances on the entanglement entropy as that one was experimentally (numerically) observed.

**Results** The first result of this paper is to establish the form (2.7) based on constructions of (Imbrie, 2016). The form (2.7) was never explicitly stated in the original paper. Once we have the form, it allows the use of most advanced techniques of information theory to prove the following:

- If  $U$  is a circuit with no resonances, then for a local operator  $X$  both  $UXU^\dagger$  and  $U^\dagger XU$  have exponential tails.
- $|\psi\rangle$  of any eigenstate of  $H$  (the Hamiltonian diagonalized by  $U$ ) has an efficient matrix-product state description.
- $|\psi\rangle$  satisfies a stronger condition: it can be created by a finite-depth local circuit with local precision.

Let's take a moment here and try to formulate the last statement precisely. Based on the infinite circuit  $U$  without resonances, we construct a circuit

$$U_F = \otimes_{j=1}^D \otimes_{i=1}^{L/2} U_{ij} \quad (3.2)$$

containing only nearest neighbor 2-qubit gates (2-spin rotations), such that any qubit is acted upon by at most  $D$  gates.  $D$  is called the depth of the circuit. Such circuit is called finite-depth local circuit.

We know that an eigenstate  $|\psi\rangle = U|\pi\rangle$ , where  $|\pi\rangle$  is a product state. The circuit  $U_F$  is constructed so that  $|\psi_F\rangle = U_F|\pi\rangle$  approximates  $|\psi\rangle$ . For a system size  $L$ , we

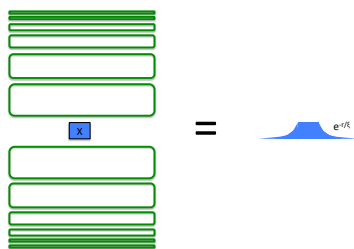


Figure 3.1: First way to conjugate a local operator.

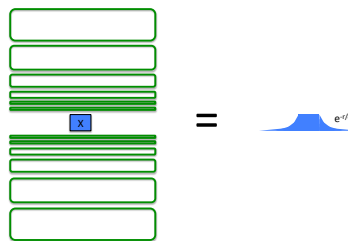


Figure 3.2: Second way to conjugate a local operator.

could require approximation of a state as a whole  $\| |\psi\rangle - |\psi_F\rangle \|$  to be small. That would imply system size dependent depth  $D(L)$  (in fact, one can show  $D(L) \sim L$  in this case). We'd like  $D$  to be independent of  $L$  (thus the name finite-depth), so we need to relax the approximation requirement: let's only care about local observables, and approximate  $|\psi\rangle$  so that one is unlikely to distinguish  $|\psi_F\rangle$  from it by any local measurement. This is done by considering density matrices  $\rho = \text{tr}_{\bar{R}} |\psi\rangle\langle\psi|$  and  $\rho_F = \text{tr}_{\bar{R}} |\psi_F\rangle\langle\psi_F|$  over any region  $R$  of  $|R| < R_0$  consecutive spins. Now we require

$$\forall R, \quad \|\rho - \rho_F\| < \epsilon. \quad (3.3)$$

The result is that there indeed exist triples  $(\epsilon, R_0, D)$  such that it is possible to fulfill the above requirement for any eigenstate  $|\psi\rangle$ . We note that it is not always possible to have "flat" circuit - that is, for the region to be longer than the circuit is deep:

$$D = D(R_0, \epsilon) < R_0. \quad (3.4)$$

For not too small errors (compared to  $\chi$ ) it is possible. Note that  $U_F$  approximates any eigenstate of  $H$  with the same chosen precision  $\epsilon$  over regions of chosen size  $R_0$ . It is one circuit for all basis states.

A general Hamiltonian  $H$  will also have resonances. They modify the circuit above: on top of each resonance, there's a local increase in depth. We proceed with a list of our results about  $U, H$  and its eigenstates  $|\psi\rangle$ :

- States  $|\psi\rangle$  satisfy area law (as expected from states approximated by matrix product states). We can bound the entanglement across the cut as

$$S_{\text{cut}} = S(\rho_{\text{left}}) < 16\chi. \quad (3.5)$$

Entanglement across the cut:

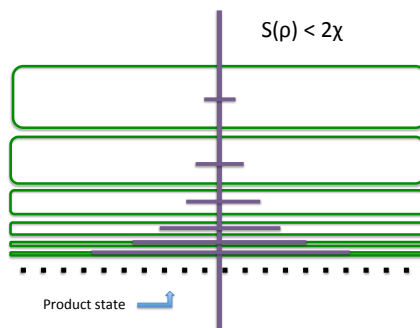


Figure 3.3: Entropy across the cut in the system with no resonances

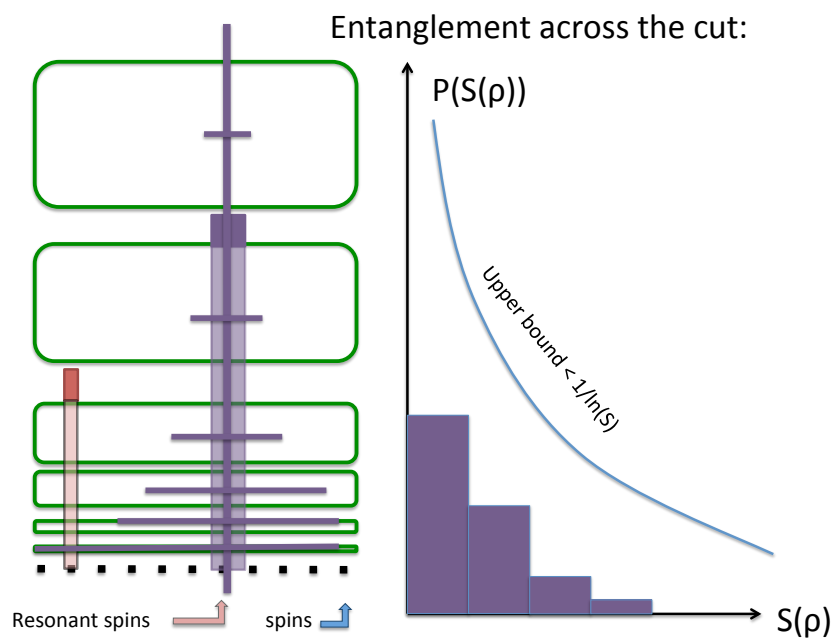


Figure 3.4: Entropy across the cut, generic.

- The presence of resonances modifies the entanglement entropy in the following way: if the cut is across the resonance,  $S_{\text{cut}} < \text{size of the resonant region}$ . Recall that the total density of resonances is  $O(\epsilon)$ , and the distribution of their sizes is  $P(n_r) \leq \epsilon^{\ln^2 n_r}$ . Thus for different realizations of disorder, as well as for different locations of the cut, we should observe the following tail of the distribution of entanglement entropies:

$$P(S_{\text{cut}} > X) \leq \text{const} \cdot \epsilon^{\ln^2 X}. \quad (3.6)$$

As we noted before, the largest resonance in a system of size  $L$  is approximately logarithmic in  $L$ . Thus we should find entropies as big as logarithmic in system size for a given disorder realization. The bound on the expectation value of entanglement is now dominated by step-1 resonances:

$$\overline{S_{\text{cut}}} \leq 16\chi + 4\epsilon, \quad (3.7)$$

as  $\epsilon \gg \chi$  in Imbrie's construction.

- We can bound correlations in states of  $H$ . Imbrie provided a result for static correlation functions in the eigenstates, which can be easily derived from exponential tails of local operator  $UXU^\dagger$ , written in the form of the *telescopic sum* (see Appendix B). The correlations are exponentially decaying with distance. The bounds are modified by resonances, the probability of large deviations being bounded in (Imbrie, 2016).

We begin the investigations of the dynamics of correlations developed by  $H$ . We prove a Lieb-Robinson bound for the case of no resonances:

$$\|[A, B(t)]\| \leq at e^{-cx} = at(Z\chi)^x, \quad (3.8)$$

where  $B(t) = e^{iHt} B e^{-iHt}$ . Here  $Z$  is a system-independent number. We note that the decay in  $x$  is much stronger than for generic Hamiltonian, which has  $e^{-cx}$  with  $c$  a system-independent number. In our case,  $c \sim -\ln\chi$ . We can see the logarithmic light cone  $x \sim \ln t$ . The effect of the resonances is such that, again, the bound becomes probabilistic - in the rare event that resonance is found between supports of  $A$  and  $B$ , the light cone is linear in that region. We also note that since  $\ln t$  is non-analytic at  $t = 0$ , the logarithmic light cone should be thought of as linear for the first lattice site and then logarithmic.

We provide an original proof of LRB in Appendix B. We note, however, that once the bound on tails of the  $UXU^\dagger$  is established, it is easy to transform the

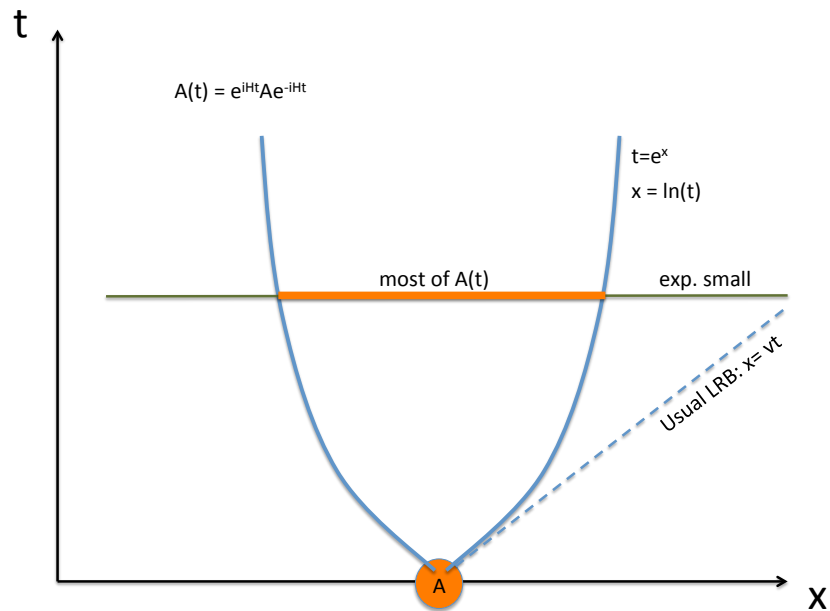


Figure 3.5: Dynamics as in LRB.

Hamiltonian into a sum of tailed commuting terms as  $U^\dagger H U$ . Then it satisfies the definition of MBL given in (Kim, Chandran, and Abanin, 2014). This reference contains an independent proof of Lieb-Robinson bound, as well as the proof of the logarithmic growth of entanglement after quench.

## Chapter 4

## ALONG THE ADIABATIC PATH

Consider setting up a chain of spins in the D-wave machine. The input consists of a classical random 1d Ising model:

$$H_z = \sum_i J_{i,i+1} Z_i Z_{i+1} + h_i Z_i, \quad (4.1)$$

where  $J_i, h_i \in [-1, 1]$  are random variables. Other Hamiltonian terms are a transverse field and a coupling to environment that acts by phase flips ( $Z$  operators):

$$H_x = \sum_i X_i, \quad H_b = \sum_i Z_i B_i. \quad (4.2)$$

D-wave protocol goes as follows: start in  $H_x$  groundstate  $|-\rangle^{\otimes n}$  and interpolate to  $H_z$ :

$$H = (1 - s)H_x + sH_z, \quad \text{where } s(t) = t/T_{\text{protocol}}. \quad (4.3)$$

The time of the protocol can be varied in the machine. We plot the energy levels of the closed 6-spin system (without the term containing the environment) in figure 4.1. We ignore the midband for now, as the low energy subspace is relevant for the protocol.

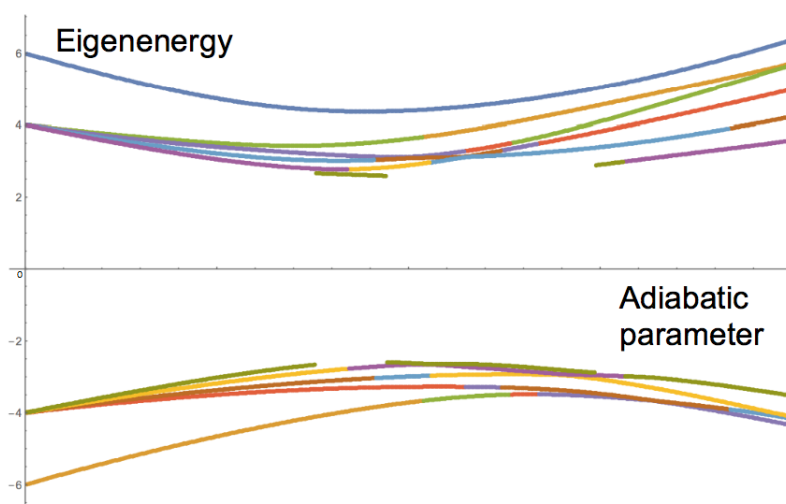


Figure 4.1: Levels along the protocol

We see that the gap of the original transverse field Hamiltonian  $H_x$  closes somewhere along the protocol, and the ground state experiences avoided crossings with the first excited state.

Let's first investigate the gap of classical  $H_z$  (the system at the end of the protocol). Consider first a simple model with just a single-site field  $h_x^i$ . The gap is given by  $2\min_i h_x^i$ . There are  $n$  random variables uniformly distributed in the interval  $[-1, 1]$ , so the smallest of them is  $O(1/n)$  on average (over the ensemble of disorder realizations). The presence of random interactions along the chain makes the problem more complicated, but doesn't change the average. We are not familiar with any theoretical results on the matter. We demonstrate it on small system sizes in Figure 4.2.

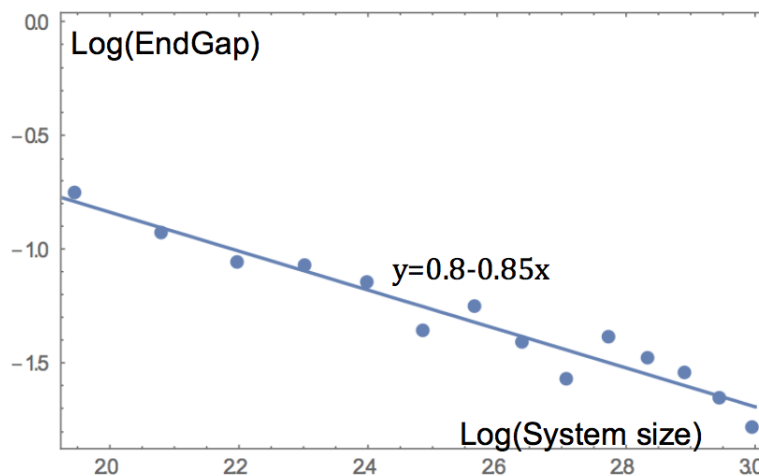


Figure 4.2: For system sizes  $n = 7$  to 20 ensemble-averaged gap approaches  $1/n$  scaling. One can extend the data to bigger system sizes in poly-time, as outlined in appendix A.

We expect that the gap along the protocol is also  $O(1/n)$  for ensemble average. But for the matter of avoided crossings, we care about minimal gap along the protocol, and that is given by exponentially short intervals  $\Delta s$  where the gap is exponentially small in  $n$ . Numerically it is not feasible to observe that, as checking for minimal gap along  $s$  is exponentially more expensive than checking for a gap at a specific  $s$ . We can only access system sizes up to  $n = 9$ . Typical minimal gaps for those sizes are not much different from the end gap of the corresponding disorder realization of  $H_z$ . Figure 4.3 shows distribution of gaps for an ensemble of 100 realizations.

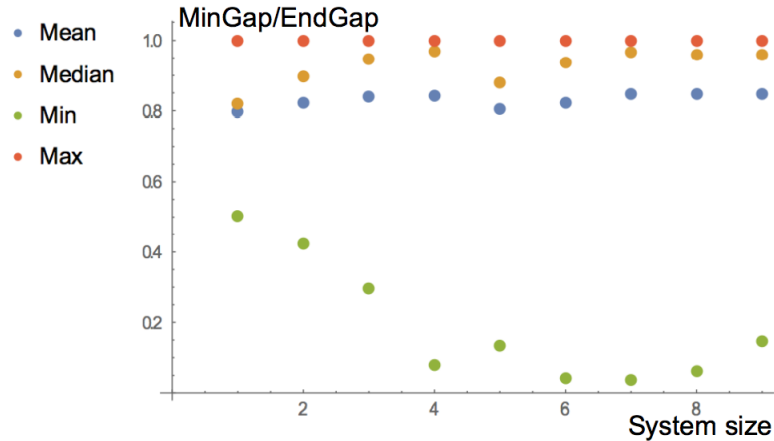


Figure 4.3: For system sizes  $n = 1$  to  $9$  the smallest gap of avoided crossing that ground state encounters is expected to be  $e^{-n}$  — not observed for small systems. (B. Altshuler, Krovi, and Roland, 2010) presents a poly-time procedure for collection of this data for big systems sizes, assuming MBL.

We note that suppression by a factor of 10 is present in at least one of those 100 systems. However  $n < 10$  is nowhere near the regime where exponentially small minimal gap is typical, so these numerics do not qualify as an evidence of existence of such regime. We note that since the evolution time of the D-wave is around  $10^5$ , the smallest gaps measurable by it would be  $\sqrt{n/10^5}$ , so roughly 0.01. Using the fit for gap of  $H_z$  above, one finds that at system sizes  $n \approx 100$  the gaps surely become smaller than what's measurable on D-wave. However they can do so much earlier - a more ambitious estimate is the gap of ferromagnetic chain with no magnetic field — that one becomes unmeasurable over the D-wave protocol time already for  $n = 10$ .

## Chapter 5

### SLOPES

So far we have established what MBL means for a Hamiltonian that is close to z-basis. However, along the adiabatic path considered in the previous section, only the  $s \approx 1$  region is that way. The  $s \approx 0$  region is close to a Hamiltonian diagonal in another basis (x-basis), but that Hamiltonian is not disordered so we don't expect Imbrie's proof to apply. However, this does not show that approximately diagonalizing it locally is impossible. We would like to have some measure that distinguishes the two cases, ideally based on our understanding of what basis-independent properties the MBL has. Finally, in the middle of the path ( $s \sim 0.5$ ) the perturbation strength controlling Imbrie's construction is big ( $\gamma = 0.5$ ), so we expect an extended phase (antipode of the MBL phase) to appear.

The traditional indicators of MBL are level statistics and exponential decay of correlations (which can be used to derive zero conductivity). The latter is somewhat hard to confirm in systems of ED size  $L = 10$ , as the finite-size effects are strong and the data can be fit equally well by a power law. So we focus our attention on the level statistics. The commonly used quantity in level statistics is level repulsion.

Consider the differences between the two closest eigenenergies  $\delta_n = E_n - E_{n-1}$  for a particular system. We can form a dimensionless parameter:

$$r = \text{Avg}_{n,dis} \frac{\min(\delta_n, \delta_{n+1})}{\max(\delta_n, \delta_{n+1})}. \quad (5.1)$$

A random matrix theory result is that a Hermitean matrix with random entries will have  $r = 0.55$  and a symmetric real matrix has  $r = 0.53$ . At the same time, a matrix with random diagonal and all zeroes off-diagonal will have  $r = 0.39$ . Note that an MBL Hamiltonian can be reduced to sum of local terms that are statistically independent of each other (there are some correlations between neighbors, but not the ones far away). Now two different eigenstates typically have  $O(L)$  of the local terms flip signs, so their energies are random variables that are to a good approximation independent and identically distributed (i.i.d.). And nothing prevents i.i.d. random variables from being arbitrarily close, so unless there's an adversarial realization of disorder, the ones that we will find close typically are the ones that

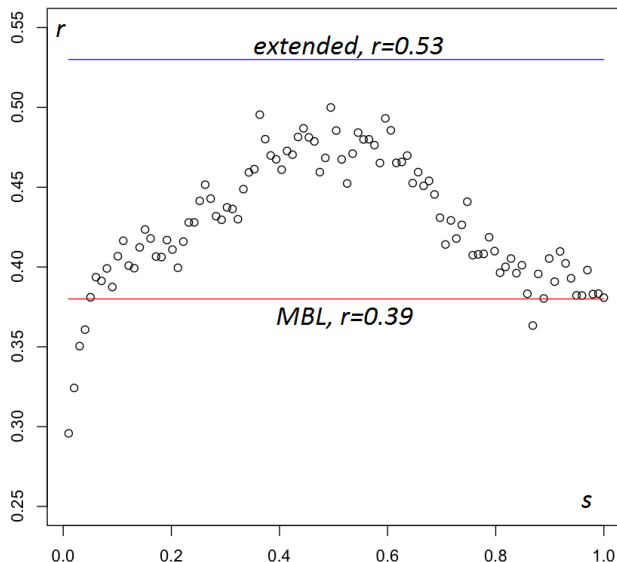


Figure 5.1: Level repulsion parameter  $r$  along the protocol, averaged over disorder. We see that it detects the extended phase, but does not distinguish between the systems close to disordered  $H_z$  and non-disordered  $H_x$

were independent. So the random diagonal approximation works for the estimation of parameter  $r$  above, and we should get  $r = 0.39$ .

Note that this argument fails outside MBL as the energy depends on the randomness in our system not like a sum over regions but like a more complicated function. We plot the level statistics parameter  $r$  along the protocol in Figure 5.1. Note that the data is very noisy even for big system sizes  $L = 15$ , and it takes a lot of time to average out the noise. If one were to claim the position of the MBL-extended transition, it would not be conclusive from this picture alone; one needs to also collect data for different system sizes to observe finite size scaling (if the points go closer to 0.53 as  $L$  increases, that should be extended phase, and MBL elsewhere). Also, we get the same behavior for two very different regimes next to  $H_x$  and  $H_z$  ( $s \approx 0$  and  $s \approx 1$ ).

In this section, we take advantage of the fact that we need to study the range of  $s$  instead of isolated Hamiltonian, and try to see how the relationship between  $H(s)$  and  $H(s + ds)$  can reveal the differences between the  $s \approx 0$  phase and the MBL phase, as well as provide a better indicator of where the transition is. Let's look again at  $E_n(s), E_{n-1}(s)$ , but now also at  $E_n(s + ds), E_{n-1}(s + ds)$ . Depending on how big we take  $ds$ , there may be an issue of how to associate level label  $n$ . For  $ds \ll \gamma^L$

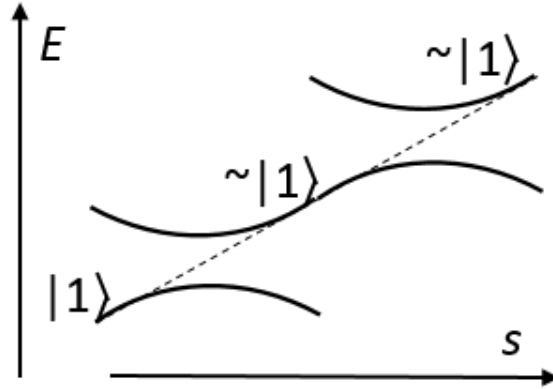


Figure 5.2: An illustration of smart level labels used to determine slopes at big  $ds$

in the MBL phase, no crossings have time to go by, and the simple ordering in energies will give the correct labels. For other two phases, we can use  $ds \ll 1/2^L$  and  $ds \ll s^L$  respectively.

However, there's another way of assigning labels, somewhat more computationally demanding. If we take  $ds > 1/2^L$ , some levels will swap places in the energy ordering. We assign label  $n$  in such a way that the state  $|n(s + ds)\rangle$  has the biggest overlap  $|\langle n(s + ds)|n(s)\rangle|$  (see Figure 5.2). That by itself is not enough, as a unitary  $U_{nm} = \langle n(s + ds)|m(s)\rangle$  connecting the eigenbases may have a states  $|n(s + ds)\rangle$  and  $|n'(s + ds)\rangle$  such that the maximum over  $m$  of overlaps  $|\langle n(s + ds)|m(s)\rangle|$  and  $|\langle n'(s + ds)|m(s)\rangle|$  is achieved on the same eigenstate  $|m(s)\rangle$ . Instead we maximize the sum of all overlaps  $\sum_n |\langle n(s + ds)|n(s)\rangle|$  over  $UP$  where  $P$  are all possible permutations of  $2^L$  elements. There are  $2^L!$  of those, so it's a computationally unfeasible task.

Instead we note that confusions happen close in energy, and restrict the permutations to  $k$  consecutive levels ordered in energy, thus requiring only  $2^L k!$  iterations. For sizes  $L > 8$ , we also find that there are apparent blocks of confused levels of size  $k > 12$ , which again makes the computation take too long. Instead of full permutation of  $k$  levels, we first deal with  $k = 2$ , but for all possible pairs within some window in energies. That removes most of the confused regions, so we can assign labels for  $L = 10$  and  $ds = 1/40$  without trouble. Higher  $L$  are also possible either by decreasing  $ds$  or by extra improvements in the code, but here we present the results for this approach.

Now that we have two ways of assigning labels (for exponentially small  $ds_1$  and for

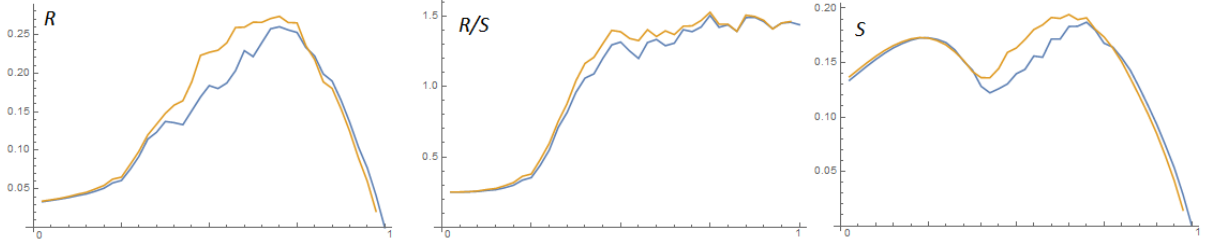


Figure 5.3: The quantities  $R(s, ds)$ ,  $R(s, ds)/S(s, ds)$ ,  $S(s, ds)$  are plotted along the protocol. Step  $ds_1$  is in blue, step  $ds_2$  with smart overlap labels is in gold

$ds_2 = 1/40$ ), we consider the following quantities:

$$S(s, ds) = \text{Avg}_{n,dis} \frac{|E_n(s+ds) - E_n(s)|}{ds}, \quad (5.2)$$

$$R(s, ds) = \text{Avg}_{n,dis} \frac{|E_n(s+ds) - E_n(s) - (E_{n-1}(s+ds) - E_{n-1}(s))|}{ds}. \quad (5.3)$$

We note that the overall scale factor contributes to  $S$  and  $R$ , and can be estimated by the standard deviation of the eigenvalues of the Hamiltonian:

$$\sigma E = \sqrt{\text{Avg}_{n,dis} E_n^2} = \sqrt{\text{tr} H^2 / 2^{L/2}} = \sqrt{s^2 \text{tr} H_z^2 + (1-s)^2 \text{tr} H_x^2 / 2^{L/2}} \approx L \sqrt{s^2 + (1-s)^2} \quad (5.4)$$

In the slopes,  $E_n(s+ds)$  can get an extra shift just by  $s$ -dependent overall rescaling of  $H$  according to  $\sigma E$  above. This trivial contribution obfuscates our results, so for the purposes of this chapter we are using the Hamiltonian:

$$H(s) = \frac{1}{L \sqrt{s^2 + (1-s)^2}} (s H_z + (1-s) H_x). \quad (5.5)$$

We plot an example of  $S$  and  $R$ , as well as their dimensionless ratio  $R/S$  for one disorder realization of  $L = 9$ , for two different step sizes  $ds_1 = 10^{-4}$ ,  $ds_2 = 1/40$ . The second one uses smart overlap labels as described above. We see how  $R/S$  distinguishes between the  $s \approx 0$  and  $s \approx 1$  phases. Indeed, near  $H_x$ , levels fan out from the  $\sum s_x$  sectors almost like straight lines. That is because each  $ZZ$  term preserves the total  $X$  magnetization, so it introduces the splitting in the first order of perturbation theory. The energies go within

$$E = E(s=0) \pm sO(L), \quad (5.6)$$

so the slopes vary by  $O(L)$  among  $\exp(L)$  levels in the fan. They all originate from the same point and do not turn, so the relative slopes will go as  $O(L)/\exp(L) \rightarrow 0$  in the thermodynamic limit. That explains the drop of the finite-size contribution

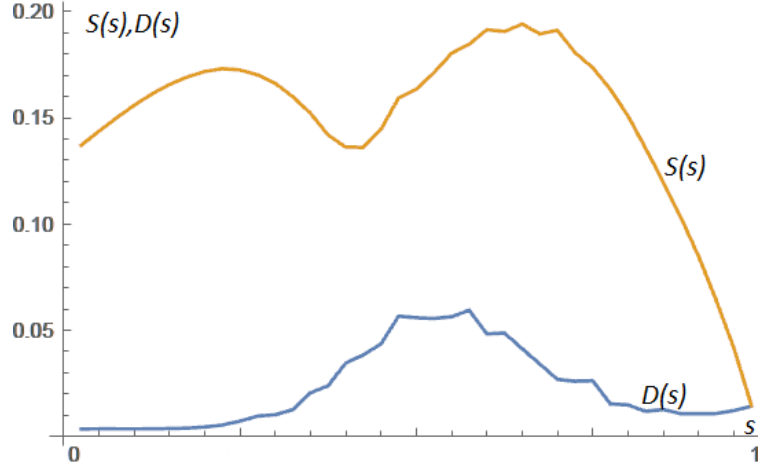


Figure 5.4: The quantity  $D(s)$  is in blue,  $S(s)$  in gold

to zero on the left. So the expectation for quantity  $R/S \sim L2^{-L}$ , whereas in both extended and MBL phases it remains constant.

We also note the linear scaling of  $S$  and  $R$  at  $s \approx 1$ , as expected from perturbation theory: the corrections to energy appear only in the second order  $\delta E \sim (1-s)^2$ , so the slopes are  $S \sim (1-s)$ . From the numerics we find the coefficient  $R \approx 1.5S \approx 1.5(1-s)$ , so we can use an estimate  $1.5L(1-s)\sqrt{s^2 + (1-s)^2}$  for the relative slopes of our original system at  $s \approx 1$ , and  $0.2L$  for  $s \sim 0.5$ . Our understanding of frequency of crossings along a level will be based on two characteristics: neighbors and slopes. We will to study the neighbors and explain the crossing data in the next chapter.

Finally, we note a subtle difference between results for  $ds_1$  and  $ds_2$ . Consider the mean absolute value of the differences observed in individual levels:

$$D(S, ds_2) = \lim_{ds_1 \rightarrow 0} \text{Avg}_{n,dis} \left| \frac{|E_n(s + ds_1) - E_n(s)|}{ds_1} - \frac{|E_n(s + ds_2) - E_n(s)|}{ds_2} \right| = \quad (5.7)$$

$$= \text{Avg}_{n,dis} \left| \left| \frac{dE_n(s)}{ds} \right| - \frac{|E_n(s + ds_2) - E_n(s)|}{ds_2} \right|. \quad (5.8)$$

We plot it in comparison with  $S$  in Figure 5.4. It is nonzero only where we expect extended phase to be according to the level repulsion parameter  $r$ . We note in Figure 5.5 that due to its fine-tuned character, it is very sensitive to noise. However, if we average out the noise over many disorder realizations, we may observe a hint of finite-size scaling (see Figure 5.6). For level repulsion  $r$ , we had a clear expectation

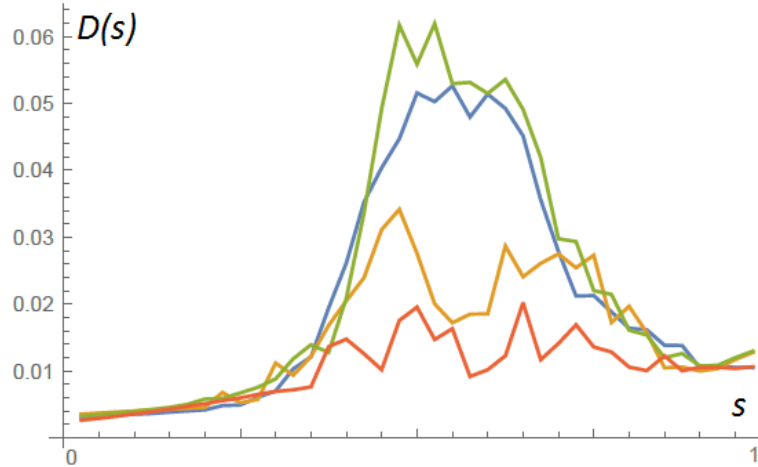


Figure 5.5: The quantity  $D(s)$  for different realizations of disorder

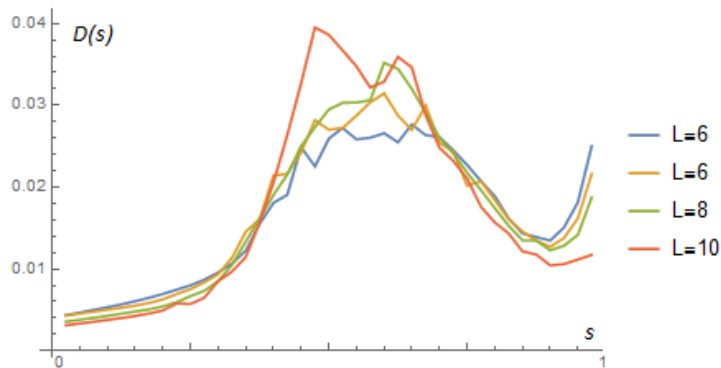


Figure 5.6: The quantity  $D(s)$  for different system sizes

of infinite system size value from random matrix theory. For  $D$ , one could also consider two random matrices  $sH_1 + (1-s)H_2$  and calculate the value. We expect the normalized by the norm value in the extended phase to be some constant. The logic for this is the following: in the extended phase, the level crossings are as big as the level distances allow. Two levels that are  $\delta E$  apart at the avoided crossing will stay  $\sim \delta E$  away from each other. That repulsion alters the slope by quantity of the same order as the slope itself. Thus the slopes are altered from their true values extracted from where the overlap travels  $O(1)$  of the time. Thus we expect  $O(1)$  difference in average slopes.

In MBL the size of the repulsion goes as  $\gamma^n$  with consecutive distance  $n$ . Here we consider non-normalized  $H$ . The probability for a level to intersect a level consecutive distance  $n$  away is  $\sim L2^n/2^L$  (see next chapter). That gives an upper bound on

the portion of energy change covered by avoidance that this level experiences:

$$\delta E_{avoid} \sim \sum_n L 2^n / 2^L \gamma^n \sim 2L\gamma / 2^L. \quad (5.9)$$

On the other hand, the distance to the next level is

$$\delta E \sim L 2^{-L}, \quad (5.10)$$

thus the fraction of values of energy at which the slopes are affected by the crossings is:

$$\delta E_{avoid} / \delta E \sim 2\gamma \quad (5.11)$$

So it is also system-size independent. However, the  $\sum_n$  may start only with  $n$  such that  $\gamma^n < ds_2$ , as the bigger avoidances are followed by the smart overlap labels. So changing  $ds_2$  should affect the result in the MBL phase as

$$D(s, ds_2) \sim \min(ds_2, \gamma). \quad (5.12)$$

In the extended phase, on the contrary, the slopes are typically results of avoided crossings with neighbors in energy, so  $D$  should remain roughly independent of  $ds_2$  as long as  $ds_2 > 1/2^L$  - some size-dependant scale. In practice it also decreases with  $ds_2$ , but is slower than linear in  $ds_2$ . So if one plots

$$D(s, ds_2) / ds_2, \quad 2^{-L} < ds_2 < \gamma, \quad (5.13)$$

one should find a static value for the MBL phase, and an unbounded growth for the extended phase. That is indeed what is observed, see Figure 5.7. We note that the quantities we defined are more sensitive to the MBL/extended transition than the level repulsion  $r$ , given the same computational resources in a numerical study. Indeed, the system size dependence of level repulsion  $r$  is shown in Figure 5.8, and the number of realizations needed to produce clean features was 500, 500, 100, 20 for  $L = 6, 8, 10, 12$ , respectively. But for the  $\frac{D(s, ds_2)}{80 ds_2}$  in Figure 5.7, we only needed  $L = 6$  and just 30 realizations. The location of the transitions can be inferred equally poorly from both. One commonly used technique for that is to search for a scaling collapse as in (Kjall, Bardarson, and Pollmann, 2014). One can then assess the benefits of our indicator by comparing the resulting uncertainty of the transition point to the one found by methods of (Kjall, Bardarson, and Pollmann, 2014). As the choice of scaling functions is subjective, we leave a careful comparison for future work. In the following section we present a somewhat more straightforward way to improve the level repulsion indicator, that does not require a sophisticated algorithm.

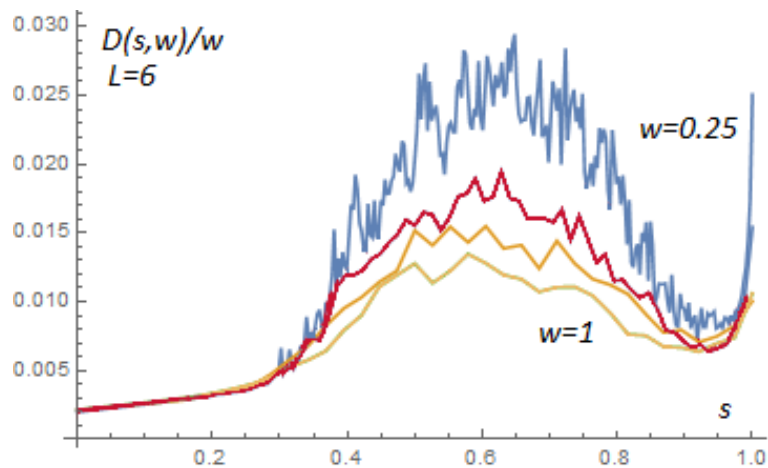


Figure 5.7: The quantity  $D(s, ds_2)/80ds_2$  for different step sizes:  $1/w = 1/80ds_2 = 4, 1, 0.5, 0.5$  for blue, red and two yellow lines correspondingly. Here  $L = 6$ .

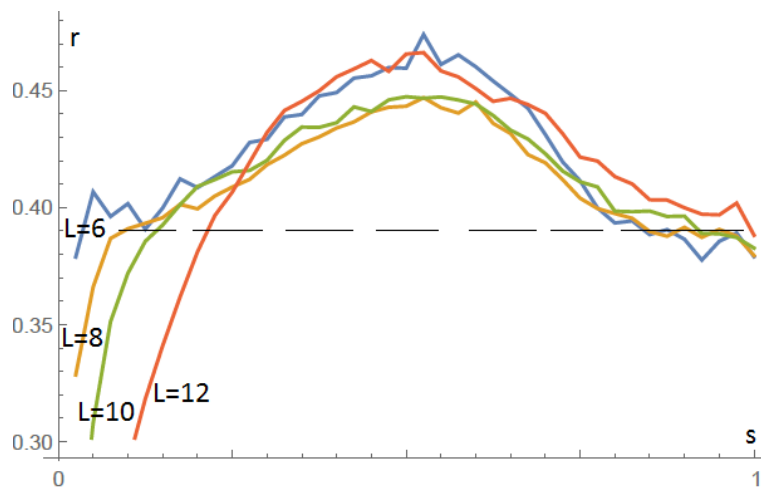


Figure 5.8: The level repulsion parameter  $r$  for the full Hamiltonian  $H$ , calculated in the mid 20% of levels where the MBL breaks down the fastest. System sizes  $L = 12, 10, 8, 6$  in blue, gold, green and red, respectively.

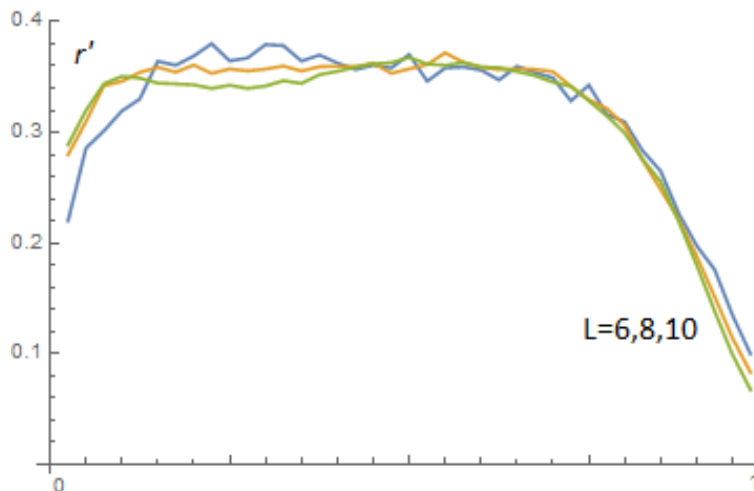


Figure 5.9: The level repulsion parameter  $r$  for time-averaged mid-chain Hamiltonian  $H'_a$ . System sizes  $L = 6, 8, 10$  in blue, gold and green correspondingly.

### 5.1 Time-averaging of Hamiltonian terms

Consider splitting the chain into two regions:  $H = H_a + H_b$ . Specifically, take a region  $a$  to be the middle 1/3 of the chain. In general  $[H_a, H] \neq 0$ , but we want to adjust it so that it commutes with  $H$ .

We construct a time-average

$$H'_a = \lim_{T \rightarrow \infty} 1/T \int_0^T e^{iHt} H_a e^{-iHt} dt; \quad (5.14)$$

this kills off-diagonal elements in the eigenbasis of  $H$ , so commutation is enforced. Note that time averaging leaves the Hamiltonian invariant:

$$H = \lim_{T \rightarrow \infty} 1/T \int_0^T e^{iHt} H e^{-iHt} dt = H'_a + H'_b. \quad (5.15)$$

So  $[H'_a, H'_b] = [H'_a, H - H'_a] = 0$  as well. The eigenstates of  $H'_a$  are those of  $H$ , but the eigenvalues might be very different. In the worst case scenario they all go to zero when the local term does not have any diagonal matrix elements. But for a sufficiently long chain the middle will carry a third of the energy, so this shouldn't be the case. What time-averaging does is that it spreads the initially local operator to the whole system, so we don't expect any degeneracies in  $H'_a$ . What we suggest is to look for level statistics in  $H'_a$ . We plot its level repulsion parameter  $r'$  in Figure 5.9. We immediately see that in the alleged MBL phase  $r'$  follows  $\gamma$ , but then stops at the Poisson value 0.39 for the extended phase. The crossover appears to be smooth. It is easy to explain the Poisson: after dropping the offdiagonal terms, we essentially end

up with a random diagonal. But in the MBL phase the levels of  $H'_a$  seem to attract each other. That is because in the MBL phase the local Hamiltonian of the mid-chain  $H'_a$  can be represented in a basis of tailed logical operators,  $U\sigma_i^x U^\dagger, U\sigma_i^z U^\dagger$ , in such a way that the coefficients of the operators far away from the middle are small as  $\gamma^d$ , where  $d$  is the distance. Then time averaging kills all the terms containing logical  $U\sigma_i^x U^\dagger$ , so we expect what's left to have  $\gamma^d$  tails around the middle. That means that the values of faraway spins only shift the spectrum by  $\gamma^d$ . So each eigenvalue of the middle has neighbors positioned roughly as energies of

$$H_{eff} = \sum_{n=1}^{L/3} \gamma^n (\sigma_n^z - 1); \quad (5.16)$$

the closest one will have a distance of  $\gamma^{L/3}$ , the next one  $\gamma^{L/3-1}$ . We can see that the ratio  $r' = \gamma$ . We see that the curves for different system sizes collapse onto each other without any rescaling. We expect that closer investigation of the transition region, and possibly the derivatives of  $r'$ , will reveal the position of the transition point using methods similar to (Kjall, Bardarson, and Pollmann, 2014), but we do not attempt it here. We also note that the decay of the tails of  $H'_a$  as well as the amplitude of the center was used in (Chandran et al., 2015) to locate the transition.

### Reduction of Any Hamiltonian

The time-averaging technique discussed here is very powerful. The properties of the infinite time-average of the Hamiltonian terms were used in (Kim, Chandran, and Abanin, 2014) as a definition of MBL, with all the mathematical properties of our Chapter 3 except the Area law following from that definition. If we time-average for a finite-time, let's bound the commutator of the two parts:

$$[H'_a, H'_b] = [H'_a, H] = \frac{1}{T} \int_0^T e^{iHt} [H_a, H] e^{-iHt} dt = \quad (5.17)$$

$$= \frac{1}{iT} \int_0^T \frac{d}{dt} e^{iHt} H_a e^{-iHt} dt = \frac{e^{iHT} H_a e^{-iHT} - H_a}{iT} \quad (5.18)$$

$$\|[H'_a, H'_b]\| \leq \frac{2S}{T}, \quad (5.19)$$

where  $S$  is the support of  $H_a$ . The spread of the local operator of any Hamiltonian can be bounded by the Lieb-Robinson bound. Let the light cone (where the bound on  $\|[A(t), B]\| \sim 1$ ) be given by  $x(t)$ , therefore time-averaging for time  $T$  should give an operator whose support outside the radius  $x(T) + \Delta x$  can be bounded as  $e^{-c\Delta x}$ , where  $c$  is a Hamiltonian-independent number for 2-local Hamiltonians (and can be

strengthened even more for MBL). Moreover, the time-averaging can be done with the Hamiltonian truncated to an  $x(T) + \Delta x$  collar of the local operator, with only exponentially small error:

$$\tilde{H}'_a = 1/T \int_0^T e^{iH_c t} H_a e^{-iH_c t} dt = H'_a + \delta_a, \quad \|\delta_a\| \leq e^{-c\Delta x}. \quad (5.20)$$

Note that  $\delta$  is a nonlocal interaction that's exponentially small in the distance. Now split the system in many regions  $a_1, a_2 \dots$ . So if we take  $H_a$  to have support  $S > x(T) + \Delta x$ , the effects of the time-averaging could be truncated in such a way that  $\tilde{H}'_{a_i}$  only overlap with their neighbors  $\tilde{H}'_{a_{i\pm 1}}$ . So we have reduced our Hamiltonian to a nearest neighbor chain of approximately commuting terms (as in Bound 5.19), with an exponentially small error:

$$H = \sum_i \tilde{H}'_{a_i} + \delta_i. \quad (5.21)$$

Now let's take even-odd pairs  $\tilde{H}'_{a_{2k}} + \tilde{H}'_{a_{2k+1}}$ . We would like to use a result by (M. B. Hastings, 2009) that reduces approximately commuting operators to exactly commuting ones, by small adjustments to each:

$$\tilde{H}'_{a_{2k}} = A_{2k} + \epsilon_{2k}, \quad \tilde{H}'_{a_{2k+1}} = A_{2k+1} + \epsilon_{2k+1}, \quad (5.22)$$

$$[A_{2k}, A_{2k+1}] = 0, \quad (5.23)$$

and the  $\epsilon$  terms are small and have the same support as the overlap of  $a'_{2k}$  and  $a'_{2k+1}$ . Now we introduce the notation

$$h_k = A_{2k} + A_{2k-1}, \quad H = \sum_k h_k + \sum_i (\epsilon_i + \delta_i), \quad [h_k, h_{k+1}] = 0. \quad (5.24)$$

We have reduced any local Hamiltonian on a chain to a nonlocal one with exponentially decaying long-range interaction, written in the form of commuting terms plus a small perturbation. We note that to repeat this in 2d one would need a version of Hastings' result for three matrices, and that one has a counterexample presented in his paper.

For chains, one may think of applying Imbrie's construction to this form of the Hamiltonian - after step 1, Imbrie's Hamiltonian has exactly this form with long range but rapidly decaying interactions! Unfortunately, the bounds for a general 1d Hamiltonian do not work out in our favor: the number of levels in the block  $S > x(T) + \Delta x$  grows as  $2^{x(T)}$ , so the minimum level distances decrease as  $2^{-x(T)}$ . However, the norm bound on  $\epsilon$  is related to Bound 5.19, which is just  $1/T$ . For

the standard Lieb-Robinson bound  $x(T) = vT$ , so the level distances are always smaller than the perturbation scale, which is the opposite to what is used in Imbrie's construction. However, in MBL with  $x(T) \sim \ln T$ , the scales may just work out. In this way, any Hamiltonian that possesses the MBL Lieb-Robinson bound can be reduced to a form "diagonal + small perturbation", even if the z-basis is not apparent from the start.

## Chapter 6

### CROSSINGS

We continue the study of Hamiltonian  $H(s)$  for  $L$  spins on a chain depending on adiabatic parameter  $s$  defined in the previous chapters. Here we focus on the region  $(1-s) < \gamma$ , where  $H(s)$  is close to the diagonal Hamiltonian in  $\sigma_z$ -basis. The strength of noncommuting local terms is quantified by a parameter  $\gamma \ll 1$ . Every eigenstate  $\psi_\sigma(s)$  corresponds to a word  $\sigma = \{\text{sign}(\langle \sigma_i^z \rangle), i = 1..L\}$  with some discontinuities where the sign changes. So for a given  $\sigma$  there are continuous fragments of  $\psi_\sigma(s)$  and jumps. We can visualize it as a plot of energies  $E_\sigma(s)$  against  $s$  for all  $\sigma$ . When a discontinuity happens, one generally finds an avoided crossing for small  $L$ . The property of MBL is that such crossings are still discernible even for large  $L$ , where there is a background of other levels. Here's how:

Note that  $(\sigma - \sigma')/2$  is an indicator of spins that differ for the two states that are exchanged at discontinuity. Define consecutive support  $S(\sigma, \sigma')$  to be the smallest connected region that contains  $S(\sigma, \sigma')$ . Add a collar neighborhood of same size at each end. Truncate the Hamiltonian to  $n = 3|S(\sigma, \sigma')|$  spins. In this Hamiltonian, the density of states is  $\sim 2^{-n}$  in the midband, and the size of the avoidance between levels is expected to be  $\gamma_{eff}^n$  for a small  $\gamma_{eff} \ll 1/2$  related to  $\gamma$  (we have briefly touched upon this in chapter 2, but here we postulate it as Conjecture 1 below). So there are no levels in the immediate vicinity of the crossing. Adding the full system of size  $L$  will add a constant energy shift, replicate the crossing many times in the spectrum, and distort it by amounts smaller than  $\gamma_{eff}^n$ . So even though many other smaller crossings may overlay on top of this one, we typically can still trace the original lines of the truncated system. We define the region  $[s_d - \Delta s, s_d + \Delta s]$ , where avoidance distorts otherwise almost straight lines of levels  $E_1(s), E_2(s)$  by an amount of order  $\delta E = \min_s |E_1 - E_2|$  (expected  $\leq \gamma_{eff}^n$ ), to be the place where avoided crossing "happens". Here  $\delta E$  is the size of the avoidance of this particular crossing,  $\Delta s = \delta E / (\partial(E - E')/\partial s)$ , and the derivative is taken as if the crossing did not happen (the slope is found by using smart overlap labels from the previous chapter, or the spin projection label defined just now).

This logic can be used as a definition of what we call an "avoided crossing" in a many-body system:

**Definition 1** Level  $|1\rangle$  experiences a crossing with  $|2\rangle$  if  $|E_1 - E_2| < 2\delta E$  where  $\delta E = \min_s |E_1 - E_2|$ , and the corresponding z-strings,  $\text{sign}(\langle 1|\sigma_z|1\rangle)$  and  $\text{sign}(\langle 2|\sigma_z|2\rangle)$ , switch places on different sides of  $|E_1 - E_2| = \delta E$ . If the positions that are flipped between  $|1\rangle$  and  $|2\rangle$  are joined in real space into the smallest interval of the chain that contains them all, that interval is called a resonance. The interval size is  $n_r$ .

To make this rigorous, a clause is implied about truncating the Hamiltonian so that there are no levels in the immediate vicinity (as explained above), and  $E_1, E_2$  are consecutive in energy.

An important thing to note is that when two lines cross, there will always be a resonance in the Imbrie circuit at some moment. Indeed, if the avoidance was bigger than the separation scale, the Imbrie circuit would have treated this place perturbatively, thus the energies of two states corresponding to these two product states will vary continuously with  $\gamma$ . The argument for it goes as follows: the Imbrie's construction in a region without resonances is a finite product where every term is a continuous function of  $s$ , times an infinite product that may be discontinuous but with its contribution to this region strongly bounded. But the continuity is strongly violated during the crossing - instead expectations of  $\sigma_z$  switch from  $\approx +1$  to  $\approx -1$ . This discontinuity has to come from the nonperturbative rotation in the circuit. This is the central idea of this paper. We formulate it as:

**Proposition 1** The range of  $\gamma$ 's where the two levels  $E_j(\gamma), E_{j+1}(\gamma)$  experience a crossing as per definition 1 is contained in the interval of  $\gamma$  when the Imbrie circuit resonance is present in the system. The spatial position of this resonance covers all the spin flips necessary to go from one of the levels to the other.

Every  $k$ -step Imbrie circuit resonance corresponds to  $O(2^{L-L_k})$  crossings in this way. In the new notation, every resonance of size  $n_r$  corresponds to  $O(2^{L-n_r})$  similar crossings, just translated in energy.

Our definition of crossings relied on the truncation. So a rigorous proof of Proposition 1 would rely on a statement like this:

*(Resonance separation condition)* For a resonance of size  $x$ , changing spins outside  $mx$  for some number  $m$  doesn't affect the resonant conditions.

Unfortunately, Imbrie proves separation only for "postprocessed" resonances. The resonances found in the brute force way above may not have any separation condition. Big resonances can appear as sequence of small ones, and the energy separations will always remain big, which can potentially confuse our method. If one carefully

draws a situation where two resonances happen in the neighboring spins, one will see that the levels of distance  $n_r = 2$  do not have to have a  $\gamma^2$  matrix element anymore, only  $\sim \gamma$ .

Consideration of such events would make the proof slightly more convoluted if one were to do it in full rigor. There may also be minor disagreements with (Imbrie, 2016) about how far around the crossing in energy should the levels be called resonant, and the size of the collar around flipped spins to include in  $n_r$ .

Now that we know the correspondence between Imbrie's work and our definition of crossings, we present the following application of it to the region of  $s \approx 1$ :

**Conjecture 1** a bound  $\delta E < (1 - s)^{an_r} = \gamma_{eff}^{n_r}$  holds for some constant  $a$ , for crossings satisfying definition 1 as long as there are no crossings of one of the same levels in the immediate vicinity in  $s$  for a given system size. If there are, but the corresponding spin flips can be identified to be far away from each other (e.g. by considering isolated portions of the system), the bound is still expected to hold. The bound could be violated if there are many small resonances appearing next to each other in space, and the level experiences an independent crossing in each of those regions.

This conjecture can be used as a definition of  $\gamma_{eff}$ . Our bound is not a strict upper bound for all splittings that we find. If the algorithm that identifies crossings discards the congested areas where many levels are close in energy and in spin flips, the bound should hold, except for rare cases where the algorithm fails to discard problematic combination of levels (with probability  $p_f < 1/2$ ). Note that even small  $p_f$  expectation value significantly: a naive upper bound on the splitting of failed case is  $\gamma$ , so the expectation value will be:

$$\overline{\delta E(n_r)} = (1 - p_f)\gamma^{n_r} + p_f\gamma \quad (6.1)$$

which can be dominated by the second term if  $\gamma \ll 1$ . Here we averaging over all observed crossings corresponding to a flip of  $n_r$  consecutive spins. The median of the distribution will not have this problem for  $p_f < 1/2$ . For a median, the bound holds in the infinite system size limit if one uses truncation of Hamiltonian to small blocks to identify crossings as per Definition 1.

One may ask how many of the resonances of a given size will our algorithm discard due to congestion? In the independent approximation, it is an easy estimate - the sites to the left and to the right of this resonance are occupied by other resonances

with  $O(\epsilon)$  probability, or  $O(c\epsilon)$  for a collar size  $c$ . So we discard  $O(\epsilon)$  if we discard the resonances that are nearest neighbors. As in the model above, we also add  $p_f$  for when the algorithm fails. Either of those small corrections should not affect the validity of our data for the purpose of measuring resonance densities (see below).

If we don't discard anything, the  $\min\delta E$  between levels can look very different from a positive random variable with mean around  $\gamma^n$  which was predicted above. For a simple estimate, let's assume that resonances are independent from each other, and each size is randomly scattered through the system with  $P^k = (C\epsilon)^{cL_k}$  for  $L_{k-1} < n_r < L_k$ . This gives

$$\frac{\gamma}{2^{n_r}} \leq \overline{\min\delta E} \leq \frac{\gamma}{n_r} \quad (6.2)$$

if a presence of a single one spin resonance in the cluster guarantees the splitting to be no less than  $\gamma$ . Of course, it is a very conservative estimate, and in a real system a single one spin resonance will not disturb as much.

Now let's ask ourselves a question how big a part of the system will we find to be involved in flips between two crossing levels such that the consecutive distance is  $n_r$ . By Proposition 1 we know that all of these regions are contained in Imbrie's resonances. But our resonances are much smaller than Imbrie's as he uses a definition of resonances that count splitting  $\epsilon = \gamma^{1/20}$  as one-spin resonant, and uses  $\epsilon^{n_r}$  as threshold for many-spin resonances. For his definition, the whole system is resonant for, e.g.  $\gamma = 0.1$ . We hope that the spirit of the bounds still applies:

### Conjecture 2

$$P(n_r) = O(\exp(-n_r)) \quad (6.3)$$

**Definition 2**  $\Delta s_r(n_r)$ : Consider an interval  $\Delta s$ . The crossings experienced by a single level in that interval have various sizes. The number of crossings of a given size  $n_r$  is on average  $\Delta s / \Delta s_r(n_r)$

$\Delta s_r$  is not specific to MBL, it is easy to estimate from density of states, slopes and neighbors. Slopes have been considered in Chapter 5. By neighbors we mean distribution in consecutive spin flip distance  $n_r$  of this particular level's neighbors in energy. If we assume a completely random neighbor (as is the case for diagonal Hamiltonian with i.i.d. random variables on diagonal), each spin can flip with probability 1/2, and distribution of neighbors is given by:

$$P^{(N)}(n_r) \sim (L - n_r + 1)2^{n_r - L} \quad (6.4)$$

the normalization is  $O(1)$ . The random diagonal model produces monotonic probabilities in  $n_r$ . Another model to consider is independent spins in random z-fields.

$$H = \sum_i h_i n_i, \quad n_i = 0, 1 \quad h_i \in [-1, 1] \quad (6.5)$$

We are interested in the neighbors of  $n_i = 0$  state. It is hard to estimate the nearest neighbor in energy, but easy to reduce it to the previous problem (random diagonal) if we instead ask for distribution of neighbors in a window  $\epsilon$  around one energy. Let  $d(\vec{n})$  be consecutive distance of a specific flip pattern. The probabilities  $P^{(N)}(n_r)$  are exactly expectation values of  $\sum_n \delta(d(\vec{n}) - n_r) \Theta(\epsilon - |\sum_i h_i n_i|)$  where the second term is an indicator of our neighbor. The sum and the expectation value can swap places:

$$P^{(N)}(n_r) = \text{e.v.} \sum_n \delta(d(\vec{n}) - n_r) \Theta(\epsilon - |\sum_i h_i n_i|) = \sum_n \delta(d(\vec{n}) - n_r) \text{e.v.} \Theta(\epsilon - |\sum_i h_i n_i|) \quad (6.6)$$

Surprisingly, the second term is essentially independent of  $\vec{n}$ . Consider  $m = \sum_i n_i$  random fields as an  $m$ -dimensional cube centered at 0. The total probability of their sum being within  $\epsilon$  is  $\sim \epsilon$  for any  $m$ . So the probability reduces to

$$P^{(N)}(n_r) \sim \epsilon \sum_n \delta(d(\vec{n}) - n_r) \sim \epsilon(L - n_r + 1)2^{n_r - L} \quad (6.7)$$

which is exactly the random diagonal model. Another quantity we need are relative slopes  $R(s)$  defined in Chapter 5:

$$\partial E / \partial s = f(\gamma) L \sqrt{s^2 + (1 - s)^2} \quad (6.8)$$

where  $f(\gamma) \sim \gamma$  in MBL and a constant (0.25 from Fig. 5.3 in extended phase. We have added a factor  $L \sqrt{s^2 + (1 - s)^2}$  as in this Chapter we're using an unnormalized Hamiltonian. Finally, the density of states is:

$$\rho = 2^L / L \quad (6.9)$$

so the average distance between levels is  $\rho^{-1} = L2^{-L}$ . That distance is traveled in  $\Delta s_{r,any} = \rho^{-1} / (\partial E / \partial s) \approx f(\gamma) 2^{-L} \sqrt{s^2 + (1 - s)^2}$ . Now for each size  $n_r$ , we need to cross  $1/P^N(n_r)$  levels to run into it. Thus

$$\frac{1}{\Delta s_r^1(n_r)} = \rho \frac{\partial E}{\partial s} P^N(n_r) \approx f(\gamma) \frac{(L - n_r + 1)2^{n_r}}{Z^N} \sqrt{s^2 + (1 - s)^2} \quad (6.10)$$

Here  $Z^N = \sum_{n_r} (L - n_r + 1)2^{n_r - L}$  is a factor needed so that probability of neighbors is normalized to 1. The answer for the case where the single level we track is the

ground state will be different as the density of states is different. For all the levels put together, we get the total number of states as an additional factor of  $2^L$ :

$$\frac{1}{\Delta s_r(n_r)} = 2^L \rho \frac{\partial E}{\partial s} P^N(n_r) \approx f(\gamma) \frac{(L - n_r + 1) 2^{n_r + L}}{Z^N} \sqrt{s^2 + (1 - s)^2} \quad (6.11)$$

### What can we say about 2d systems?

All of these results apply to a random chain. Now let's consider random 2d lattice, such that the disorder is not enough to localize the system. Specifically, let's first assume that level repulsion is present at least among some levels. Then, the bound  $\delta E < (1 - s)^{an_r}$  does not hold for those, in fact one finds large ( $O(\rho^{-1})$ ) avoidances for big  $n_r$ . Here  $\rho$  is the density of states. The difference is in the base of the exponential:  $1/\rho(n_r) \sim 2^{n_r}$  for any  $s$ , while in MBL we had  $(1 - s)^{an_r} = \gamma_{eff}^{n_r}$ . The median of avoidances of isolated crossings (when we discard the crowded regions) will show a crossover between two exponential behaviors in MBL and in extended phase.

Let's explain what I mean by "level repulsion for some levels". It is likely that random 2d lattice has Poissonian level statistics. Indeed, consider a linear sum of two independent systems with level repulsion. The resulting levels, if they overlay, will be half-way to Poissonian statistics. For random 2d lattice, there are many metastable equilibria separated by large energy barriers, so the statistics is almost poissonian. But it is not unreasonable to expect that on top of each metastable equilibrium there exists extended excitations, like in non-disordered Ising model. So it is not unreasonable to expect that 2d random Ising conducts heat at any temperatures and at arbitrary small transverse fields  $(1 - s)$ , even  $\sim O(1/L^p)$ . If that is the case, one should still be able to identify big avoidances between levels on top of the same metastable state, but maybe not as big as in the previous example. We do not know of any estimate.

### A geometrical bound on resonance density

There is a way to estimate an exponent in  $P(n) = O(\exp(-n))$  for our definition of crossings and resonances (without  $\epsilon$ ), as can be seen from purely geometrical considerations and a bound on  $\delta E$ . The argument is not rigorous though, it makes use of some extra assumption and estimates. Consider a system of size  $L$  and a crossing of maximal size  $n = L$  in it. The argument goes as follows. We note that the size of the crossing in  $s$   $\Delta s_{cr} = \delta E / (\partial(E - E') / \partial s)$  can be at most  $\gamma_{eff}^n v_{min}^{-1}$  for crossing of size  $n$  if we throw away the special cases of small relative slopes

$(\partial(E - E')/\partial s) < v_{min}$ . There is no special reason for levels to go parallel to each other in  $s$  - we expect a smooth distribution of  $v = (\partial(E - E')/\partial s)$  for all the crossings of size  $n$ . We choose a cutoff  $v_{min}$  and observe that it can be taken very small, such that the contribution of  $v < v_{min}$  to  $P(n)$  will be bounded as event of probability  $v_{min}/v_{max}$ . Now we note that there are at most  $\rho v_{max} \Delta s$  crossings that one level experiences, where  $\rho \leq 2^n/n$  is the density of states at this level's energy. The total number of crossings of all levels is  $2^n \rho v_{max} \Delta s$  then. So the typical distance between crossings is  $\Delta s_0 \geq v_{max}^{-1} 4^{-n} n$ .  $\Delta s_0$  is related to  $\Delta s_r(n = L)$  for individual level by a factor  $2^n$  - the total number of levels. On the other hand, the interval within which crossing will be counted towards  $P(n)$  is bounded as  $\Delta s_{cr} \leq \gamma_{eff}^n v_{min}^{-1}$  - that is the width in  $s$  of region where each crossing. So a bound on  $P_1(n)$  is then

$$P_1(n) \leq \frac{\Delta s_{cr}}{\Delta s_0} + v_{min}/v_{max} \leq \frac{\gamma_{eff}^n (v_{min})^{-1}}{v_{max}^{-1} 4^{-n} n} + v_{min}/v_{max} \quad (6.12)$$

which can be optimized to  $\sim \gamma_{eff}^{n/2}$ .

Here we used typical distance between all crossings  $\Delta s_0 \geq v_{max}^{-1} 4^{-n} n$  as a proxy for  $2^{-n} \Delta s_r(n = L)$  - typical distance between crossings of consecutive size  $n$  in a system of size  $L = n$ . Indeed, the typical crossings are the ones that span the whole system - we encounter them the most. Our formula works for all  $n$  which can be shown by virtue of truncation. Our bound is much stronger than what Imbrie used, which may be attributed to a weaker definition of resonance that makes every  $\Delta s_{cr}$  wider by a factor  $(\gamma_{eff}/\epsilon)^n$ .

## 6.1 Identification of crossings

The method of crossing detection is based on overlaps between consecutive states in energy  $|E_n(s)\rangle, |E_{n+1}(s)\rangle$  and the same two levels after a step  $\delta s$ :  $|E_n(s + \delta s)\rangle, |E_{n+1}(s + \delta s)\rangle$ . If the overlaps swap places, we call this a crossing. This method has its quirks that has been discussed at length in Chapter 5. One can easily see that such method will be sensitive to crossing that are faster than  $\delta s$ , but leave slow crossings undetected. One can improve the performance on slow crossings a bit by considering multiple  $\delta s$  and combining the data, but many of the big crossings in a big system are also obscured by a lot of small crossings happening "on top of them".

We use a simpler algorithm with a fixed  $\delta s = 1/40$  for the whole range  $H(s = 0) = H_x$  to  $H(s = 1) = H_z$ , where  $s$  is the adiabatic parameter from the original protocol, and the system is not MBL for some portions of the path.

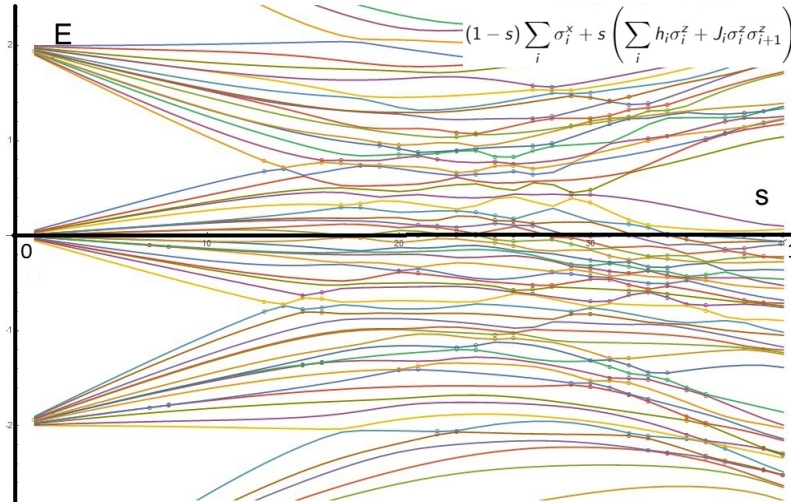


Figure 6.1: One can identify resonances as places where the state is flipped to approximately orthogonal

We can see by eye in Fig. 6.1 that for large gaps the numerical method used here stops being sensitive. One can think about it as follows:

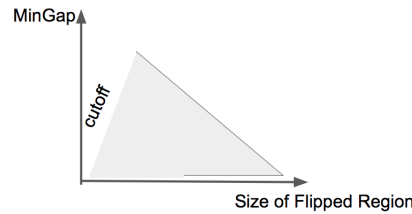


Figure 6.2: In the midband large gaps are obscured by multi-crossing.

We are content with the partial data. Consider crossing locations plotted uniformly with the eigenstate index:

We look only at isolated squares of 4-levels and discard the multi-crossing from the ensemble. On the coarse scale  $\delta s$  that we use, slopes allow levels to cross many of their neighbors, so we get a significant portion of multicrossing, which should be a true feature of extended phase, but an artifact of our approach in MBL. By zooming in, we should be able to resolve each and recover the bound  $O(\epsilon)$  derived in the previous section. One redeeming feature of keeping  $\delta s$  fixed is that each crossing of small size in space should be repeated several times throughout the spectrum in the MBL phase, as the the state of the faraway parts of the system change. So even if it is a part of multicrossing in one part of the spectrum, it might be isolated in another.

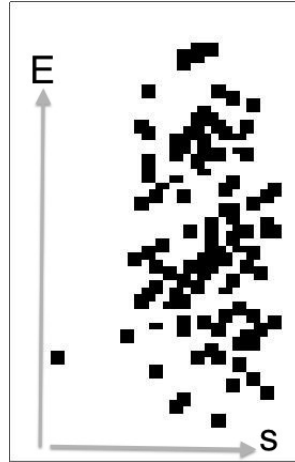


Figure 6.3: Resonances vs. level number

One quantity that can be extracted immediately is the “frequency” of resonances, or  $1/\Delta s_r(n_r)$  defined in Eqn. 6.11 - the rate of resonances encountered by a system as  $s$  changes without regard to their width in  $s$ . Recall that this quantity does not follow directly from Imbrie’s construction, instead we needed to make assumptions about neighbors in energy (that they are essentially random) The value of this quantity for chains will be important for predictions of a behavior under a slow drive. Its direct measurement from the data above is shown in Fig. 6.4. We use the consecutive distance between the two levels to determine the size of the resonance. We show that if multicrossings are included,  $1/\Delta s_r(n_r)$  is well predicted with no fitting parameters by Eqn. 6.11 that uses Relative Slopes  $f(\gamma)$  found in Chapter 5. The majority of crossings found by our algorithm are multi-crossings in energy, but the isolated ones are representative of the total distribution. As expected, the algorithm misses some crossings of small sizes as they happen over intervals longer than  $\Delta s = 1/40$ . One can also perform a direct measurement of the distribution of neighbors, which shows good agreement with our theoretical estimate in Eqn. 6.7.

## 6.2 Resonance densities

Finally we are ready to collect resonance statistics (the avoidance vs. the spin flip consecutive distance). We investigate  $L = 6$  and find avoided crossings with the splitting as small as  $\gamma^6$ , which is  $10^{-6}$  for magnetic field 0.1.

We pick a scale  $\Delta s$  first, and identify avoided crossings by overlap switches as explained before.

Then for every avoided crossing, we pick a finer scale  $\Delta s_1 = \Delta s/250$ , and measure

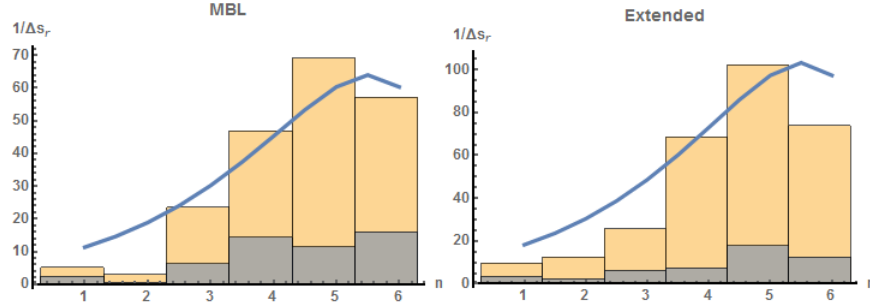


Figure 6.4: The histogram of frequencies  $1/\Delta s_r(n_r)$  collected in the last  $[7/8, 1]$  of  $s$  (left) and in the middle  $[4/8, 5/8]$  of  $s$ . Blue line is a theoretical prediction. The system size  $L = 6$ , we average over 15 disorder realizations

the minimal gap between two levels  $\Delta_{min}$  and the maximal one  $\Delta_{max}$  within each interval  $\Delta s$ . We also extract the consecutive spin flip distance  $d$ . This is a resonance when the level distance is within  $O(1)$  of  $\Delta_{min}$ , according to our definition. So of the interval  $\Delta s$ , only for about  $\frac{\Delta_{min}}{\Delta_{max}} \Delta s$  the system has resonance at that position. It contributes

$$\frac{\Delta_{min}}{\Delta_{max}} d \frac{2}{2^{L-d}(L-d)} \quad (6.13)$$

to the resonance density. The extra two factors are to account for duplicates of this resonance that should be also found in the spectrum, and for many possible positions it can occupy in the system

We then add that up for all the resonances and average over realizations. The result should be understood as average resonance density, and unsurprisingly it exceeds 1 in the extended phase:

We proceed to extract the data about minimal splittings. We described above how to mark different places in  $(s, E)$  with  $(\delta E, n_r)$  whenever there is a crossing. Then one collects all the pairs  $(\delta E, n_r)$  for a given  $s$  (putting together different energies). Then one puts the data together for  $N$  realizations of disorder.

We take a median of  $\delta E$  for all realizations of disorder for an interval of  $s$ . That is the quantity that should be bounded by our conjecture. One can check the bound  $\delta E < \gamma_{eff}^{nr}$  by looking at those plots. Note that one needs a very small finer scale  $\Delta s_1$  such that  $\Delta s_1 \frac{\partial E}{\partial s} = 10^{-6}$ . We don't quite get there with  $\Delta s_1 = \Delta s/250 = 10^{-4}$ . If we keep making it smaller, the medians for  $s = 1/8$  will lie on the straight line.

We also note that in extended phase the consecutive distance does not mean anything, so the splitting is essentially flat as a function of it

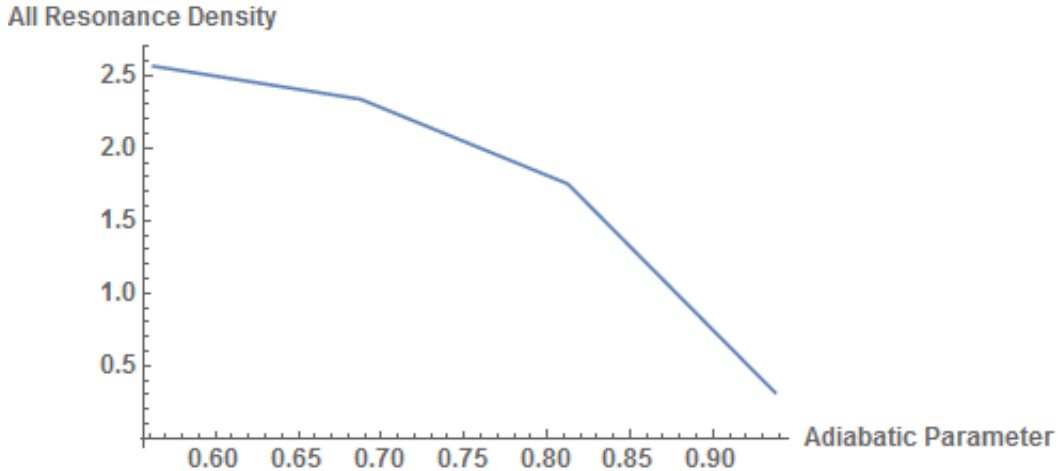


Figure 6.5: Total density of resonances plotted along the protocol

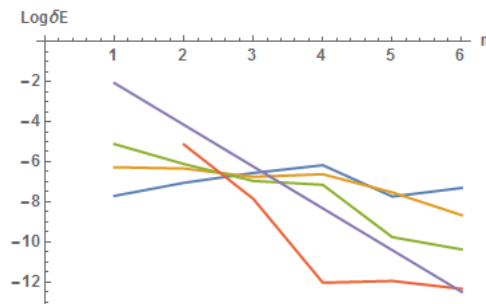


Figure 6.6: Median of  $\delta E$  with resonance size for length-1/8 intervals of  $s$  along the protocol, from  $[4/8, 5/8]$  in blue to  $[7/8, 1]$  in red. The theoretical fit (purple) with  $\gamma_{eff} = 1/8$  is plotted to guide the eye

A good proxy that would tell us which gaps are small enough for MBL and which are typical for extended phase is  $2^{-L}$  - indeed that is of the same order of magnitude as the median found for extended phase in Fig. 6.6.

But there's extra information in those plots — the resonance probability as a function of  $d$  which is calculated as an average of  $\frac{\Delta_{min}}{\Delta_{max}} d \frac{2}{2^{L-d}(L-d)}$  over all observed instances of size  $d$ .

Recall that Imbrie proves weak bound on it using  $\epsilon = \gamma^{1/20}$ . If we try to do that in our code, we will find everything overlapping. So the density of resonances for reasonable values of magnetic fields is 1 if we use Imbrie's definition. We can still follow "the spirit" of his bound and use our own bound  $\gamma_{eff}^{n/2}$ . That will be contrasted with the extended system where the resonances we find are dominated by sizes  $O(L)$  (because typical two states are away by  $L/2$  spin flips and  $\sim L$  consecutive flips)

So if we observe a peak at  $L$  in the resonance probability data, that's a sign we're extended.

We can extract the plots that look consistent with  $\gamma_{eff}^{n/2}$  for MBL, and growing for extended, if we throw away the multi-crossing in energy (we also drop the factor  $2^{L-d}$  from the formula as most of the duplicates are also involved in multicrossings): Unfortunately, there's a form of a cutoff in our data collection method at small

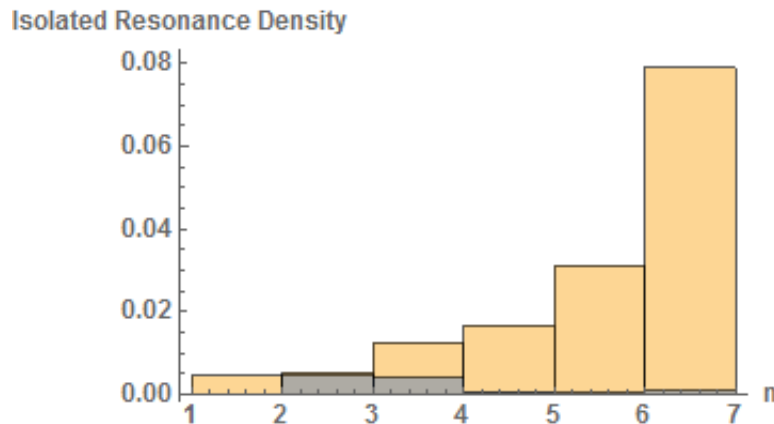


Figure 6.7: Resonance density with size. Extended in gold, MBL in blue. We see that large ( $\sim L$ ) resonances are always present in the extended system

resonance sizes, so  $\gamma_{eff}^{n/2}$  is not very apparent. Cutoff stems from insensitivity to crossings with big avoidances. In numerics, one can directly see from the Fig. 6.1 that some crossings are missed, because they happen on a scale bigger than the discretization step, so the algorithm considers them to be just levels that are changing continuously. A better algorithm would catch all of those. But then there's another reason for cutoff - resonance overlap. It is not clear how to write an algorithm that works for big systems and treats this case correctly.

## Chapter 7

### SLOW DRIVE

The MBL is expected to hold for a sufficiently small  $\gamma$ . Also it is expected to be stable with respect to other sufficiently small static perturbations.

Let us consider the MBL Hamiltonian changing in time from a perturbation parameter  $\gamma$  to  $a\gamma$ . Here  $a = O(1)$ ,  $a \neq 0$ . Here for simplicity the system will start in an eigenstate, but one can straightforwardly translate our result to easy-to-prepare states (Gibbs state, or product state). Our goal is to say something predictive about the state at the end of the evolution. This is the simplest case to analyze, yet other paths within the MBL regime are possible (e.g. from one realization of disorder to another). We will draw the intuition from changing  $\gamma$ , other paths can be considered in a similar way. One may think of changing  $\gamma$  as a possible parameter drift in an actual physical system exhibiting MBL. Even when restricted to changing only  $\gamma$ , one can engineer many other types of paths that are physically relevant: creation of a state (from  $\gamma = 0$  to some nonzero value, relevant for proofs in the spirit of quasi-adiabatic evolution by Matthew B. Hastings and Michalakis, 2015), and the slow random motion of  $\gamma$  around some average (parameter drift in actual systems is a random walk). The method we will use only works for small drive rates and breaks down at the drive rate  $\frac{T}{\Delta\gamma} \approx 1$  That sets the distinction between fast and slow.

Our theoretical prediction for the dynamics is as follows:

**Proposition** At  $T/\Delta\gamma = v^{-1} \gg 1$  the result of the evolution will remain close to an eigenstate almost everywhere and we can neglect the diabatic errors. Spin flips of resonances will be observed starting from  $v^{-1} \geq \gamma^2$ . In the range of velocities:

$$\frac{T}{\Delta\gamma} = v^{-1} < (v^*)^{-1} = \frac{a+1}{4\pi} \left( \frac{1}{\sqrt{|a-1|\gamma}} \right)^{5.8\ln(1/\gamma_{eff})+2} \quad (7.1)$$

the total density of flipped regions is  $< 1$ . The configuration of flips changes with the drive speed in discrete steps of the shape of the original system's resonances. New and typically bigger resonances are added to the flipped region as the  $v$  decreases. After it decreases past the value in Eq. 7.1, system is no longer in approximately a product state. One can no longer identify local flips by varying  $v$ , as large portions of the system appear to flip simultaneously.

Let's elaborate on what the theorem means. Consider the energy scale  $E_v = \gamma\sqrt{|a-1|}/2\pi$  set by our drive speed. The relationship between  $E_v$  and the splitting energy  $\delta E_n$  of the individual resonances determines whether they are flipped along the drive. In the special case when  $E_v \approx \delta E_n$ , we can selectively create an entanglement between the two resonant states. This entanglement will be visible in the  $z$ -basis measurement as the expectation value is now given by a superposition of the corresponding product states. When resonances start to overlap, flip of one of them can influence the other (because one state has the corresponding crossing and the other one doesn't), so even a rare resonance such that  $E_v \approx \delta E_n$  makes the whole system a superposition of two possible paths. Thus long range entanglement is introduced for  $v < v^*$

Other contributions to the evolution are adiabatic and diabatic losses. The latter is bounded by a value small in  $\gamma$ . We use the term "adiabatic losses" implying an honest application of Landau-Zener formula. The competitor probabilities found in it are bounded in the distance between  $E_v$  and  $\delta E_n$  for all the resonances along the path.

*Proof* The average relative slope of the levels is found in Chapter 5:

$$\frac{dE}{dt} = \frac{dE}{d\gamma} \frac{d\gamma}{dt} \approx \gamma(t)L \frac{\gamma|a-1|}{T} \quad (7.2)$$

We will use the average slope for simplicity for all level intersections, the argument can be repeated with only minor modifications for a random distribution of slopes around the average. The contribution of a crossing of a consecutive size  $n$  at position  $\gamma(t_x) = a_x\gamma$ ,  $a_x = O(1)$  is given by a Landau-Zener formula:

$$\delta P = 1 - \exp\left(-2\pi \frac{\delta E_x^2}{na_x\gamma^2|a-1|}T\right) = 1 - \exp\left(-\frac{\delta E_x^2}{na_xE_v^2}\right) \quad (7.3)$$

where  $\delta E_x$  is the splitting and  $E_v = \gamma\sqrt{|a-1|}/2\pi$ . Only the slopes of the section of the system where the resonance is matter. To find the losses along the evolution, we need to sum the above contributions for each level for those that are passed fast, and  $1 - \delta P = \exp\left(-\frac{\delta E_x^2}{na_xE_v^2}\right)$  for slow passage. We sum corrections over all crossings. We can neglect the corrections from slow passage as they are exponentially small. The big contribution comes only from unlucky levels with the splitting at the crossing close to  $\sqrt{na_x}E_v$  (or more carefully, the right fraction of the splitting and the slope of that level matches that value). If for some of the resonances the exponent is close to 1, we consider them to be mixing corresponding spins, but not affecting the other regions.

To estimate the number of regions with such mixing, we again need the relative slopes and the density of states:

$$\rho \sim \frac{2^L}{L} \quad (7.4)$$

the total number of crossings over an interval  $\Delta\gamma = |a - 1|\gamma$  is then

$$N = \rho \frac{dE}{d\gamma} \Delta\gamma = \frac{2^L}{L} \gamma L \gamma |a - 1| = 2^L \gamma^2 |a - 1| \quad (7.5)$$

We see that it grows with the system size. But we only care about  $\delta E_x \approx E_v$ , where  $\delta E_x \approx \gamma_{eff}^n$ . So the sizes of the crossings we care about are limited roughly to  $n < \ln E_v / (\ln \gamma_{eff})$ . If we keep all the factors,  $\delta E_x = \sqrt{n a_x} E_v = \sqrt{n a_x} \gamma \sqrt{v} |a - 1| / 2\pi$ . We will replace  $a_x$  by its average  $\bar{a} = (a + 1)/2$ . Now denote

$$n^* = \frac{\ln \sqrt{n^* \bar{a}} E_v}{\ln \gamma_{eff}} = \frac{\ln \gamma}{\ln \gamma_{eff}} + \frac{1}{2 \ln \gamma_{eff}} \left( \ln \frac{|a - 1|}{T} + \ln n^* + \ln \frac{\bar{a}}{2\pi} \right) \quad (7.6)$$

The first term is  $O(1)$ ; the second depends on the relationship between  $|a - 1|/T$  and  $\gamma_{eff}$ . The last two terms in the brackets are subleading. We find  $n^* = 4$  for  $\gamma = 0.1$  and  $T = 10^5$ .

The number of crossings of size  $n$  per site is given by the same expression as the total number of them for a system size  $n$ :

$$N_n = 2^n \gamma^2 |a - 1| \quad (7.7)$$

Now we note that there are 2 times as many crossings of size  $n + 1$  as those of size  $n$ . So the typical one that's not jumped is of size  $n^*$ . The total density of crossings that experience flips is then:

$$p_f = \sum_{n \leq n^*} n N_n = n^* 2^{n^*+1} \gamma^2 |a - 1| \quad (7.8)$$

if  $2^{n^*+1} \gamma^2 |a - 1| < 1$ , we resolve individual resonances with this procedure. For our  $n^* = 4$  and  $\gamma = 0.1$ , and  $|a - 1| = 1$ , we get  $2^{n^*+1} \gamma^2 |a - 1| = 1.3$  so the flips start to overlap. Every spin will be found in some entangled state away from its original  $z$  configuration. More generally, this relation gives us the idea that to witness bigger resonances, besides exponentially long drive times, we need to narrow down our range in  $\gamma$  and  $a$ .

A few remarks about this result:

1. We can plug in the value of  $n^*$  to obtain the expression in Eq. 7.1.  $\gamma_{eff}^{n^*} = \sqrt{n^* a} E_v$  which gives  $2^{n^*} = \gamma_{eff}^{(\ln 2)n^* / \ln \gamma_{eff}}$  in:

$$p_f = n^* \gamma^2 |a - 1| \left( \sqrt{n^* a} E_v \right)^{\ln 2 / \ln(\gamma_{eff})} \quad (7.9)$$

$p_f < 1$  if  $\sqrt{n^* a} E_v < (n^* \gamma^2 |a - 1|)^{\ln(\gamma_{eff}) / \ln 2}$  which we express via the drive speed:

$$\gamma \sqrt{v |a - 1|} / 2\pi < \frac{1}{\sqrt{n^* a}} (n^* \gamma^2 |a - 1|)^{\ln(\gamma_{eff}) / \ln 2} \quad (7.10)$$

or in terms of the protocol time:

$$\frac{T}{\Delta\gamma} = v^{-1} > \frac{a + 1}{4\pi} (1/\gamma)^{5.8 \ln(1/\gamma_{eff}) + 2} (n^* |a - 1|)^{2.9 \ln(\gamma_{eff}) - 2} \quad (7.11)$$

the last multiplicative term can be dropped as it is  $\sim \ln 1/\gamma_{eff}$ .

2. A careful error estimates counts the contribution from terms like  $\delta P = 1 - \exp\left(-\frac{\delta E_x^2}{n a_x E_v^2}\right)$  for jump crossings  $n > n^*$  as they give bigger, non-exponentially small error.  $\delta P \approx \frac{\delta E_x^2}{n a_x E_v^2}$  that is suppressed for sizes  $n^* + 1$  by a factor of  $\gamma_{eff}^2$  compared to  $n$ . Consider contributions of resonances of size  $n^*$ . Even if all of them happen to have  $\delta E_x$  that are fine-tuned to our speed of the drive, the effect will still be contained to the regions of flips that occupy  $< p_f$  of the system. If we ask for an average local deviation from the product state  $1 - P_{max,z}^{loc}$  it is bounded by  $p_f$ . There are also contributions that are a factor of  $\gamma_{eff}^2$  smaller from the resonances at the step  $n^* + 1$ . Even though their density is two times bigger, they don't affect the leading order of the error.  $p_f$  is proportional to  $\gamma^{|\ln \gamma_{eff}|}$ . Assuming that is small, we find  $1 - P_{max,z}$  in a system of size  $L$ . We need to add the probabilities of different locations in the system:

$$1 - P_{max,z} \leq L p_f, \quad L > n^* \quad (7.12)$$

For a patch of a bigger system, we get:

$$1 - P_{max,z} \leq (L + n^* - 1) p_f \quad (7.13)$$

For our parameters and  $L = 1$  this gives 2.5 so the bound is useless, but for smaller  $\gamma$  or shorter  $T$  it can be the other way.

We note that for small system sizes it's the same as the expression for  $p_f$ , besides a subleading  $L, n^*$ -dependent factor. So the same condition on velocity can be derived from it. Whenever the crossings are well-resolved, on average the system is still in the product state.

3. All along we used resonance size  $n$  as a proxy for splitting  $\delta E_x$ . But in fact those splittings are random variables taking values around the mean we've used. As well as the randomness in slopes, that can be accounted for and does not change the results.
4. Landau-Zener formula we have used is only exact for just two levels measured infinitely far away after the crossing. if the LZ protocol is stopped  $E_{end}$  away from the crossing point with the splitting  $\delta E$ , the LZ result gets adjusted. As in the remaining portion the time-dependent p.t. is applicable, we expect deviations from LZ result to be small in  $\delta E/E_{end}$ . In our case, the adjustment of amplitudes is  $O(\gamma/\epsilon)^n$  as according to Imbrie we can endow every crossing with a window of energies of  $\epsilon^n$  size. Indeed in our time-dependent p.t. analysis below we will confirm that scaling.

### 7.1 Finite velocity perturbation theory

To conclude the proof, we need to account for another loss of probability which is fully perturbative and is just due to the fact that we're not evolving infinitely slowly. It's present even if there are no distinctive avoided crossings in the levels. This effect is discussed in the literature as error bounds on the adiabatic theorem (Cheung, Høyer, and Wiebe, 2011; Jansen, Ruskai, and Seiler, 2007). Let's get familiar with these results. Consider the evolution of our Hamiltonian and assume that there is a gap  $> \Delta$  between all the eigenstates. Then the probability loss per unit length can be bounded naively (theorem 1 in Cheung, Høyer, and Wiebe, 2011) by

$$\frac{\delta P^{p.t.}}{L} \leq \frac{1}{\Delta^4 T^2} + O\left(\frac{1}{T^3}\right) \quad (7.14)$$

and using a more refined bound (theorem 2 in Cheung, Høyer, and Wiebe, 2011):

$$\frac{\delta P^{p.t.}}{L} \leq \frac{\gamma_{max}^2}{T^2 \Delta^2} + O(T^{-3} \gamma_{max}^p) \quad (7.15)$$

Here  $\gamma_{max} = \max(\gamma, a\gamma)$  and to derive this form we used a special time-dependent basis for the Hamiltonian (see below). Here  $p > 2$  is some constant power. In fact, the first term have even more detailed structure according to Wiebe

$$\delta P^{p.t.} \leq \frac{1}{T^2} \sum_{\alpha} \frac{|V_{0\alpha}|^2}{\Delta_{\alpha}^2} + O(T^{-3} L \gamma_{max}^p) \quad (7.16)$$

here  $V_{0\alpha}$  is a matrix element that decreases as  $(\gamma/\epsilon)^{\{\alpha\}}$  where  $\{\alpha\}$  is a consecutive support of difference between the state  $\alpha$  and the initial state. If all the states are

nonresonant,  $\Delta_\alpha > \epsilon^{\{\alpha\}}$ , so the sum converges as

$$\frac{1}{T^2} \sum_\alpha \frac{|V_{0\alpha}|^2}{\Delta_\alpha^2} \leq \frac{1}{T^2} L(\gamma_{eff} + \gamma_{eff}^2 + \dots)^2 \leq \frac{2}{T^2} L\gamma_{eff}^2 \quad (7.17)$$

here  $\gamma_{eff} = \gamma/\epsilon^2$  to indicate that renormalization can change this quantity. This sum can be thought as a partition function. Note that for big systems  $L\gamma_{eff}^2/T^2 \gg 1$ , so the typical state is one of the excited states, not the initial one. But our bound on adiabatic theorem applies to all states in the spectrum, as all of them have bounds on gaps when they are nonresonant. So each of states that have weight  $\gamma_{eff}^2/T^2$  will have its own errors accumulate, until the partition function takes the form:

$$\delta P \leq \frac{1}{T^2} L\gamma_{eff}^2 + (L\gamma_{eff}^2/T^2)^2 + \dots = (e^{L\gamma_{eff}^2/T^2} - 1) \quad (7.18)$$

This bound is saturated in  $O(L)$  time. It is roughly that of a chain of independent spins each with probability  $p = v^2\gamma_{eff}^2$  of flipping. A configuration with  $n$  (not consecutive) spins flipped will have a probability  $p^n(1-p)^{L-n}$ . We note that probability loss per unit length can be translated into density of deviations in density matrices (the error of density matrices over region  $R$  goes as  $2\gamma_{eff}^2 R/T^2$ ). Indeed,

$$\delta P^{p.t.} = \sum_\alpha \delta P_\alpha \quad (7.19)$$

If we only look at the  $\frac{1}{T^2} \sum_\alpha \frac{|V_{0\alpha}|^2}{\Delta_\alpha^2}$  term, we note that

$$\delta P_\alpha \leq (\gamma_{eff}/T)^{2|\alpha|} \quad (7.20)$$

Now we split the system into region  $R$  and its complement  $\bar{R}$ . Thus we change notation  $\alpha \rightarrow \alpha\bar{\alpha}$

$$\frac{1}{R} \|\rho_R - \text{tr}_{\bar{R}}|\phi_{s=1}\rangle\langle\phi_{s=1}|\|_1 = \frac{1}{R} \sum_{\alpha \neq 0} \sum_{\bar{\alpha}} \delta P_{\alpha\bar{\alpha}} \leq \frac{2\gamma_{eff}^2}{T^2} \quad (7.21)$$

Here we have used a nontraditional version of the trace norm that we removes all offdiagonal elements of the density matrix in a basis of interest.

Unfortunately, we cannot choose different gaps  $\Delta_\alpha$  for terms that Wiebe collects into the other contribution  $O(T^{-3}L\gamma_{max}^p)$ . Pessimistically, those terms get  $1/\Delta^{min} \sim 2^L$  and the norm gets a factor exponential in the system size. Still, those bounds are useful for small system sizes.

Note that the error does not depend on time as  $\sim T$  for  $T > O(L)$  - instead there are some cancellations and evolution that started at a state 0 will in  $O(L)$  time saturate the bounds above and remain within them for the rest of the time.

The proofs in Cheung, Høyer, and Wiebe, 2011 are quite sophisticated, instead we will present an *estimate* that gives the same answer. Besides coinciding with the above bounds on small system sizes, our estimate has the prospect of avoiding  $\sim 2^L$  terms in the same way as they are avoided in Imbrie's construction. So our intuition is that a proof of a bound consistent with our estimate is possible, although we do not attempt it here. First let's derive what is the operator  $V$  that we have used above.

**MBL, finite velocity evolution** We take advantage of our knowledge of MBL phase: at each point  $s$  along the path  $\gamma(s) = a\gamma s + \gamma(1 - s)$  we know the circuit that diagonalizes the system:

$$U(s) = \prod_k e^{A^{(k)}(s)} \quad (7.22)$$

Here we are interested in perturbative effects, so we'll assume there are no resonances. Then  $U(s)$  is a continuous function. Here  $\gamma_{max} = \max(\gamma, a\gamma)$  and we will omit the difference between  $\gamma$  and  $\gamma_{max}$  as  $a = O(1)$ . The time-dependent Schrodinger equation is:

$$i \frac{d}{dt} \psi(t) = H(s(t)) \psi(t) \quad (7.23)$$

Here  $s(t) = t/T$  for our purposes, and  $v = \Delta\gamma/T$  is the velocity. We'd like to recover adiabatic theorem in the  $v \rightarrow 0$  limit, and find the first perturbative correction to it. We would like to choose a time dependent basis of instantaneous eigenstates of  $H(s(t))$ :

$$U(s)H(s)U(s)^\dagger = E(s), \quad \psi(t) = U(t/T)^\dagger a(t) \quad (7.24)$$

we substitute it into the Schrodinger equation:

$$i(U(s) \frac{d}{dt} U(s)^\dagger) a(t) + i \frac{d}{dt} a(t) = E(s) a(t) \quad (7.25)$$

From this equation, we get a new time-dependent Hamiltonian:

$$H_x(s) = E(s) - (U(s) \frac{d}{dt} U(s)^\dagger) \quad (7.26)$$

We call the second term  $V$

$$V = -(U(s) \frac{d}{dt} U(s)^\dagger) \quad (7.27)$$

From the properties of  $U(s)$  for Imbrie spin chain,

$$V = \frac{1}{T} \sum_i^L \sum_k (U^{(k+)}(s) \frac{dA_i^{(k)}}{ds} U^{(k+)}(s)^\dagger) \quad (7.28)$$

$V$  is strictly offdiagonal. We get the following bound on  $V$ :

$$|V_{\alpha\beta}| \leq \frac{1}{T}(\gamma/\epsilon)^{|\alpha-\beta|} \quad (7.29)$$

where  $\{\alpha - \beta\}$  is the consecutive support of nonzero elements in the bitstring  $\alpha - \beta$ .

With this property, the convergence of Ineq. (7.17) follows:

$$\delta P^{p.t.} \leq 4 \sum_{\alpha} \frac{1}{T^2(E_{\alpha} - E_0)^2} |V_{\alpha 0}|^2 \quad (7.30)$$

We use  $|E_{\alpha} - E_0| > \epsilon^{|\alpha|}$ . We can split the summation into size  $n_r$  spin flips starting at site  $i$  from the initial state.

$$\delta P^{p.t.} \leq 4L \sum_{n_r} \sum_{\alpha(n_r, i)} \frac{1}{T^2} (\gamma/\epsilon^2)^{2n_r} \quad (7.31)$$

The question is whether  $\sum_{\alpha(n_r, i)}$  contains a factorial. It doesn't - it is bounded by  $2^{n_r}$ . Thus the sums converge, are dominated by the first term, and we arrive at

$$\delta P^{p.t.} \leq \frac{4L}{T^2} (\gamma/\epsilon^2)^2 \quad (7.32)$$

We note that we can transfer to the interacting picture with  $V$  considered as a perturbation. The resulting time-dependent Hamiltonian is small in  $\gamma$ . That's how we can use Wiebe's bounds. Let's derive the estimate of the probability loss stated in the beginning of this section.

**probability loss** We use first order time dependent perturbation theory for evolution with  $H_x$ :

$$a(t) = a^{(0)}(t) + a^{(1)}(t) \quad (7.33)$$

In the equation

$$i \frac{d}{dt} a(t) = (E(s) + V(s))a(t) \quad (7.34)$$

There are no transitions in zeroth order:

$$i \frac{d}{dt} a^{(0)}(t) = E(s)a^{(0)}(t) \quad (7.35)$$

$$a^{(0)}(t) = e^{-i \int E(vt) dt} a(0) \quad (7.36)$$

In the first order, we find

$$i \frac{d}{dt} a^{(1)}(t) = E(s)a^{(1)}(t) + V(s)a^{(0)}(t) \quad (7.37)$$

$$a^{(1)}(t) = e^{-i \int E(t/T) dt} \int e^{i \int^{\tau} E(t/T) dt} V(s) e^{-i \int^{\tau} E(t/T) dt} d\tau a(0) \quad (7.38)$$

The coefficient  $c_\alpha$  of the excited state  $\alpha$  for a system started in the ground state  $a(0) = |0\rangle$  is:

$$c_\alpha(t) = e^{-i \int E_\alpha(t/T) dt} \int e^{i \int^\tau E_\alpha(t/T) dt} V_{\alpha 0}(s) e^{-i \int^\tau E_0(t/T) dt} d\tau \quad (7.39)$$

We can proceed if we make simplifications:  $V_{\alpha 0}(s) = V_{\alpha 0}$  time-independent in the first order,  $E_\alpha(t/T) = E_\alpha$  time-independent (the first time-dependent correction is  $O(\gamma^2)$ ). Then

$$c_\alpha(t) = e^{-i E_\alpha t} \frac{1}{E_\alpha - E_0} (e^{i(E_\alpha - E_0)t} - 1) V_{\alpha 0} \quad (7.40)$$

More generally, this is the first contribution from integration by parts of the integral above:

$$c_\alpha(t) = e^{-i \int E_\alpha dt} \left( \frac{V_{\alpha 0}(t)}{E_\alpha(t) - E_0(t)} e^{i \int (E_\alpha - E_0) dt} - \frac{V_{\alpha 0}(0)}{E_\alpha(0) - E_0(0)} \right) \quad (7.41)$$

The next contributions drop a power of  $\frac{1}{T}\gamma$  each as  $\frac{d}{dt} = \frac{1}{T} \frac{d}{ds} = \frac{\gamma}{T} \frac{d}{d\gamma}$ , so it is justified to neglect them (this is a well known situation with rapidly oscillating integrand, so all the oscillations cancel out). Then we make  $V_{\alpha 0} \rightarrow \frac{1}{T} V_{\alpha 0}^s$  by changing  $d/dt \rightarrow d/ds$ . The  $V^s$  doesn't depend on  $T$  to the first order. The total probability loss is:

$$\delta P^{p.t.} = \sum_\alpha |c_\alpha|^2 \leq 4 \sum_\alpha \frac{1}{T^2 (E_\alpha - E_0)^2} |V_{\alpha 0}^s|^2 \quad (7.42)$$

We arrived at the desired result. We see that the difference establishes itself over times  $(E_\alpha - E_0)^{-1} \sim 1$ , and then remains bounded while our approximations of neglecting higher orders in integration by parts and smallness of the population of excited states remain valid. Wiebe's bound for small system sizes suggests that it stays such even beyond those approximations. For big system sizes, we can bootstrap the argument for all levels as described above/ We believe that the corresponding bound

$$\delta P^{p.t.} / L = \frac{1}{R} \|\rho_R - \text{tr}_{\bar{R}} |\phi_{s=1}\rangle \langle \phi_{s=1}|\| \leq \frac{4}{T^2} (\gamma/\epsilon^2)^2 \quad (7.43)$$

remains valid for big system sizes. There are two major concerns with this argument:

- As usual in MBL, the low system size estimates might be misleading. One needs to show that  $n$ 'th order of time-dependent p.t. is always smaller than the first, and that the approximations can be justified.
- The Imbrie's bounds used relatively tight combinations of parameters. We have seen that the dynamics enhances both the perturbative and the resonant contributions. Maybe  $\gamma_{eff}$  becomes  $O(1)$  faster than in the static construction, so one needs to confine oneself with even smaller range around  $H_z$ .

**Now putting it all together** We have discussed losses due to perturbation theory and exact nonperturbative LZ losses. Now we'd like to have an understanding how to glue/compare those two. Note that the LZ effect happens on timescales  $\sim 1/\gamma^{n_r-2}$ . For higher-order crossings  $1/\gamma^{n_r-2} \gg T$  so a simple  $\delta P^{p.t.}/L \sim T/\gamma^{n_r-2}$  bound gives good enough suppression. For the sake of an easier proof, we may also consider a deformed Hamiltonian where all the jumped avoided crossings are turned into actual crossings of levels. There is some theory for that case (Avron and Elgart)

The crossings with smaller  $n_r$  are followed, not jumped. So they are in the range of applicability of the diabatic corrections theorem. The bound should coincide for the two, but our theorem appears to be not tight: our bound for  $\gamma_{eff} = 1$  gives  $\frac{1}{T^2}$  probability of error, not  $\exp(-T)$  like in LZ.

Adding the two, we get the average error to be:

$$\frac{1}{R} \|\rho_R - \text{tr}_{\bar{R}}|\phi_{s=1}\rangle\langle\phi_{s=1}|\| \leq 4 \frac{1}{T^2} (\gamma/\epsilon^2)^2 + n^* 2^{n^*+1} \gamma^2 |a-1| \quad (7.44)$$

where  $n^*$  as defined before is the characteristic resonance size that has nontrivial LZ probabilities, and is logarithmic in  $v$ . The resulting  $v$ -dependence of the second term is some power-law  $v^{-1/(\ln\gamma_{eff})}$  - some small positive power. We note that the second term grows the longer is our path in the space of Hamiltonians, while the first terms stays fixed.

But the two contributions are easy to separate experimentally: while perturbative effects are evenly spread in the system, the LZ flips happen with those particular sites involved in the resonance. Their total density over all time of the evolution may still be small for the range of parameters discussed in LZ section. So if we look at the local density matrix, it will only notice the resonances with probability (over disorder configurations) proportional to resonance total density, otherwise its deviation from the eigenstate will be bounded by our diabatic bound.

We note that the choice of  $\epsilon$  still has some freedom. For bigger  $\epsilon$ , the diabatic term is better controlled, while the second term seems to remain the same. But remember that now our diabatic estimate is not applicable  $\epsilon$  of the time. So naively  $\epsilon < 1$ , which gives:

$$\frac{1}{R} \|\rho_R - \text{tr}_{\bar{R}}|\phi_{s=1}\rangle\langle\phi_{s=1}|\| \leq 4 \frac{v^2}{|a-1|^2} + O(v^{-1/(\ln\gamma_{eff})}) \gamma^2 |a-1| \quad (7.45)$$

Finally, do we understand this evolution well enough to predict it? As the estimates show,  $n^* \approx 4$  for realistic drive. MBL systems also possess exponential decay

of correlations, so the resonances will flip in the same locations approximately independent of the edges. It should be enough to simulate truncated Hamiltonian of 10-spin patches of the chain, either by trotterizing the evolution, or by investigating the crossings. Then the behavior of spins in the center will be a good predictor for what will happen in that location in the infinite system. The error will be augmented by  $\gamma^3$  via the influence of the edges, but the above two errors will be reduced if we actually do careful trotterization of evolution. They stay if we just point at the product state after investigating the crossings. Trotterization introduces additional error, which can be made arbitrarily small given enough resources, and we will still count it as polynomial in system size. We note however that as soon as the flips start overlapping, one will need to keep track of many entangled trajectories. A method based on matrix product states will give slight advantage for simulating such dynamics, but eventually the amount of resources required will become exponential. Thus we have a long window in protocol time where the simulation is efficient, but not infinitely long.

We also note that such systems allow for Quantum computation with a decent error given by estimates above, with the only experimental knob being the magnetic field. Indeed, by tuning it back and forth at various speeds, one can perform gates at every crossing. This idea has been used in Quantum dots (Cao et al., 2013) before. The cost of apparent simplicity is that the fabrication has to be very precise, so that we know exact parameters of the system, and the preprocessing that turns a computational routine into a  $h(t)$  is not trivial.

## 7.2 Floquet

We now consider a special case of periodic driving  $H(t) = H(t + T)$ . To be consistent with the calculations above, we will vary the transverse magnetic field  $\gamma = \gamma(t)$ . There are two simple realizations of the time dependence: a periodic drive  $\gamma(t) = \gamma \cos 2\pi t/T$  and a sequence of quenches

$$\gamma(t) = \begin{cases} \gamma, & t \in [Tn, T/2 + Tn] \\ 0, & t \in [T/2 + Tn, T(n+1)] \end{cases} \quad (7.46)$$

for integer  $n$ . Our analysis of the slow drive only applies to the first case. However, the second case is easier to analyze numerically if one wishes to access infinite times. Indeed, one just needs to study the eigenvalues and eigenvectors of the unitary evolution operator:

$$U_{\text{floquet}} = e^{i(H_z + H_x)T/2} e^{iH_z T/2} \quad (7.47)$$

we will also discuss the Hermitean Floquet Hamiltonian:

$$iH_{\text{Floquet}}T = \ln(e^{i(H_z+H_x)T/2}e^{iH_zT/2}) \quad (7.48)$$

The logarithm is ill-defined so every eigenvalue of  $H_{\text{Floquet}}$  can be shifted up or down by  $2\pi/T$ . In  $T \rightarrow 0$  limit the Baker-Campbell-Hausdorff formula is applicable, and the eigenvalues are too small to wrap around in this way, so

$$\lim_{T \rightarrow 0} H_{\text{Floquet}} = H_z + \frac{1}{2}H_x \quad (7.49)$$

in fact, the BCH expansion converges for  $\|H_z + H_x\|T/2 + \|H_zT/2\| < \ln 2$ , so for  $T = O(1/L)$ . The Floquet Hamiltonian acquires small in  $1/L$  terms like  $[H_z, H_x]T^2$ .

Even though for bigger  $T$  our formal perturbative expansion diverges, the eigenvalues of the Floquet Hamiltonian are expected to be found near the original eigenvalues of the big  $H_z$  term modulo  $2\pi/T$ , with the following exceptions. Repeat the energy levels of  $H_z$  in steps of  $2\pi/T$  on energy axis. For a pair of levels, there will be situations when the perturbative mixing of the appropriate order by  $H_x$  is bigger than the new level distance. In these situations we will find eigenvalues of  $H_{\text{Floquet}}$  to deviate from those of  $H_z$ . The level distance is now calculated as a minimum over all possible shifts by  $2\pi/T$  of one of the levels, so faraway levels can now experience a resonance. In other words, the denominators  $E_\alpha - E_\beta$  appearing in the perturbation theory are now replaced by  $\min_n(E_\alpha - E_\beta + 2\pi n/T)$ .

We can confirm the above intuition by studying a two-level system (a single spin) exactly. Let  $H_z = r\sigma^z$  where  $r$  is a random number uniformly distributed in an interval  $[-1, 1]$ , and  $H_x = \gamma\sigma^x$  where  $\gamma \ll 1$ . We would like to find how close the eigenstates

$$e^{i(H_z+H_x)T/2}e^{iH_zT/2}|\phi\rangle = e^{i\phi}|\phi\rangle \quad (7.50)$$

are to the z-basis:

$$X(\gamma, r, T) = 1 - (\langle\phi|\sigma^z|\phi\rangle)^2 \quad (7.51)$$

In particular, we're interested in disorder average:

$$\text{Av.}X(\gamma, T) = \frac{1}{2} \int_{-1}^1 dr (1 - (\langle\phi|\sigma^z|\phi\rangle)^2) \quad (7.52)$$

In the two level system, the quantity  $X(\gamma, r, T)$  can be evaluated exactly:

$$X(\gamma, r, T) = \frac{n_x^2 \text{Sin}^2(ET/2)}{n_x^2 \text{Sin}^2(ET/2) + (\text{Cos}(ET/2)\text{Sin}(rT/2) + n_z \text{Cos}(rT/2)\text{Sin}(ET/2))^2} \quad (7.53)$$

where  $E = \sqrt{r^2 + \gamma^2}$ ,  $n_x = \gamma/E$  and  $n_z = r/E$ . From our intuition, we expect a peak in this expression at  $ET = \pi n$  as the levels are  $2E$  apart. Indeed, we find a sequence of peaks as a function of  $T$ , of width  $\gamma/E$  for odd  $n$  and  $\frac{\gamma^2}{E^2}$  for even  $n \neq 0$ . For smaller  $r$ , we can essentially look at corresponding value of  $X$  at  $T = rT_0$ ,

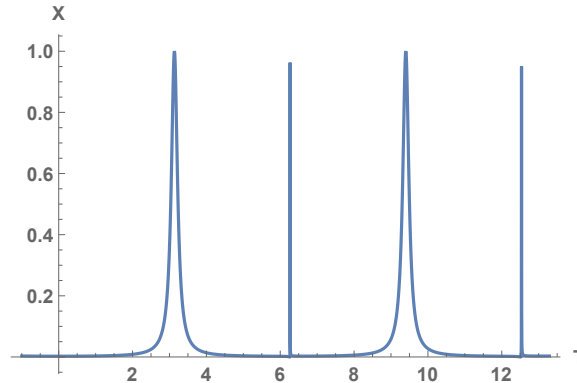


Figure 7.1: The peaks in  $X(\gamma = 0.1, r = 1, T)$

Indeed,  $X$  is a function of just two independent parameters  $rT$  and  $\gamma T$ . As long as the second one is small,  $X(T)$  at  $r = 1$  and  $X(r)$  at  $T = 1$  essentially coincide. Only for  $r \approx 0$  there's a difference:  $X(r)$  experiences a peak corresponding to a resonance in the original (with no level wrapping) system. For bigger  $T$ 's, the picture shrinks so that the peaks appear in the interval of integration  $r \in [-1, 1]$ . we note how the

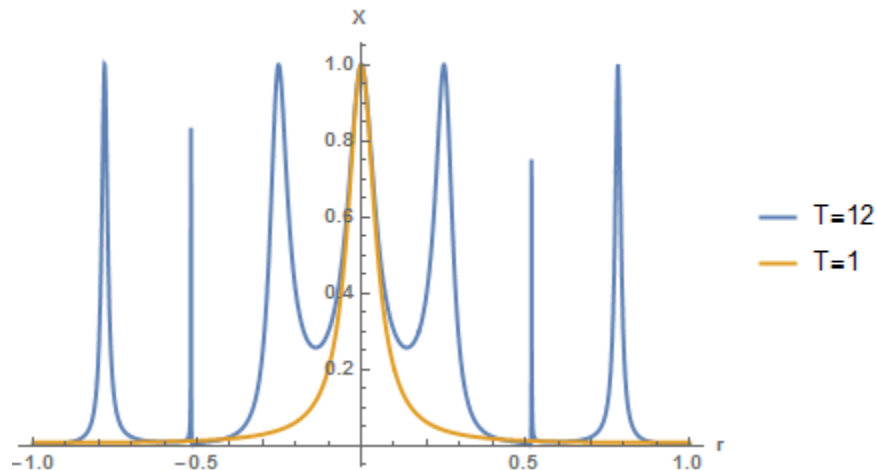


Figure 7.2: The peaks in  $X(\gamma = 0.1, r, T = 6)$  (blue) and  $X(\gamma = 0.1, r, T = 1)$  (gold)

area under peaks increases by at least a factor of 3 thanks to wrapping of the levels. Since our probability distribution of  $r$  has a discontinuity at  $r = \pm 1$ , it appears as

a discontinuity in the limit  $\gamma \rightarrow 0$  in the integrated value  $\text{Av}.X(\gamma, T)$ . Even for moderate  $\gamma = 0.1$  it is still very sharp. At  $T \rightarrow \infty$ , the value  $X(\gamma, T)$  saturates to  $\sim 4\gamma$ . The  $T \rightarrow 0$  value was  $\sim 1.5\gamma$ , so the system is 3 times as likely to experience a resonance as the non-driven one! We confirm that the enhancement is linear so

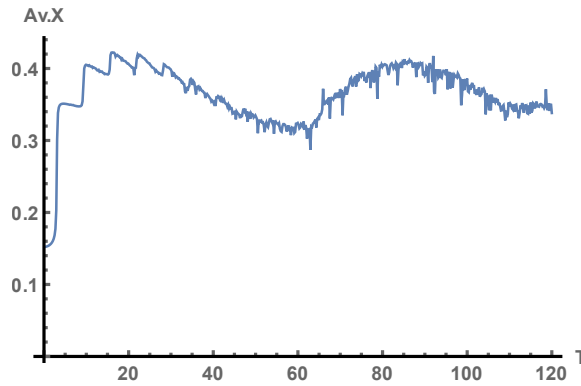


Figure 7.3: Saturation of  $\text{Av}.X(\gamma = 0.1, T)$ . The narrow peaks lead to a numerical noise.

$\text{Av}.X(\gamma = 0.1, T) \sim \gamma$ . Now that we've understood this one-spin effect, let's see

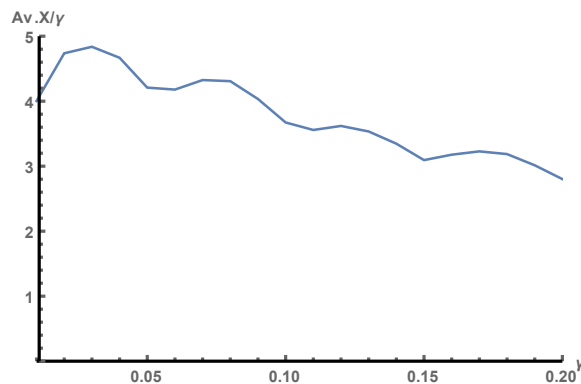


Figure 7.4: Enhancement  $\text{Av}.X(\gamma, T = 500)/\gamma$  in the limit of long times

what happens in a many-spin system. First, note that our effect appeared for all  $(E_\alpha - E_\beta)T > 2\pi$ . In a block of size  $n$ , there are  $4^n$  pairs of levels. Their perturbative mixing is  $\gamma_{eff}^{n'}$ , where  $n'$  is their consecutive distance. We restrict our attention to those that have  $n' = n$ , as they are typical and moreover, the smaller  $n'$  could be considered in the smaller block sizes. From above considerations of two level system, we know that a particular pair will be resonant  $4\gamma_{eff}^n$  fraction of the time. The total probability of size  $n$  resonance is then  $4^{n+1}\gamma_{eff}^n$ . For sufficiently small  $\gamma_{eff}$  it will still be suppressed in  $n$ .

This naive consideration predicts that densities of resonant blocks are enhanced by a factor of  $4^n$ . It does not account for the fact that the true suppression of the density is weaker than the splittings at the crossing ( $\gamma_{eff}^{n/2}$  according to our estimates or  $\epsilon^{cn}$  according to Imbrie). The cases where multiple resonances are in the neighboring blocks need to be accounted carefully as in Imbrie's construction. Finally, the reduction of  $2^L$  level system to  $4^L$  two-level systems is not legitimate — there may be three-level collisions after we allow for  $2\pi/T$  shifts.

One redeeming quality of this naive estimate is that it works very well to predict the behavior up to  $L = 10$ . Consider again

$$U_{floquet} = e^{i(H_z+H_x)T/2} e^{iH_zT/2}, \quad (7.54)$$

but now  $H_z+H_x$  is the spin chain Hamiltonian we investigate in this paper. Individual spins has magnetic fields along  $z$   $h_i \in [-1, 1]$  and the couplings  $J_i \in [-1, 1]$ . Surprisingly, the jump when one-spin levels start to wrap around is still clear and almost unchanged for all system sizes up to  $L = 10$ . We divide the  $\text{Av}.X(\gamma, T)$  by  $\gamma$  so that the plots for different  $\gamma$  approximately lie on top of each other. The position of the jump is now at  $T \approx \pi/2$ . The many-body slopes at small  $\gamma$  appear to be renormalized by a factor of two as well with the addition of  $J_i \sigma_i^z \sigma_{i+1}^z$  terms. Long-time behavior appears to be saturating to a value  $\sim 4\gamma$  with a slight positive  $\gamma^2$  corrections in the  $L = 10$  system.

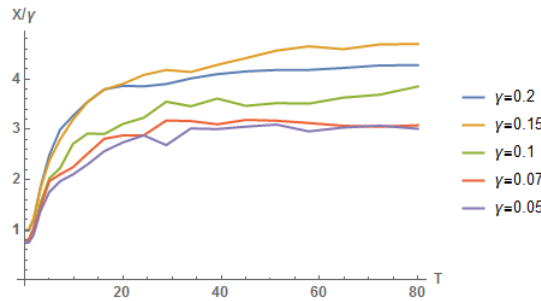


Figure 7.5: The jump in  $\text{Av}.X(\gamma, T)/\gamma$  for  $L = 10$  system

This lead Ponte et al., 2015 to conclude that the floquet Hamiltonian is also MBL in a strong sense (admitting an Imbrie circuit using the notation of our paper). That is, for example, that:

$$iH_{floquet}(t_1 + t_2) = \ln(e^{i(H_z+H_x)T/2} e^{iH_zT/2}) \quad (7.55)$$

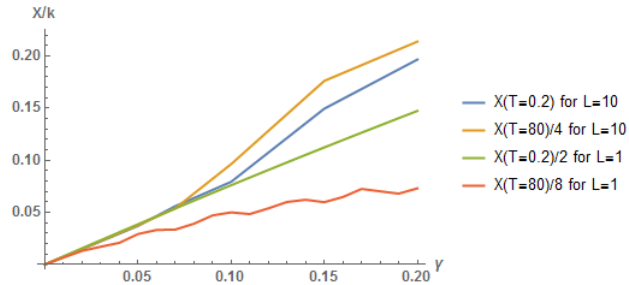


Figure 7.6: The values of  $\text{Av}.X(\gamma, T)/k$  before and after the jump. An integer  $k$  is chosen to approximately match the small  $\gamma$  slope.

has local with exponential tails form and can be diagonalized by Imbrie circuit. To get around the ill-defined logarithm we say that the local structure exists for one choice of  $2\pi n/T$ .

Since the eigenstates are close to the product states except for a few resonances, the evolution of a product state under  $U_{f\text{loquet}}$  may actually preserve the regions outside resonances up to infinite times. That is indeed what has been observed in the numerical study (Ponte et al., 2015). A many body system that preserves a local density matrix up to infinite time is demonstrating non-thermalizing behavior: hot and cold systems put together do not reach the same temperature. Instead they stay how they started.

There's a consensus in the literature that MBL systems under any weak local periodic driving do not heat up to infinite temperature. Thus in particular the driving  $\gamma(t) = \gamma \cos 2\pi t/T$  should not completely destroy the state even for large  $T$ . Note that it does not immediately follow from our results about slow drive of  $\gamma(t)$ : we can predict what happens for a few periods of the drive, but eventually the diabatic errors and the LZ drain could explore the whole configuration space. However, the diabatic loss may be reversible — in the same integration by parts as above the periodic drive over infinite time in principle keeps the error the same over many periods. The LZ effects that are big are constrained locally. So the only contribution that remains uncontrolled is a polynomially small correction from high-order flips that are jumped by LZ. Surprisingly, this effect seems to remain controlled at least in a limit of weak drive up to infinite times, as demonstrated in (Abanin, Roeck, and Huvneers, 2016) by constructing an analogue of perturbation theory that would allow an equivalent of Imbrie's construction. For stronger drives and higher frequencies, see a detailed numerical study in (Rehn et al., 2016).

## Chapter 8

### D-WAVE

Consider again a disordered spin chain Hamiltonian

$$H = s(t)H_z + (1 - s(t))H_x, \quad H_z = \sum_i J_i \sigma_i^z \sigma_{i+1}^z + h_i \sigma_i^z, \quad H_x = \sum_i \sigma_i^x \quad (8.1)$$

where  $s(t) = t/T$  and  $J_i, h_i$  are random numbers drawn from a uniform distribution on an interval  $[-1, 1]$ . Denote the number of spins by  $L$ . In this section we will focus on the interaction with environment via

$$H_e = \sum_i \sigma_i^z B_i \quad (8.2)$$

where  $B_i$  are operators acting on the environment. To obtain the system evolution in a closed form, a set of approximations can be made in the weak coupling limit  $C_{ij}(t) = \langle B(t)_i B_j \rangle \rightarrow 0$ . The derivation of a master equation in this setting is can be found in Mozgunov, 2016. Such environment acts on the MBL phase at  $s \approx 1$  primarily by dephasing: the off-diagonal elements  $\rho_{nm}$  of the density matrix in the eigenstate basis are lost at a rate  $\kappa L = \sum_i \langle n | \sigma_i^z | n \rangle \langle m | \sigma_j^z | m \rangle \int C_{ij}(t) dt$ . From Johansson et al., 2009 we know that for one spin  $\kappa = O(1)$  — it is of the same scale as the local terms in the Hamiltonian. That allows us to focus our attention on the diagonal of the master equation. It is well known that the Lindblad equation decouples the evolution of diagonal density matrix elements in the eigenstate basis. Such evolution can be written as a Markov process: an evolution of a probability vector  $P_E = \langle E | \rho | E \rangle$  via the rate matrix:

$$\dot{P}_n = M_{nk} P_k, \quad M_{nk} = \sum_i |\langle n | Z_i | k \rangle|^2 \int C_{ii}(t) e^{-iE_{nk}t} dt, \quad \text{for } n \neq k \quad (8.3)$$

Here we assumed an independent noise on each spin. The matrix element between two states  $|n\rangle, |k\rangle$  given by their labels  $n_{prod}, k_{prod}$  in  $Z$ -basis is:

$$\langle n_{prod} | (1 + \sum c_1(1-s)X + \dots) Z (1 + \sum c_2(1-s)X + \dots) | k_{prod} \rangle \sim (1-s)^{n_r} \quad (8.4)$$

Here  $(1 + \sum c_1(1-s)X + \dots)$  stands for a Taylor expansion of the Imbrie circuit, and  $n_r$  is the consecutive distance between  $n_{prod}$  and  $k_{prod}$ . If the two levels are resonant, the matrix element can get  $O(1)$ . However for  $\kappa = O(1)$  the weak coupling

limit is no longer applicable, so we can't trust this equation for the diagonal rates. The effective rates were presented in Johansson et al., 2009 and derived via Fermi's golden rule in Amin and Averin, 2008

$$M_{n,k} = \frac{(1-s)^{2n_r}}{\kappa} e^{-\frac{\beta E_{nk}}{2} - \frac{E_{nk}^2}{4\kappa^2} - \frac{1}{4}\beta^2 \kappa^2} \quad (8.5)$$

where  $\beta$  is the inverse temperature that is also  $O(1)$  according to Johansson et al., 2009. The noise is also low-frequency (Amin and Averin, 2008), so technically even Born approximation fails and the use of master equation has uncontrolled error. We believe that error bounds special for this case can still be derived, but we are not aware of any work in this direction. We will use a simpler form for just one spin flips below:

$$M_{n,k} = (1-s)^2 e^{-\frac{\beta E_{nk}}{2}}, \quad n_r = 1 \quad (8.6)$$

and ignore the rest. Here we note that the reduction to the diagonal of the density matrix doesn't do justice to the LZ transitions - all of them are followed adiabatically in this approach. So for an accurate description, we don't use the exact  $E(s)$  obtained by diagonalizing  $H(s)$ , instead we keep only the perturbative part of the Hamiltonian  $U^\dagger H(s)U$  on logical spins whenever the resonance corresponds to a crossing that is jumped. We discuss it further in the Subsection 8.2.

The final part of the protocol is a readout: the  $s = 1$  state is measured in  $Z$  basis, that is, a bitstring is sampled from the final probability distribution  $P_E$ . The question we address here is whether running this protocol on the MBL system captures any features of that elusive phase.

**Comparison** The conventional way to test for MBL will be to prepare a nonequilibrium state (e.g. an even-odd pattern of spins) and see if that state persists for long times. This is a special case of a quench experiment, where we prepare an eigenstate of  $H_z$  and that turn on small magnetic field instantly. What happens is that all resonances present at this value of the field will start turning, and if one measures several times after waiting for different intervals, the rare spins that will be found flipping will belong to resonances. One can map out the resonances, and as a consequence everywhere where the system is nonresonant ( $1 - O(\gamma)$  of sites) the even-odd pattern will survive if it was put in initially.

This protocol is simple, can give valuable information in finite time (does not require the protocol time to grow with the system size) and is already implemented in other settings. What possible benefit or an interesting effect can the adiabatic evolution

show that the above cannot? We find no immediate advantages of using it. The only motivation is that it's a chance to use an already available D-wave machine, but we will find that the open system effects and the limit on the evolution times smears the data so much that it would be infinitely better to just do the quench experiments.

So we cannot measure an "order parameter" of MBL on the machine directly. Nonetheless, if the methods described in this section predict the results of a run of the D-wave machine well, the underlying system has an MBL phase present at the end of the protocol (and possibly other phases before it). So the error in our prediction of the outcome becomes such an "order parameter" for the MBL phase.

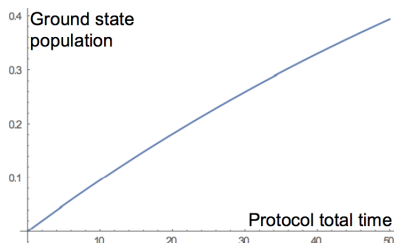
### 8.1 Failure of the collection of $(\delta E, n_r)$ data

First we would like to answer how well can a D-wave machine collect a similar data to what our exact diagonalization of small system sizes was collecting in Chapter 7, and list all the complications that arise. Even though we will find a negative answer, this will provide us with valuable intuition for the following Sections. Let's review the physics of the Landau-Zener transition.

If there is one avoided crossing that the GS encounters, the probability to stay in GS will depend on protocol time by LZ formula:

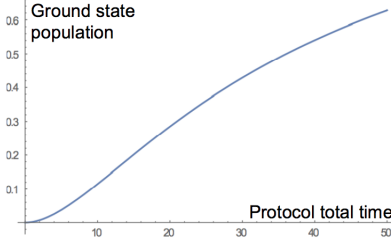
$$P_{gs} = 1 - e^{-2\pi\Delta^2 T/v} \quad (8.7)$$

here  $\Delta$  is the minimal gap and  $v = \partial(E_{gs} - E_e)/\partial s$ . The protocol time dependence looks as follows:



If there's two crossings that ground state experiences, the early times go as  $T^2$ :

But the late times behavior always depends on the minimal gap encountered along the path. We can extract it from the late times by taking a logarithm of  $1 - P_{gs}$  and fitting a line through its dependence on the protocol time. This is true for a closed system. For an open system, one needs to be more crafty, as  $1 - P_{gs}$  is generally nonzero for all protocol times because of the thermal occupation of excited states.



We can estimate the effect of the decay by considering the decay rate of a difference in density matrices between the current state and the instantaneous Gibbs state  $\tau_s = \rho_s - \rho_{G,s}$ . It depends on the adiabatic parameter like  $(1-s)^2$ . Indeed, the state that is away from the ground state by  $n_r \gg 1$  spin flips does not have to relax to the ground state directly. Each decaying state can always go to states that are energy  $O(1)$  (constant energy barrier in 1d systems) away by  $(1-s)$  matrix element, and then keep flipping until it reaches a state 1 spin flip away from the ground state, all within  $O(1)$  energy window. The actual time dependence of the ground state depletion  $\langle g|\tau_s|g\rangle$  will go as  $1 - O(((1-s)^2 t)^{n_r})$  for small times, and  $\text{poly}(t)e^{-\kappa e^{-\beta(1-s)^2 t}}$  for long times, as probabilities take some time to redistribute themselves among the intermediate states. The half-life of the depletion is still governed by an exponential and is  $\sim 1/(1-s)^2$ . Here by half-life we mean the time when depletion changes by half, since its time dependence is not a simple exponential decay. It is also what we measure from long-time tail of  $\ln(1 - P_{g,s})$ . Of course, this kind of model neglects many contributions: for instance the entropic contribution of multiple possible paths to the decay. So it's not going to give the right answer for every system (especially if the answer is that decay time grows with the system size - there are many models that have an energy barrier but are not expected to be good memories). But it gives the right intuition for the case of a chain, as is shown in (Alicki, Fannes, and M. Horodecki, 2009) in the non-disordered case.

There is also a simpler framework that we will find useful. According to (Alicki, Fannes, and M. Horodecki, 2009), there's a gap  $\Delta M$  in singular values of a matrix  $M_{EE'}$  between singular value 0 corresponding to the Gibbs state and all the other ones. we claim that the same statement holds for our disordered chain. Consider the rate of decay of the deviation from the ground state  $\tau_s$  for a very special  $\tau_s$  that is zero everywhere except for the ground state and the first excited state.  $\langle g|\tau_s|g\rangle = P_e^{Gibbs} - P_g^{Gibbs}$  and  $\langle e|\tau_s|e\rangle = P_g^{Gibbs} - P_e^{Gibbs}$ . The rate of decay of such  $\tau_s$  is lower bounded by a decay with the Markov process with a transition matrix in which all nonzero singular values are the same (equal to the gap of the original process  $\Delta M$ ).

And that one has a very simple  $\tau_s e^{-\Delta M \Delta t}$  behavior. In our case,  $\Delta M = \kappa(1-s)^2$  as  $(1-s)^2$  is an overall factor appearing through the matrix elements  $\sum_i |\langle E | Z_i | E' \rangle|^2$  that define every  $M_{E,E'}$ .

Let's consider the protocol with  $s = t/T$  and see which LZ transitions are feasible to observe and which ones will have their effects smeared by the decay. The fact that the relaxation depends on  $s$  as  $(1-s)^2$  alters the result by a constant factor in the exponential. One also takes into account the time  $\sim (1-s^*)$  left till the end of the protocol, where  $s^*$  is the position of the avoided crossing of the ground state and first excited state. With decay, we expect the end population after one LZ transition at  $s^*$  to be:

$$P_{gs} - P_{gs}^{gibbs} = (P_e^{gibbs} - P_{gs}^{gibbs}) \text{poly}_{n_r}(\kappa(1-s^*)^3) T_{prot} e^{-(\Delta^2/v_{s^*} + \kappa(1-s^*)^3) T_{prot}} \quad (8.8)$$

Even if for some reason the half-life does depend on consecutive spin flip distance  $n_r$  to the excited state, it will only do so linearly or weaker. The gap in  $\Delta^2/v_{s^*}$  is exponential in  $n_r$ , so its contribution to the exponent is negligible for most  $n_r$ .

We have dropped the terms that would come when occupations of the excited states  $P_e$  are comparable to that of the ground state  $P_{gs}$ . This approximation is valid for small system sizes and small temperatures as the ground state has the most of the population. The approximation can be thought of as follows: fully occupied groundstate experiences crossings with different states, but decays back. Decay is so strong that before  $s_{min}$  s.t.  $\kappa(1-s_{min})^3 T_{prot} = 1$  we expect the LZ occupations to decay and be not so well measurable. For our Hamiltonian,  $\kappa \approx 1$  and  $T_{prot} \approx 10^5$ . Thus  $s_{min} = 0.98$  - well into the MBL regime. So the  $Z$  phase flips actually help focus the data on the Hamiltonians close to  $H_z$ . The decay will also obscure (make negligible) the  $\Delta^2/v_{s^*}$  contribution of all resonances of sizes  $n_r > 2$ , which is almost all of them. The time  $T_{s_{min}}$  is called a freezing time.

Suppose we measure  $1 - P_{gs}$  for different protocol times. The long times log-slope will give  $(\Delta^2/v_{s^*} + \kappa(1-s^*)^3)$  for  $s^*$  - the position of the last crossing. So if interpreted as the closed system result would be, it will overestimate some of the small  $\Delta^2/v_{s^*}$ , especially the ones away from  $H_z$ . So some of the small gaps will be reported as big ones. The same effect was already present in the closed system case due to the variability in velocities  $v = \partial(E_{gs} - E_e)/\partial s$ . We expect  $v_{s^*} \leq v_{max} \sim \|H\|$ , but in principle it can be very small. This will bloat the small gaps as well. One redeeming feature is that if the small gap is bloated by either of the two factors, another one comes in its place. If there are two or more small gaps encountered

by the system, the long times log-slope will be given by one of them, such that  $\text{Min}(\Delta^2/v_{s^*} + \kappa(1 - s^*)^3)$  is achieved. That condition prefers the cases where the corrections are weaker.

An experimentalist can collect the data for the factor in front of  $T_{prot}$  in the exponential for different disorder realizations and system sizes. We also want to record the number of spins  $n_r$  that are flipped between the ground state and the state the smallest gap transition was to. We can't get that information from D-wave directly: in practice, it's hard to find which state the smallest  $(\Delta^2/v_{s^*} + \kappa(1 - s^*)^3)$  LZ transition was to. But it is likely to be the last one. So instead we use the consecutive flip distance to the lowest excited state at the end of the protocol (or the average over the distance to a few lowest excited states).

Smallest gap  $(\Delta^2/v_{s^*} + \kappa(1 - s^*)^3)$  has the typical gap that an avoided crossing would have in our system. Indeed, the distribution of neighbors is what governs the resonance sizes (see Chapter 6), and most of the weight is concentrated around size  $n_r \sim L$ . One of  $n_r \sim L$  resonances will have the smallest  $(\Delta^2/v_{s^*} + \kappa(1 - s^*)^3)$ . We expect  $s^*$  to be in MBL phase, if any crossings fall into the range  $[s_{min}, 1]$  at all. In the minimal gap estimates of Chapter 4, we did not find any avoided crossings at all at sizes  $L < 10$ . Since the fully occupied ground state approximation breaks down pretty fast with system size (at  $L > \beta \approx 1$ ), our prediction here is that small system sizes where it is valid will not see any crossing that would allow one to extract  $(\Delta^2/v_{s^*} + \kappa(1 - s^*)^3)$ .

Moreover, even though there's a possibility for two terms to be comparable, the expectation is that the closed system contribution is orders of magnitude smaller for all the cases we'll see. Note that running a system size many times to collect statistics with exponential precision takes exponentially long time. If we were to look at  $L = 10$ , we can plug in the numbers directly.  $k(1 - s)^3 T = 10^4$ , and  $\Delta^2 T/v = 10^2$ . There's no way in the world to measure  $e^{-10^2}$  difference in population.

It takes exponentially long in the system size to collect  $(\delta E, n_r)$  data for avoided crossings by relying on exact diagonalization as in Chapter 6. If one doesn't know where the crossings are in advance, it will also take exponentially long to collect such data using a fully operational quantum computer (since they are exponentially small). But note that not all of them are like that. We can still collect  $(\delta E, n_r)$  for big  $\delta E$ . Conveniently the gap between the ground state and the first excited state is  $O(1/L)$ , so the crossing we're measuring can have a splitting as big as  $\sim 1/L$ . Suppose we wanted to search for this kind of crossings involving the ground state in

the vicinity of  $s = 1$ . That can be done in polynomial time on a quantum computer by essentially running the closed system protocol described in this section. Now can we use D-wave to perform the same task?

Such a task is easier if we allow *adjustments to the D-wave protocol*. First of all, we suggest a simple quench protocol where a state in z-basis at  $s = 1$  experiences a sudden change to  $s \neq 1$ . After some time, the state is measured in z-basis. This protocol will allow to detect resonances of sizes up to  $n_r = 2$  in our MBL system, that is, almost all of them at this  $s$ . Bigger resonances will be obscured by thermal decay. One can also deduce their splitting by investigating the time-dependence of the observed z-projection. So we can collect a clean ( $\delta E, n_r \leq 2$ ) data by carefully analyzing the data from the same experiment as what is conventionally done to detect MBL in cold atoms. Alternatively, we can consider a protocol that also starts with a state in z-basis (not in x-basis like the D-wave machine) and then quenches to  $s_1$  and evolves to  $s_2$  over a time  $T$ . That has the benefit of higher chances of running into bigger  $n_r$  (smaller  $\delta E$ ). Both protocols will be useful for a search for  $O(1/L)$  crossing that the ground state can experience. Below we discuss possible implications of such measurements.

Recall that Imbrie's bound on  $\delta E$  is proven throughout the whole spectrum of energies, not just the crossings between the ground state and the first excited state. One can imagine the strong MBL property shown by Imbrie to fail, while the ground state splitting of crossings is still bounded by  $\gamma_{eff}^{n_r}$  at the crossing. That happens if at any nonzero  $(1 - s)$  the mobility edge is present in the system: all the eigenstates above it are extended, and below — localized. Such situation is not very likely for a generic system, since we're infinitesimally close to a z-Hamiltonian, but the intensive and extensive mobility edges are discussed in the literature (Cuevas et al., 2012). We illustrate the possibilities in the figure below: The current D-wave machine can distinguish between (c) and the rest, whereas the adjusted protocol will be able to detect the mobility edge in (b). Indeed, the relationship  $\delta E \leq \gamma_{eff}^{n_r}$  is only present in the MBL phase, the extended phase is essentially flat in  $n_r$  as shown in Chapter 6. We note that possibilities (b),(c) are not going to be present in 1d disordered  $(1 - s)H_x + sH_z$  systems generically (as per Imbrie's proof). To see them, we either need a very atypical family of disorder realizations, or to look at a higher-dimensional (or long-range) Hamiltonian.

So the application of a D-wave machine to physics using the method of this section could be to study the MBL phase found in (a) and to measure the quantities used in the

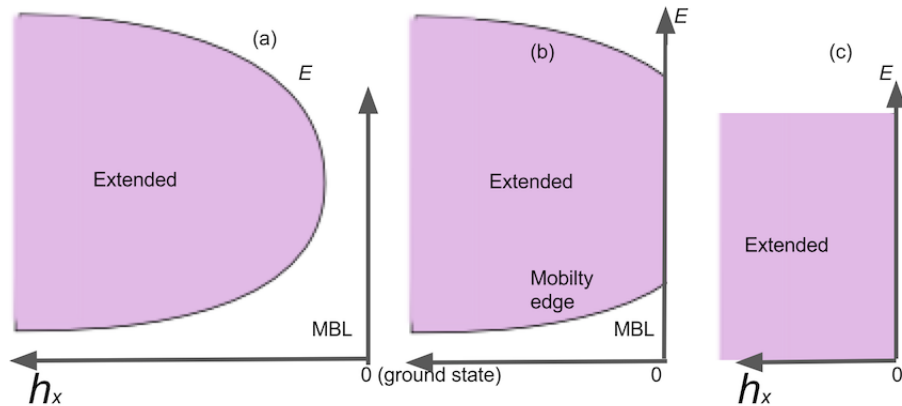


Figure 8.1: Phase diagram (a) is expected for our spin chain. Mobility edge (b) and a fully extended phase (c) is shown for comparison.

Imbrie's proof (e.g. splitting), albeit with very strong limitations (only  $n_r < 2$ ,  $L < \beta$  can be accounted for), and everything it can do so far can be reproduced by exact diagonalization. In the next Section we will go with our predictions beyond the ED lengthscale. Let's note a crucial feature of the usage of the D-wave machine we seek: the task of mapping out a phase diagram of a many-body system is a non-commercial scientific application of independent interest. So far it has only been used to (i) study itself and (ii) approximately solve instances of an optimization problem. It was shown to be not very suitable for either of those tasks, but we believe that it can perform well at the task of simulating physical systems of independent interest (quantum simulation task).

To sum up: in this approximation, there are 3 regimes in terms of the speed of the drive and the system size: (i) all is thermal, because the last crossing has had plenty of time to relax (ii) the last crossing didn't completely relax, so a jump + thermal relaxation describes it (iii) the last crossing wasn't too small so a full LZ + thermal relaxation describes it. The most frequent regime for small system sizes is (i), followed by (ii) and the most rare of all, (iii). The regime (iv) that will be explained in the following is when deviations from the Gibbs distribution become more complex.

Larger than ED system sizes are *never* in the regimes (i-iii). So if we want to extract anything at all from the runs of the D-wave on big sizes, we need to expand our understanding.

## 8.2 Prediction about distribution deviating from Gibbs

Consider a so called stoquastic Hamiltonian corresponding to a Markov chain describing the evolution of the energy level population:

$$\dot{P}_E = \sum_{E'} M_{E' \rightarrow E} P_{E'} \quad \Leftrightarrow \quad |\dot{\psi}\rangle = H_M |\psi\rangle, \quad P_E = \sqrt{P_E^{Gibbs}} \langle E | \psi \rangle \quad (8.9)$$

We note that the  $P^{Gibbs}$  (and  $|g\rangle$  for the equivalent quantum problem) is the steady state of the time-independent chain. In our case, the generator of the evolution  $M_{E' \rightarrow E}$  changes with time slowly: the energy levels drift so the would-be fixed point changes as  $P^{Gibbs}(t)$  (or  $|g(t)\rangle$ ). We plan to apply the above equation for the MBL part of the path  $s > 0/8$ , assuming everything is Gibbs before that. The transitions rates contain an overall factor  $(1 - s)^2$  that can be taken out by rescaling of time  $\tau = T(1 - (1 - t/T)^3)$ . The Hamiltonian (or Markov chain) after that has a constant gap (constant gap of 1D Ising relaxation has been proven by Alicki, Fannes, and M. Horodecki, 2009). We again use a simplification where all singular values are equal to the gap  $\Delta M$ . After the rescaling,  $\Delta M \sim \kappa$  and contains Gibbs factors of transitions that are  $O(1)$  in energy. Since  $\beta = O(1)$ , we can just set the whole thing to one  $\Delta M = 1$  up to a constant factor:

$$H_M(\tau) = - \sum_e |e(\tau)\rangle \langle e(\tau)| = -(1 - |g(\tau)\rangle \langle g(\tau)|) \quad (8.10)$$

Here  $|e(\tau)\rangle$  are the instantaneous excited states of  $H_M$ . Since we're working with a Hamiltonian, we used the fact that its eigenstates form a resolution of the identity:  $|g(\tau)\rangle \langle g(\tau)| + \sum_e |e(\tau)\rangle \langle e(\tau)| = 1$ . In practice some of the exponentially many excited states relax even faster than the rate we set, but it will not alter the estimates below. Recall that before we identified a timescale  $s^* = 0.98$ . Looking at  $H_M$ , nothing peculiar stands out about last  $0.000008T$  of  $\tau$  (which corresponds to  $s > s^*$ ). It is defined as the place where if the big changes in the state are introduced, they don't have time to completely relax. It is an upper bound on the time the changes actually start to persist until the end of evolution. The source of changes is hidden in the time dependence of eigenstates  $|g(\tau)\rangle, |e(\tau)\rangle$ : energy differences start to curve with singular slopes as  $\tau \rightarrow T$ . But the crossing physics is lost as soon as we replaced the full density matrix evolution with just the energy level population. Since we know that crossings are jumped for most of the intersections, we should truncate the  $z$ -Hamiltonian used to define energy levels at a low order of the construction, so that it automatically ignores all the resonances  $n > n^*$  defined in Chapter 7 (let the levels  $E$  used to define  $M_{E,E'}$  pass through each other with populations intact). The

construction will still send the populations of levels for  $n < n^*$  adiabatically. This idea is similar to the 6th order of perturbation theory used by (B. Altshuler, Krovi, and Roland, 2010) to map out the energy levels near  $s = 1$ .

A side note to alleviate a possible confusion: the stoquastic hamiltonians in imaginary time always have positive amplitudes in the ground state, so it cannot experience a genuine LZ transition with anything. Other levels too because of imaginary time, so we should not apply our ideas about LZ transitions to this one. All the dynamics is in the changes of the eigenvector itself.

Now we use the same method of finding the diabatic corrections as in Chapter 7. Consider the imaginary time Shroedinger equation:

$$|\dot{\psi}(\tau)\rangle = H_M(\tau)|\psi(\tau)\rangle == -(1 - |g(\tau)\rangle\langle g(\tau)|)|\psi(\tau)\rangle \quad (8.11)$$

Using the resolution of the identity again,  $|\psi(\tau)\rangle = |g(\tau)\rangle\langle g(\tau)|\psi(\tau)\rangle + \sum_e |e(\tau)\rangle\langle e(\tau)|\psi(\tau)\rangle$ . Then we can derive the time-evolution:

$$\frac{d}{d\tau}\langle g(\tau)|\psi(\tau)\rangle = \langle \dot{g}(\tau)|\psi(\tau)\rangle + \langle g(\tau)|H_M|\psi(\tau)\rangle \quad (8.12)$$

The second term is zero as the ground state is annihilated by  $H_M$ . Now insert the resolution:

$$\frac{d}{d\tau}\langle g(\tau)|\psi(\tau)\rangle = \langle \dot{g}(\tau)|g(\tau)\rangle\langle g(\tau)|\psi(\tau)\rangle + \sum_e \langle \dot{g}(\tau)|e(\tau)\rangle\langle e(\tau)|\psi(\tau)\rangle \quad (8.13)$$

Now the first term is zero as we can see if we take derivative of  $\langle g(\tau)|g(\tau)\rangle = 1$ , and use the fact that for stoquastic Hamiltonian we can always choose all the states to be real, so  $\langle g(\tau)|\dot{g}(\tau)\rangle = \langle \dot{g}(\tau)|g(\tau)\rangle$ . The second terms contain amplitudes in the excited states  $\langle e(\tau)|\psi(\tau)\rangle$  which we assume to be small by p.t. So in the first order,

$$\frac{d}{d\tau}\langle g(\tau)|\psi(\tau)\rangle = 0, \quad \langle g(\tau)|\psi(\tau)\rangle = 1 \quad (8.14)$$

Now for the evolution of amplitudes of the excited states, we find (again, neglecting the higher orders of p.t.):

$$\frac{d}{d\tau}\langle e(\tau)|\psi(\tau)\rangle = \langle \dot{e}(\tau)|g(\tau)\rangle\langle g(\tau)|\psi(\tau)\rangle - \langle e(\tau)|\psi(\tau)\rangle \quad (8.15)$$

The steady state is such that the r.h.s vanishes, and is reached in  $O(1)$  time:

$$\langle e(\tau)|\psi(\tau)\rangle|_{steady} = \langle \dot{e}(\tau)|g(\tau)\rangle \quad (8.16)$$

Here we have used that  $\langle g(\tau)|\psi(\tau)\rangle = 1$ . Also note that  $\langle e(\tau)|g(\tau)\rangle = 0$ , thus  $\langle \dot{e}(\tau)|g(\tau)\rangle = -\langle e(\tau)|\dot{g}(\tau)\rangle$ . Finally, we can write the full steady state vector:

$$|\psi(\tau)\rangle|_{steady} = |g(\tau)\rangle - \sum_e |e(\tau)\rangle\langle e(\tau)|g(\tau)\rangle \quad (8.17)$$

We can collect the resolution of the identity (remember that  $\langle g(\tau)|g(\tau)\rangle = 0$ ):

$$|\psi(\tau)\rangle|_{steady} = |g(\tau)\rangle - |\dot{g}(\tau)\rangle \quad (8.18)$$

Now recall that the steady state takes  $O(1)$  time to equilibrate. So any changes in it that happen in the last interval  $\tau \in [T-1, T]$  will not have time to take effect. That "screens" the singularity in  $|\dot{g}(\tau)\rangle$ . Note that  $\tau^* = T-1$  is the same condition as  $(1-s^*)^3 T = 1$  which gave us  $s^*$ .

So what we expect from  $|\psi(T)\rangle$  is that it is well approximated by the steady state one relaxation time away, that is:

$$|\psi(T)\rangle \approx |\psi(T-1)\rangle|_{steady} = |g(\tau^*)\rangle - |\dot{g}(\tau^*)\rangle|_{\tau^*} \quad (8.19)$$

If we use the Taylor expansion around  $\tau^*$ :

$$|g(T)\rangle = |g(\tau^*)\rangle + |\dot{g}(\tau^*)\rangle|_{\tau^*} + O(|\ddot{g}(\tau^*)\rangle|_{\tau^*}) \quad (8.20)$$

The derivatives will turn out to be small, so we get a factor of two:

$$|\psi(T)\rangle \approx |g(T)\rangle - 2|\dot{g}(\tau^*)\rangle|_{\tau^*} \quad (8.21)$$

How far it is from the Gibbs state depends on the size of the correction  $|\dot{g}(\tau^*)\rangle|_{s^*}$ :

$$\langle E|\dot{g}(\tau^*)\rangle = \frac{d}{d\tau} \frac{e^{-\beta E/2}}{\sqrt{Z}} = \frac{1}{T} \frac{dt}{d\tau} \frac{dE}{ds} \frac{-\beta e^{-\beta E/2}/2}{\sqrt{Z}} - \frac{1}{2T} \frac{dt}{d\tau} \frac{e^{-\beta E/2}}{\sqrt{Z}} \frac{d \ln Z}{ds} \quad (8.22)$$

where we can use the numerical slopes to estimate  $\frac{dE'}{ds} \sim L(1-s)$  in the first term. We denote the amplitude of the deviation  $|\langle E|(-2)|\dot{g}(\tau^*)\rangle| = f(s)$ :

$$f(s) = \frac{1}{T} \frac{dt}{d\tau} \frac{dE}{ds} \frac{-\beta e^{-\beta E/2}}{\sqrt{Z}} \sim \frac{L}{\sqrt{Z}T} \frac{1}{(1-s)} \quad (8.23)$$

The second term adjusts overall scale of the steady state compared to  $|g(\tau)\rangle$ . Markov chain preserves the sum of probabilities, so we expect the equivalent dynamics to respect that, and that terms makes that happen.

The components of  $|g(\tau^*)\rangle$  are of order  $1/\sqrt{Z}$ . So at least while  $f\sqrt{Z} \ll 1$ , the probabilities will not be too far from their equilibrium values - the decay is working.

Intuitively, at position  $s$  the nonequilibrium state's amplitude deviation from the steady state is bounded by  $f$ . Let's calculate when  $f\sqrt{Z} = 0.1$ :

$$\frac{L}{T} \frac{1}{(1-s)} = 0.1 \quad \Rightarrow T(1-s)/(10L) = 1 \quad (8.24)$$

for  $L > 200$  this condition gives  $s < s^* = 0.98$ . Another way to put it:

$$\sqrt{Z}f(s^*) = \frac{L}{T} \frac{1}{(1/T)^{1/3}} = \frac{L}{T^{2/3}} \approx L/2000 \quad (8.25)$$

So this is the bound on relative deviation of amplitudes of  $|\psi(T)\rangle$  from  $|g(s^*)\rangle$ . Recall that the observed probability distribution is related to  $|\psi(T)\rangle$ :

$$|\psi(T)\rangle = P_G^{-1/2}P \quad (8.26)$$

Here  $P_G$  is a Gibbs state at  $s = 1$ .

If we square and add up the amplitudes of  $|\psi(T)\rangle - |g(T)\rangle$ , the relative error becomes an absolute error:

$$f\sqrt{Z} = \sqrt{((P - P_G)P_G^{-1/2})^T(P - P_G)P_G^{-1/2}} = \|(P - P_G^*)/\sqrt{P_G}\|_2 \leq L/2000 \quad (8.27)$$

That is the norm for which we predict a bound for D-wave. The precise number 2000 is to be taken with a grain of salt, as we dropped numerical factors along the way and didn't use the true relaxation rates for a chain. But we see that this construction lets one arrive to a bound on error  $< L/10L^*$  with some  $L^*$ . We also note that distributions can be traced over the complement of a region  $R$ . Let's look at the expression again:

$$P = P_G^{1/2}|\psi(T)\rangle = P_G - 2P_G^{1/2}|g(\tau)\rangle|_{\tau^*} = P_G - \frac{1}{T(1-s^*)^2} \frac{dE - \beta e^{-\beta E}}{ds} + \text{norma-n} \quad (8.28)$$

First lets express the correction in terms of spins in z-basis:

$$P(s_z) = P_G(s_z) \left( 1 + \beta \frac{1}{T(1-s^*)^2} \frac{dE^{s^*}(s_z)}{ds} + \text{norma-n} \right) \quad (8.29)$$

The factor  $L$  comes from  $E^{s^*}(s_z)$  - the energy of the level corresponding to  $s_z$  at  $s^*$ , for which the perturbative expression is valid. Denote:

$$\frac{dE^{s^*}(s_z)}{ds} = (1-s^*) \sum_i O_i(s_z) \quad (8.30)$$

where each  $O_i(s_z)$  is a norm  $O(1)$  tailed function (operator) of  $s_z$  around site  $i$ . We truncate it with some constant collar  $c$ . Now we take a trace over  $\bar{R}$ :

$$\mathrm{tr}_{\bar{R}}P(s_z) = \mathrm{tr}_{\bar{R}}P_G(s_z) \left( 1 + \beta \frac{1}{T(1-s^*)} \sum_{i \in R+c} O_i(s_z) + \text{norma-n} \right) \quad (8.31)$$

We see that the only spin-dependent corrections are from operators  $O_i$  that are in the collared region  $R + c$ . The rest just contribute to the overall normalization. So the deviation of the distribution observed in  $R$  from the trace of a Gibbs state is:

$$\mathrm{tr}_{\bar{R}}P(s_z) - \mathrm{tr}_{\bar{R}}P_G(s_z) = \beta(1-s^*)^2 \mathrm{tr}_{\bar{R}}P_G(s_z) \sum_{i \in R+c} O_i(s_z) + \text{norma-n} \quad (8.32)$$

The sum of the absolute values of the differences (the 1-norm) is bounded as:

$$\|\mathrm{tr}_{\bar{R}}P(s_z) - \mathrm{tr}_{\bar{R}}P_G(s_z)\|_1 = \beta(1-s^*)^2(R+2c) = \frac{R+2c}{T^{2/3}} \quad (8.33)$$

Unfortunately, it's not easy to calculate either of the two norms for a distribution from which we only have a sample. But we see that all the deviations come from operators  $O_i$  that have a tailed decay with a small exponent  $1/(-\ln\gamma)$ . So we expect all the deviations of  $P$  from  $P_G$  to come from traced distributions over just a few neighbors.

### 8.3 Distributions as slopes, small systems

Here we will discuss how slopes of levels near the ground state can be measured after the protocol. First of all, let's define the relative slopes carefully: there is an overall scale factor that contributes to every slope. For example, for the counting of the number of crossings the relative slopes generated by a Hamiltonian  $sH$  (where  $H$  is independent on  $s$ ) should be counted as zero (because there are no crossings) even though the levels appear to go at different angles. We can exclude the effect of rescaling the Hamiltonian by adding the scale transform. As the first step of it, one needs to find average slopes at different ranges of energy. Then one finds the point where they intersect (or average of those intersections), and rescales the slopes so as to send that point to infinity.

The relative slopes are  $O(L)$  in the system size. The density of states is exponential as  $L \exp(\sqrt{L})$  even in the constant window of energies above the ground state (see the Supplementary material to Cuevas et al., 2012). Correspondingly, one gets  $O(L^2 e^{\sqrt{L}})$  level crossings with the ground state throughout the protocol. The coefficient should be such that at  $L = 10$  there's still 0 to 1 crossings. Let's assume

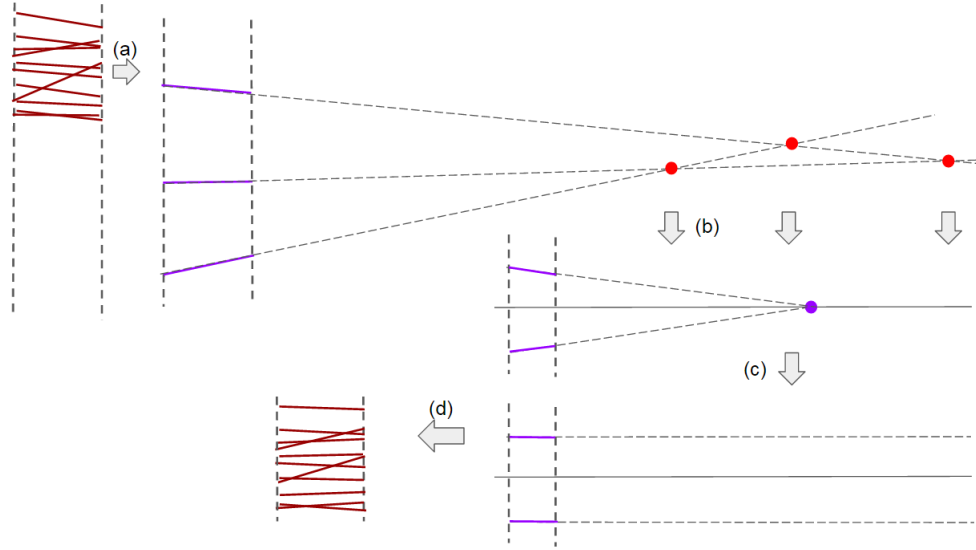


Figure 8.2: The Hamiltonian rescaling procedure used to determine slopes involved in *frequency* of resonances. Steps (a) and (b) are averaging, then at step (c,d) the transformation is found and applied to original slopes

$L^2 e^{\sqrt{L}}/2000$  dependence. There's a special point  $s^* = 1 - (1/T\kappa)^{1/3} = 0.98$ , before which the effects of the crossings have enough time to be washed away by the environment.

How many crossings are in  $[0.98, 1]$ ? If the slopes obey  $1 - s$  like they do for the midband, we'll get an extra numerical suppression of  $(1 - s)^2 = 0.0004$  of the total number. Now it's  $0.0004 L^2 e^{\sqrt{L}}/2000$ . So there will be a system size  $L^* = 60$  when the first crossing falls into this range. Among the crossings there are a few ones of size 1, 2 such that their slow passing can significantly mix the occupancies. But the probability that those fall into the range of  $[0.98, 1]$  remains very small for all sizes D-wave has to offer. So we don't need to worry about LZ formula, just the Gibbs probabilities of the appropriate logical spin Hamiltonian. We also note that for excited states crossings appear for system sizes smaller than  $L^*$ .

A simplified model derived above is that the end state is

$$P(s_z) = P_G(s_z) \left( 1 + \beta(1 - s^*) \frac{dE^{s^*}(s_z)}{ds} + \text{norma-n} \right) \approx P_G^{s^*}(s_z) \quad (8.34)$$

which corresponds to the Gibbs distributions at energies  $E(s^*)$ . So the D-wave machine is preparing a Gibbs distribution at  $s^* = 0.98$ , from which for small system sizes we can extract the energies. Note that every population whose statistics have been observed ( $\{P_i\}$  for different states  $i$ ) can be interpreted as energies via

$E_i = T \ln P_i$  where  $T = 1/\beta$  is the temperature. There's an overall constant that remains arbitrary. It can be set by setting the smallest energy to zero. This allows one to extract energy slopes near z-Hamiltonian from D-wave data! Pictorially, one just positions two sets of levels 0.02 apart in  $s$ , one for z-Hamiltonian, and ones extracted from the "permuted" distribution. Note that in the actual system levels go as  $(1 - s)^2$ , not as straight lines, which introduces a factor of two in the estimate. Of course, if the p.t. is valid, one can extract the same picture the way (B. Altshuler, Krovi, and Roland, 2010) did it in poly-time, so the D-wave doesn't offer any speedup here. Also, for any big system it takes exponentially long to collect the distribution precisely.

In reality the extracted  $E_i$  can be placed on the level at  $s_i$  somewhere between, say,  $s_1 = 0.9$  and  $s = 1$ . Indeed, at  $s_1$  the state is Gibbs with a good precision. The equation  $E_i = T \ln P_i$  will obtain an exact match with the spectrum if applied for  $s_1$  populations. Then the system fails to follow the level changes, so the populations remain closer to the past Gibbs state at  $s_1$ . How close depends on the rate of decay of an individual level, and the detail of the Markov process. To the zeroth approximation, all of the  $s_i = s^* = 0.98$ . In practice there is a scatter, in some extreme cases some points lie even outside  $[0.9, 1]$ , but we neglect that.

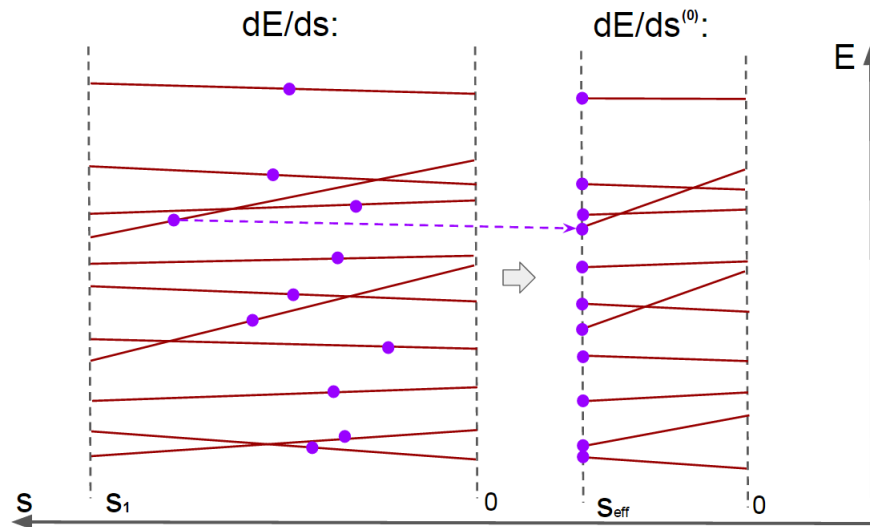


Figure 8.3: The data processing procedure where end populations are interpreted as points along the evolution of the level, and then they are collapsed to  $s^* = 0.98$  and used to determine a first approximation to slopes.

The zeroth approximation  $dE/ds^{(0)}$  can be obtained by investigation just one probability distribution for a specific  $T_{prot}$ . The position of  $s^*$  depends on  $T_{prot}$ .

To obtain the first approximation, one needs to use the specific properties of the underlying Markov process. We do not control the error between the zeroth and the first approximation. Both adjustments are really weak in  $1 - s_{eff} = 0.02$ , but they are of the same order. So one needs to study the Markov process to fit those (supposedly small for small system sizes) differences between  $P$  and  $P_G$ . Now we know that those differences are only due to local  $O_i$ , so simulating a small system size and then truncating a few sites at each end should give the same  $\text{tr}_{\bar{R}} P(s_z)$  as the real experiment.

Let's discuss what can be done with a Markov process. The Markov matrix has rates  $P_{i \rightarrow j}$  obeying the detailed balance:

$$\frac{P_{i \rightarrow j}}{P_{j \rightarrow i}} = e^{\beta E_{ij}} \quad (8.35)$$

So  $P_{i \rightarrow j} = \kappa_{ij} e^{\beta E_{ij}}$ . This equation can be derived from a Lindblad equation as described in the beginning of the Chapter. The diagonal and offdiagonal evolution decouples for it, and the offdiagonal terms decay really fast. What's left for the diagonal is the Markov process obeying the above. The Lindblad equation itself is theoretically not a good approximation for a strong bath, one may consider looking at the Redfield instead. In practice we did not see any serious differences.

The specific terms in Lindblad are well known, but one needs exact eigenstates to calculate the matrix elements  $\langle \phi | Z | \psi \rangle$ . Or one uses the first few steps of the Imbrie circuit and neglects all the rest. Approximate calculation of these matrix elements is possible (one should be contempt with elements between states one spin flip away), since the Imbrie's procedure is poly-time for a finite number of steps, so one can obtain the form of the Markov chain.

Since we only talk about small system sizes here, all the approaches are feasible. The Redfield is probably the best compromise between computational efficiency and simplicity: one can easily simulate ED sizes. We note that a patch in a bigger system can be selected and the distribution can be traced to what's in the center of the patch. Now back in the approximation where all the decay singular values were the same, the nonequilibrium state is a Gibbs state of the Hamiltonian at another time. The validity of the truncation to a small patch can be checked if we compare  $\text{tr}_{\bar{C}} e^{-\beta H}$  for different total system sizes. By the transfer matrix method outlined in the Appendix, this distribution converges starting from some system size  $C + 2\xi$  where  $\xi = O(1)$  is the distance at which classical correlations decay. We hope that the same applies to nonequilibrium states extracted using true decay rates.

Now note that comparing the slopes extracted from  $\ln(\text{tr}_{\bar{c}} P)$  for different  $s'$  may contain an indicator of the MBL phase vs. the extended phase, just like the closed system slopes did in Chapter 5. The boundary effects introduced in the truncation can be estimated using the Gibbs state approximation. After blocking the effective Hamiltonian into 2-site terms, each truncated side just introduces an effective magnetic field on the corresponding end spin. The dependence of that magnetic field on  $s$  is not much stronger than dependence of other couplings. So we expect it to contribute a system-size independent constant into the slope. Of course, in our system it's always MBL near the ground state and the z-Hamiltonian. Even if there exists a rapidly mixing system with disorder that becomes delocalized at  $s^*$ , only at a very large system sizes will the band around energy  $\sim$  temperature  $T$  with level spacings  $\exp(-\sqrt{L})$  start to get delocalized.

To conclude, let's answer a somewhat simpler question: what would be the ground state population of a chain at the end of the protocol depending on the system size? It varies from disorder realization to realization, but for small sizes it is the Gibbs state, so the occupation of one state is  $O(\exp(-L))$  and random (occupies a band around  $\exp(-L)$  if sampled from different realizations). There are corrections to the Gibbs value because of the failure of decay at the very end regardless of crossings. We get the Gibbs value for  $s = 0.98$  roughly, and it stops changing after that. What happens at  $L^* = 60$  when the first crossing appears is that the end probabilities of the ground and the first excited state can now be out of order in magnitude. Surprisingly, we see it much earlier in the numerics.

### **Non-monotonic population**

For a simulation of a 1d MBL chain in the D-wave protocol one observes an irregularity in populations of final states. Instead of population following the Gibbs state with some smooth correction, there are preferred states appearing that depend on the speed of the driving and the level layout. This is contrasted with non-MBL systems, where preferred states are not expected to appear, at least the populations should remain smooth typically. Such irregularities are a suppressed remnants of the preferred states in the closed system adiabatic evolution. It is indeed observed for many disorder realizations, at least for smaller protocol times  $T = 1000$  and system sizes  $L = 10$ . However, even for clean transverse field Ising model we observe step-like behavior in populations that is sometimes non-monotonic in energy.

One would think that investigating monotonicity will lead to an indicator of the

MBL vs. extended phase. The biggest problem with this approach is that the non-monotonicity is a qualitative, not quantitative feature. One interesting quantitative consequence of the non-monotonicity is the possibility of a work extraction. Even from the monotonic non-Gibbs states one can extract some work. We investigated some of the measures from quantum thermodynamics, related to the majorization and resource theories, following a picture from (Michał Horodecki and Oppenheim, 2013). But we don't think there can be any quantitative measure that works as an "order parameter" related to the non-monotonicity of the level populations with energy.

#### 8.4 Distributions too thin to sample

So, a run of a size  $L = 100$  chain on the D-wave machine will return a sample from a distribution  $P(s)$ , where we won't see two states twice unless we run it for an exponential time. We can still trace out most of the spins to calculate local density matrices. Those should be fairly consistent with the local Gibbs state.

Only sizes up to  $L = 20$  are accessible for direct comparison with the Gibbs state due to memory limitations of the classical software and a high number  $2^{20} = 10^6$  of runs of the machine. For bigger sizes, the overall error grows as  $L$ , but it is just compounded from small local errors. When at  $L^* = 60$  the first predicted jump crossing introduces a permutation in the global probability, it is still reflected in the global Gibbs state at  $s'$  if we use z-projections as state labels. Will this effect be washed out by the influence of truncation in simple local Gibbs states? If we only compare local density matrices, one may be concerned that something global is missing from the picture. Here we introduce a possible measure of error that is applicable when we can only sample from a distribution: the Bayesian likelihoods. Essentially we calculate the logprobability of the observed data with the assumed distribution. We expect the logprobability to grow if one uses Gibbs state at  $s'$  as compared to classical system Gibbs state. One can improve the likelihood even more by using the decay models, or other numerical methods. If one has a hypothesis as a matrix product density operator, one can easily calculate logprobability.

Let's see how to compute likelihoods (= free energies) for the Gibbs cases. We get a bitstring. With ED, we find eigenstates for  $H(s')$  of patches that match the bitstring. Then we calculate the expectation value of the Hamiltonian terms in the middle of the patch. By scanning like this, we can get energy that is this eigenvalue, thus logprobability. We can compare that to pure z. Constants are partition functions of

pure  $z$  Hamiltonian and the quantum one. The first one can be calculated via the transfer matrix method, the second one - via trotterization of  $e^{-\beta H}$  and contraction of it. Both poly-time. The likelihood is calculated as:

$$-\frac{\log P}{N_{runs}} = Av_{s_n} X(s_n) + \ln \sum_s e^{-X(s_n)} \quad (8.36)$$

where  $X(s_n)$  is the  $\beta E(s_n)$  of string  $s_n$  we're trying to use. One can easily see that the function on the right is minimized for  $X^*$  s.t. strings are distributed  $\sim e^{-X^*(s_n)}$ . The value at the minimum is the entropy of this state. One can plug in the classical Hamiltonian  $X = \beta H_z$  at the end of the protocol as the prior, and the diagonalized quantum Hamiltonian  $X' = \beta U H' U^\dagger$  as the competing hypothesis. The second one should be closer to the underlying entropy of the distribution we sample.

For calculation of quantum partition function, one can do without trotter. Note that  $\langle \lambda | H | \lambda \rangle = \sum_i \langle \lambda | H_i | \lambda \rangle$ , and each  $H_i$  just spreads by a small amount by the Imbrie circuit. Take  $L$  blocks around each  $H_i$  at the biggest size that is accessible by ED. Label the states by  $z$ -spin expectations rounded to  $\pm 1$ . Now use the found averages of  $H_i$  to build a classical Hamiltonian that is local on ED size. Its free energy can be calculated via the transfer matrix.

## GENERALIZATION TO OTHER SYSTEMS

**9.1 Efficient simulation of big systems via master equation**

Consider a more general system  $sH_z + (1 - s)H_x$ , possibly in 2d. Assume that at  $s = 0.8$  the protocol is stopped and the system thermalizes for arbitrary long time. The thermal state is expected to be described by a tensor network for any system with exponentially decaying correlations. For the further evolution one just needs to update it via a local master equation (it is easier to use the equivalent stochastic shroedinger equation though). It is only known how to do the required tensor contractions and the truncation of entanglement in the case of Matrix Product States (1d systems). Now there's another method that is so naive no one to our knowledge seriously investigated it, but somehow it seems to be applicable at least in this work. One initially assumes that the state is thermal along the way. Then one can calculate time-dependent correlation function along the protocol. Master equation for a patch of a closed system depends on the full dynamics only through  $C_{ij}(t) = \langle A_i(t)A_j \rangle$  on the boundary. If  $C_{ij}(t)$  decays sufficiently fast with  $|i - j|$ , we can self-consistently simulate big systems! One can evolve each patch in a bath of thermal time-dependent correlation functions of its neighbors. This will give some evolution of the patches computed in poly-time. Then one can use these patches to calculate correlation functions one more time, to plug in the new evolution. One repeats the steps of this procedure until convergence. There's no guarantee it converges, or does so in poly-time. But if it does, we get a self-consistent answer. That is, we know density matrices everywhere, and we know that their local time-evolution looks like the generator was our time-dependent Hamiltonian.

A simple counterexample when this method fails will be two wavepackets after the beamsplitter. In time that's related to a Lieb-Robinson bound of the system and the size of the patch this will fail to describe reality. All the interference is lost. So some effects like weak localization correction will also be out of reach, or will get adjusted by a correction depending on the size of the patch. But besides that, maybe the long-range interference is not that important for D-wave. It will be a good method to compare the experimental results to.

Another interesting application for this method are all-to-all connected systems. The

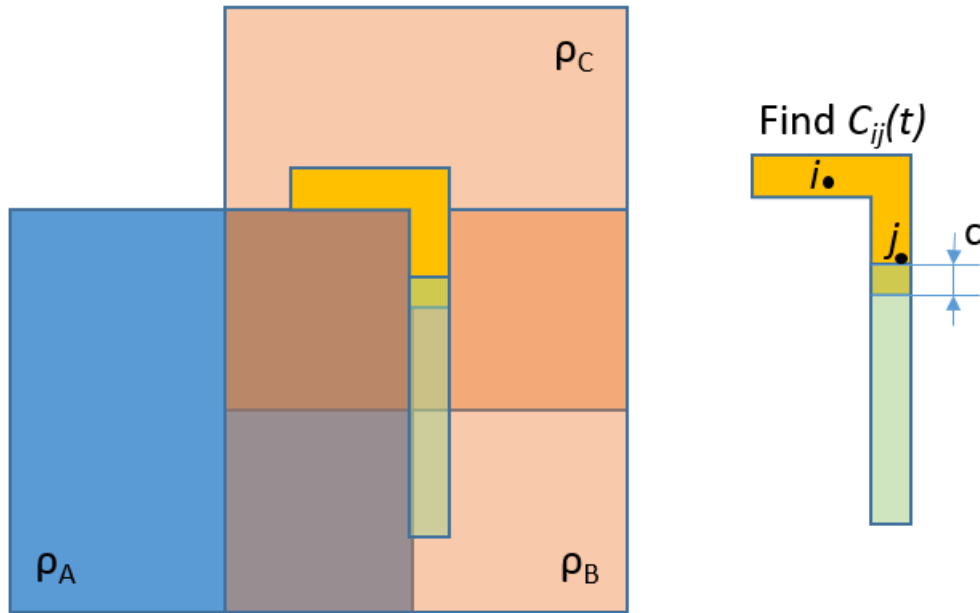


Figure 9.1: Layout of paths for a 2d system

mean field is exact in some calculations like the cavity method, and this method may also benefit from a boost in accuracy like that. The only to our knowledge relevant result in mathematical physics is LRB on a complete graph (Lashkari et al., 2013), which allows the authors to prove that for  $t \sim \log L$  ( $\log k$  for coordination number  $k$ ) the state of the system can be approximated by a pure product state. Clearly it proves the validity of method suggested here for at least that time. A more tight error estimate for it is an open question.

We can also use the logarithmic LRB for MBL systems to establish that for some patch size  $n$  the time for which the above method is valid is  $\exp(n) > T(1 - s^*)$  that's left to travel to  $z$ -Hamiltonian. Our work proved that one is allowed to use a much smaller patch for 1d chains.

## BIBLIOGRAPHY

- Abanin, Dmitry A., Wojciech De Roeck, and François Huveneers (2016). “Theory of many-body localization in periodically driven systems”. In: *Annals of Physics* 372, pp. 1–11. URL: <http://www.sciencedirect.com/science/article/pii/S000349161630001X>.
- Alicki, R., M. Fannes, and M. Horodecki (2009). “On thermalization in Kitaev’s 2D model”. In: *Journal of Physics A: Mathematical and Theoretical* 42.6. URL: <http://iopscience.iop.org/article/10.1088/1751-8113/42/6/065303/meta>.
- Altshuler, B., Hari Krovi, and Jérémie Roland (2010). “Anderson localization makes adiabatic quantum optimization fail”. In: *PNAS* 107.28, pp. 12446–12450. DOI: 10.1073/pnas.1002116107. URL: <http://www.pnas.org/content/107/28/12446.short>.
- Amin, M. H. S. and Dmitri V. Averin (2008). “Macroscopic Resonant Tunneling in the Presence of Low Frequency Noise”. In: *Phys. Rev. Lett.* 100, p. 197001. URL: <https://journals.aps.org/prl/abstract/10.1103/PhysRevLett.100.197001>.
- Anderson, P. W. (1958). “Absence of Diffusion in Certain Random Lattices”. In: *Phys. Rev.* 109, p. 1492.
- Bardarson, Jens H., Frank Pollmann, and Joel E. Moore (2012). “Unbounded Growth of Entanglement in Models of Many-Body Localization”. In: *Phys. Rev. Lett.* 109, p. 017202. URL: <https://journals.aps.org/prl/abstract/10.1103/PhysRevLett.109.017202>.
- Basko, D.M., I.L. Aleiner, and B.L. Altshuler (2006). “Metal–insulator transition in a weakly interacting many-electron system with localized single-particle states”. In: *Annals of Physics* 321 (5), pp. 1126–1205.
- Bauer, Bela and Chetan Nayak (2013). “Area laws in a many-body localized state and its implications for topological order”. In: *J. Stat. Mech.* P09005. URL: <https://arxiv.org/abs/1306.5753v2>.
- Bravyi, S., M. B. Hastings, and F. Verstraete (2006). “Lieb-Robinson bounds and the generation of correlations and topological quantum order”. In: *Physical Review Letters* 97.050401. URL: <http://arxiv.org/pdf/quant-ph/0603121v1.pdf>.
- Bravyi, S. and Robert Koenig (2012). “Disorder-assisted error correction in Majorana chains”. In: *Communications in Mathematical Physics* 316 (3), pp. 641–692. URL: <https://link.springer.com/article/10.1007%2Fs00220-012-1606-9?LI=true>.

- Cao, Gang et al. (2013). “Ultrafast universal quantum control of a quantum-dot charge qubit using Landau–Zener–Stückelberg interference”. In: *Nature Communications* 4.1401. URL: <https://www.nature.com/articles/ncomms2412>.
- Chandran, Anushya et al. (2015). “Constructing local integrals of motion in the many-body localized phase”. In: *Phys. Rev. B* 91, p. 085425. URL: <https://journals.aps.org/prb/abstract/10.1103/PhysRevB.91.085425>.
- Chen, Xie et al. (2012). “Symmetry-Protected Topological Orders in Interacting Bosonic Systems”. In: *Science* 338 (6114), pp. 1604–1606. DOI: 10.1126/science.1227224. URL: <http://science.sciencemag.org/content/338/6114/1604>.
- Cheung, Donny, Peter Høyer, and Nathan Wiebe (2011). “Improved error bounds for the adiabatic approximation”. In: *Journal of Physics A: Mathematical and Theoretical* 44.41. URL: <http://iopscience.iop.org/article/10.1088/1751-8113/44/41/415302/meta>.
- Childs, A. M., D. W. Leung, and G. Vidal (2004). “Reversible simulation of bipartite product Hamiltonians”. In: *IEEE Transactions on Information Theory* 50 (6). URL: <http://ieeexplore.ieee.org/abstract/document/1302297/?reload=true>.
- Cuevas, Emilio et al. (2012). “Level statistics of disordered spin-1/2 systems and materials with localized Cooper pairs”. In: *Nature Communications* 3.1128. DOI: 10.1038/ncomms2115. URL: <https://www.nature.com/articles/ncomms2115>.
- Dickson, N.G. et al. (2013). “Thermally assisted quantum annealing of a 16-qubit problem”. In: *Nature Communications* 4, p. 1903. URL: <https://www.nature.com/articles/ncomms2920>.
- Gosset, David and Evgeny Mozgunov (2016). “Local gap threshold for frustration-free spin systems”. In: *Journal of Mathematical Physics* 57.9. URL: <http://aip.scitation.org/doi/abs/10.1063/1.4962337>.
- Hamza, Eman, Robert Sims, and Günter Stolz (2012). “Dynamical Localization in Disordered Quantum Spin Systems”. In: *Communications in Mathematical Physics* 315 (1), pp. 215–239. DOI: 10.1007/s00220-012-1544-6. URL: <https://link.springer.com/article/10.1007%2Fs00220-012-1544-6?LI=true>.
- Hastings, M. B. (2009). “Making Almost Commuting Matrices Commute”. In: *Communications in Mathematical Physics* 291 (2), pp. 321–345. URL: <https://link.springer.com/article/10.1007%2Fs00220-009-0877-2?LI=true>.
- Hastings, Matthew B. and Spyridon Michalakis (2015). “Quantization of Hall Conductance for Interacting Electrons on a Torus”. In: *Communications in Mathematical Physics* 334 (1), pp. 433–471. URL: <https://link.springer.com/article/10.1007%2Fs00220-014-2167-x>.

- Horodecki, Michał and Jonathan Oppenheim (2013). “Fundamental limitations for quantum and nanoscale thermodynamics”. In: *Nature Communications* 4.2059. DOI: 10.1038/ncomms3059. URL: <https://www.nature.com/articles/ncomms3059>.
- Imbrie, John Z. (2016). “On Many-Body Localization for Quantum Spin Chains”. In: *J. Stat. Phys.* 163, p. 998. DOI: 10.1007/s10955-016-1508-x.
- Jansen, Sabine, Mary-Beth Ruskai, and Ruedi Seiler (2007). “Bounds for the adiabatic approximation with applications to quantum computation”. In: *Journal of Mathematical Physics* 48, p. 102111. DOI: <http://dx.doi.org/10.1063/1.2798382>. URL: <http://aip.scitation.org/doi/10.1063/1.2798382>.
- Johansson, J. et al. (2009). “Landau-Zener transitions in a superconducting flux qubit”. In: *Phys. Rev. B* 80, p. 012507. URL: <https://journals.aps.org/prb/abstract/10.1103/PhysRevB.80.012507>.
- Khemani, Vedika and Rahul Nandkishore and S. L. Sondhi (2015). “Nonlocal adiabatic response of a localized system to local manipulations”. In: *Nature Physics* 11, pp. 560–565. URL: <http://www.nature.com/nphys/journal/v11/n7/abs/nphys3344.html>.
- Kim, Isaac H., Anushya Chandran, and Dmitry A. Abanin (2014). “Local integrals of motion and the logarithmic lightcone in many-body localized systems”. In: URL: <https://arxiv.org/abs/1412.3073>.
- Kitaev, Alexei (2009). “Periodic table for topological insulators and superconductors”. In: *AIP Conference Proceedings* 1134 (22). DOI: <http://dx.doi.org/10.1063/1.3149495>. URL: <http://aip.scitation.org/doi/abs/10.1063/1.3149495>.
- Kjall, Jonas A., Jens H. Bardarson, and Frank Pollmann (2014). “Many-Body Localization in a Disordered Quantum Ising Chain”. In: *Physical review letters* 113, p. 107204. URL: <http://journals.aps.org/prl/pdf/10.1103/PhysRevLett.113.107204>.
- Knabe, S. (1988). “Energy gaps and elementary excitations for certain VBS-quantum antiferromagnets”. In: *J. Stat. Phys.* 52 (3-4), pp. 627–638. DOI: <http://dx.doi.org/10.1007/BF01019721>. URL: <https://link.springer.com/article/10.1007/BF01019721>.
- Lashkari, Nima et al. (2013). “Towards the fast scrambling conjecture”. In: *Journal of High Energy Physics* 2013:22.2059. URL: <https://link.springer.com/article/10.1007%2FJHEP04%282013%29022>.
- Lieb, E. H. and D. W. Robinson (1972). “The finite group velocity of quantum spin systems”. In: *Communications in Mathematical Physics* 28, pp. 251–257. DOI: 10.1007/BF01645779. URL: <https://link.springer.com/article/10.1007%2Fs00220-012-1544-6?LI=true>.

- Medvedyeva, Mariya V., Tomaž Prosen, and Marko Žnidarič (2016). “Influence of dephasing on many-body localization”. In: *Phys. Rev. B* 93, p. 094205. URL: <https://journals.aps.org/prb/abstract/10.1103/PhysRevB.93.094205>.
- Mozgunov, Evgeny (2016). “Local Master Equation for Small Temperatures”. In: *arXiv:1611.04188*. URL: <https://arxiv.org/abs/1611.04188>.
- Oganesyan, Vadim and David A. Huse (2007). “Localization of interacting fermions at high temperature”. In: *Phys. Rev. B* 75, p. 155111. URL: <http://journals.aps.org/prb/abstract/10.1103/PhysRevB.75.155111>.
- Ponte, Pedro et al. (2015). “Many-Body Localization in Periodically Driven Systems”. In: *Phys. Rev. Lett.* 114, p. 140401. URL: <https://journals.aps.org/prl/abstract/10.1103/PhysRevLett.114.140401>.
- Rehn, Jorge et al. (2016). “How periodic driving heats a disordered quantum spin chain”. In: *Phys. Rev. B* 94, 020201(R). URL: <https://journals.aps.org/prb/abstract/10.1103/PhysRevB.94.020201>.
- Serbyn, Maksym, Z. Papić, and Dmitry A. Abanin (2013). “Local conservation laws and the structure of the many-body localized states”. In: *Physical review letters* 111 (12), p. 127201.
- Thouless, D. J. (1977). “Maximum metallic resistance in thin wires”. In: *Physical Review Letters* 39 (18), pp. 1167–1169.

*Appendix A*

## TRANSFER MATRICES

Is there a local representation of the disordered z-chain? We're interested in being able to sum over spins up to position  $i_0$ . The probabilities are:

$$P(s) = \frac{1}{Z} \prod_i e^{-\beta H_i(s_i, s_{i+1})} \quad (\text{A.1})$$

Consider a left portion of the chain up to spin  $i_0$ :

$$H^{(i_0)} = \sum_{i < i_0} H_i(s_i, s_{i+1}) \quad (\text{A.2})$$

In this chain, the probabilities of different values of  $s_{i_0}$  can be found:

$$P^L(s_{i_0}) = \frac{1}{Z_{i_0}} \sum_{s_i, i < i_0} e^{-\beta H^{(i_0)}} \quad (\text{A.3})$$

Note that the numerator  $P^L(s_{i_0})Z_{i_0}$  can be found recursively:

$$P^L(s_{i_0})Z_{i_0} = \sum_{s_{i_0-1}} e^{-\beta H_{i_0}(s_{i_0-1}, s_{i_0})} P^L(s_{i_0-1})Z_{i_0-1} \quad (\text{A.4})$$

The normalization factor can be chosen at every step such that  $\sum_s P^L(s) = 1$ . One can also include the normalization factors into the equation on probabilities:

$$P_{i_0}^L = T P_{i_0-1}^L \quad (\text{A.5})$$

where  $T$  is a 2x2 transfer matrix. Computing transfer matrices and their products takes poly-time. Using transfer matrices, any correlation function of local operators can also be computed in poly-time. In particular, we can compute a joint probability of finite number  $k$  of (possibly distant) spins. That would be equivalent to knowing (after poly-time of effort) any density matrix of size that can fit in our memory.

But note that it doesn't give us low-lying states immediately! Even though we know the probability  $P(s) = \frac{1}{Z} \prod_i e^{-\beta H_i(s_i, s_{i+1})}$  of every state (can compute it for one state in poly-time), we don't know which are the likely states. That's counterintuitive because we seem to have what we like to call "efficient description", yet to produce a sample from this distribution we need some extra work.

**Proposition:** we can find polynomially many low-lying states in poly-time.

Unfortunately, they're not going to contain  $> 1/2$  of all the probability distribution. One can imagine a system at high-infinite temperature, where one needs to know exponentially many likely states to get to  $1/2$  of probability distribution. But note that if energies scale as  $O(L)$ , then this argument requires corresponding temperature also scales as  $O(L)$ . For temperature that stays finite, it really all depends on the density of states. One needs to solve the following system:

$$Z = \int dE \rho(E) e^{-\beta E}, \quad \int dE \rho(E) = 2^L, \quad Z/2 = \int_0^{E^*} dE \rho(E) e^{-\beta E} \quad (\text{A.6})$$

where  $E$  is counted from the bottom of the band. Then the number of states that we want to know (that we will see in the machine) is:

$$N = \int_0^{E^*} dE \rho(E) \quad (\text{A.7})$$

if it were  $N = \text{poly}(L)$ , then the method below is useful. If  $N = \exp(L)$ , there's no way to list so many levels, but we can sample from them with Gibbs probability using Monte Carlo. On the experimental size, we'll need to spend exponential time sampling from this distribution to collect any data about underlying many-body probabilities. Shorter samples can still be compared to theory using Bayesian methods as was discussed in "Distributions too thin to sample".

Could it be that for a chain Hamiltonian  $N = \text{poly}(L)$ ? No. Note that for random diagonal that's  $O(L)$  in width  $N = \exp(L)$ . Indeed, temperature is finite, and we integrate exponentially big density of states over a finite interval. Random chain is more like independent spins in random field. In that case, density of states is  $L e^{\sqrt{L}E}$  according to Feigelman, Cuevas. This will give  $E^* \sim e^{L/\beta^2}$  and  $N^* = \exp(L)$ . Let's see if we can arrive to this.

Let's start with a non-random chain. The energy only depends on magnetization, the degeneracies of equally spaced levels are  $1, L, L^2/2, L^3/6, \dots$ . That suggests that for a finite interval around the ground state the density of states is  $O(L)$ . If one prepares a thermal state of this system though, each spin just has a probability  $p_e \sim e^{-\beta h}$  to be excited, and  $1 - p_e$  to be down. That means that any one configuration has probability  $< \max(p_e, 1 - p_e)^L$ . So one needs to sum at least  $N \sim \exp(L)$  of them to get anything finite. Same arguments hold for a random chain with lower bound on absolute value of local magnetic field.

If there's no lower bound, one may just consider the half of spins that have a lower bound, and repeat an argument for them. Even if the rest can be represented by just

one state, the resulting representation will still have  $N \sim \exp L$  states. So the two limiting cases both have  $N \sim \exp L$  typical states. The precise calculation for a chain is not as simple, but we expect that it also has  $N \sim \exp L$  typical states. In the main text we were also using an estimate on the typical probabilities  $P(E) \sim \exp(-L)$  that can be derived from the above expressions.

Let's still describe how to find poly $L$  lowest states in poly-time. It's not clear what we would need it for at the moment. The ground state can be found by the following procedure that scans the chain from one end to another. We start with two possibilities: spin up and spin down. We keep both of them in memory. The next spin is also up or down. If it is up, there are two states where the previous was up or down respectively. We compare their energies up till this point. The one with bigger energy surely will not be the ground state, because it will have at least the same energy in the remaining part. So we forget that one from the memory. Same for the last spin down. We again have two states written in our memory, different by the last spin at the very least, and their energies. We repeat the step with the next spin. At the end of the chain, we choose the smallest out of two.

The procedure above gives us an unambiguous ground state in  $O(L)$  time. It's harder to find first excited state. We know that it should be different from GS in at least one spin. We try flipping each one of  $L$  spins, and then repeat the minimization procedure with that spin fixed. That takes  $O(L^2)$ , but the smallest energy we find is the 1st excited state. We also record all the other energies we find. For the 2nd excited state, we need to try to flip every spin of the 1st excited state, and compare all the  $2L-1$  energies we have for flips away from GS or excited state. The smallest of those will be 2nd excited state. The procedure can be repeated as many times as one wants, finding next excited state always takes  $O(L^2)$ .

Finally, let's say a few words on locality. If the state has decay of correlations (which 1d essentially always has), then the transfer matrix multiplied several time will approximately have rank 1. That means that after a few sites the boundary conditions do not matter. And that means that we can just use the Gibbs state of a patch of Hamiltonian to estimate the density matrix (= joint probability distribution) in the middle of the patch. The accuracy will be related to the width of the collar of the patch. If correlations decay exponentially, the accuracy will be exponential in the width, if polynomially - polynomial.

So we don't even need to calculate transfer matrices - just calculate the distribution for a patch of, say, 20 spins, and then take the trace over the 7-spin collar on each

site, to obtain something close to the true distribution of the middle 6 spins.

Now we are ready to discuss the quantum case. By Imbrie's construction, it is reduced to the above by finite depth circuit (we throw away exponentially small rotations). The only difference is that the Hamiltonian is not nearest neighbor, but instead has exponentially decaying long-range interactions. To deal with that, we block sites until we can throw away non-nearest neighbor interactions. Then we are back to nearest neighbor classical chain, and can apply the techniques above. Of course, it's nontrivial to show that exponential tails lead to exponentially small errors in any of the quantities of interest. It is possible that it can only be shown in the presence of exp. decay of correlations. But we do not concern ourselves with those proofs here.

There's an easier way to obtain something like transfer matrix approach. The Gibbs state  $e^{-\beta H}$  can be trotterized, and then split into local gates. Then we can contract legs of the left portion of the tensor network to come up with an equivalent of  $P_i^L$ , but now with a lot (but still finite number) of virtual legs sticking out. Then we consider a vertical array of local gates that advances that tensor by 2 steps. That would be our new transfer matrix. The same consideration about decay of correlation and approximate rank 1 applies, even though contraction can be performed in poly-time. Using this object, we demonstrate that again the patch density matrices should give a good approximation if the approximate rank 1 condition holds.

But how do we sample from a distribution? A local density matrix can be fully reconstructed, but then what? Same question for classical case, how do we sample from Gibbs, instead of just finding low-lying states one by one? Markov chain Monte Carlo is one thing that definitely does that after the "equilibration time" that is somewhere between const and  $\text{poly}(L)$ . How to do it for the quantum case? Well it only takes poly-time to find one joint probability of measuring a spin string (by contracting with appropriate projectors). Then one can attempt an MC step to another string, and find accept probability by finding the probability of that string. Since the distribution is given essentially by a z-Hamiltonian, we expect the relaxation time of that chain to be likewise between 1 and  $\text{poly}(L)$ .

Another thing we might want though are the Gibbs occupations of the quantum Hamiltonian. And for that one needs to know exact energies. One might do the scanning again, calculating the expectation values of the Hamiltonian terms at the center of the patch in the eigenstate of the patch that matches the desired spin pattern.

*Appendix B*

PROOFS OF PROPERTIES OF IMBRIE CIRCUIT

**B.1 Telescopic sum for Imbrie circuit**

**Small unitary expansion**

We consider a generator  $A$  of a unitary evolution  $e^A$  (corresponding to step  $k$ ) such that  $A = \sum_i A_i$  where  $\|A_i\| \leq \chi^{L_k}$  and each  $A_i$  is supported on  $L_{k+1}$  consecutive sites. We would like to study the structure of a local operator  $X$ , evolved as  $e^A X e^{-A}$ . We prove

**Proposition:**

$$e^A X e^{-A} = \sum_j X_j \tag{B.1}$$

where  $\text{Supp} X_j \leq \text{Supp} X + 2j(L_{k+1} - 1)$  and  $\|X_j\| \leq L_{k+1}^j \chi^{jL_k} \|X\|$

So the operator  $X$  acquires exponential tails after conjugating with  $e^A$ .

*Proof:*

$$e^A X e^{-A} = \sum_n \frac{A^n}{n!} X \sum_m \frac{(-A)^m}{m!} \tag{B.2}$$

collecting the terms that have the same power of  $A$

$$= \sum_k \sum_{i=0}^k \frac{A^{k-i}}{(k-i)!} X \frac{(-A)^i}{i!} \tag{B.3}$$

Compare this to the expansion of  $k$ 'th order commutator

$$[A[A \dots [A, X]]]^{(k)} = \sum_{i=0}^k C_k^i A^{k-i} X (-A)^i \tag{B.4}$$

where  $C_k^i = \frac{k!}{(k-i)!i!}$

$$\sum_k \sum_{i=0}^k \frac{A^{k-i}}{(k-i)!} X \frac{(-A)^i}{i!} = \sum_k \frac{1}{k!} [A[A \dots [A, X]]]^{(k)} \tag{B.5}$$

Now denote  $X_j = \frac{1}{j!} [A[A \dots [A, X]]]^{(j)}$ . We found that

$$e^A X e^{-A} = \sum_j X_j \tag{B.6}$$

Each commutator  $[A, X]$  increases the support of  $X$  by at most  $2(L_{k+1} - 1)$  sites (left and right included). Thus

$$\text{Supp}X_j \leq \text{Supp}X + 2j(L_{k+1} - 1) \quad (\text{B.7})$$

To find the norm of  $\|X_j\|$ , one needs to recall that  $A = \sum_i A_i$ , and only the overlapping terms can contribute to the commutator. If one counts carefully the overlap of supports of the terms in the nested commutators, it cancels the factorial:

$$\|X_j\| \leq L_{k+1}^j \chi^{jL_k} \|X\| \quad (\text{B.8})$$

where we neglected the original support of  $X$ , that doesn't cancel the factorial. The same factor of  $L_{k+1}^j$  will appear again in the recursion relation below.  $\blacktriangleleft$

Note that with this tool we can have a bound for collared  $\tilde{X} = e^{A_c} X e^{-A_c}$ , where  $c(L_{k+1} - 1)$  is the extra support on each side of  $X$ . By bounds above, we see that  $X$  and  $\tilde{X}$  only differ in terms starting from  $X_c$ . So the difference is bounded by their sum:

$$\|e^A X e^{-A} - \tilde{X}\| \leq \sum_k L_{k+1}^c \chi^{cL_k} \|X\| \leq 4L_{k+1}^c \chi^{cL_k} \|X\| \quad (\text{B.9})$$

One can relax the above bound to a simpler expression:

$$\|e^A X e^{-A} - \tilde{X}\| \leq 4(2\chi)^{cL_k} \|X\| \quad (\text{B.10})$$

for all  $k$ . Indeed, the second expression differs by multiplication of  $2^{cL_k}/L_{k+1}^c > \min_{x>1, c>0} (2^x/x)^c = 1$  which can be easily confirmed by noticing that slope of  $2^x$  is bigger than of  $x$  already at  $x = 1$ . In this fashion, we will always replace inconvenient polynomial (in  $L_k$  etc.) factors by bigger bounding numbers, as we only care about exponential decay for these bounds. We have proven:

**Proposition:** If one conjugates a local operator  $X$  with  $L_k$ -locally generated 1d evolution  $e^A$  for small time  $\chi^{L_k}$ , operator  $X$  acquires exponential tails. Two equivalent expressions exist for an operator with exponential tails - telescopic sum:

$$e^A X e^{-A} = \sum_j X_j \text{ where } \text{Supp}X_j \leq \text{Supp}X + 2j(L_{k+1} - 1) \text{ and } \|X_j\| \leq (2\chi)^{jL_k} \|X\| \quad (\text{B.11})$$

and error of the collared neighborhoods:

$$\|e^A X e^{-A} - \tilde{X}\| \leq 4(2\chi)^{cL_k} \|X\| \text{ where } \tilde{X} = e^{A_c} X e^{-A_c} \text{ and } \text{Supp}A_c = \text{Supp}X + 2c(L_{k+1} - 1) \quad (\text{B.12})$$

where we have "simplified" the bound on  $X_j$  to  $2\chi$  as well.

**Aside: comparison with LRB** It is much stronger result than if we apply LRB for small  $\chi$  for propagation of tails beyond the collar, but becomes trivial for  $\chi = 1$ . Here's this LRB estimate for comaparison - it still gives nontrivial answers even for big  $\chi$ :

$$\|e^A X e^{-A} - \tilde{X}\| \sim \exp\{-(ac - L_{k+1}\chi^{L_k})\} \|X\| \quad (\text{B.13})$$

Here  $a$  is just some number  $< 20$  much smaller than  $L_k/(-\ln\chi)$ . We shall use the stronger first bound as in our case  $\chi \ll 1$ .

### Infinite product of unitaries

Now we'd like to use our bound to estimate precision of collar approximations to:

$$\prod_{k=1} e^{A_k} X \prod_{k'=1} e^{-A_{k'}} \quad (\text{B.14})$$

as in the total Imbrie circuit without resonances. The order in the product turns out to be unimportant for our bound. From the point of view of the physical meaning, if smaller  $k$  act on the operator  $X$  first, then  $X$  is a physical operator and evolved  $X$  represents the action on "logical" spins, or integrals of motion. In particular, for the diagonalization of the Hamiltonian, smaller  $k$  act on the physical Hamiltonian first. If smaller  $k$  act last, then  $X$  is a logical operator, and its evolved form will be the representation of such operator on physical spins.

In the proof below  $\chi = \gamma/\epsilon$ . We now present and prove the bound:

**Proposition:** If we add a collar of  $c$  sites to the support of  $X$ , and take  $A_{k,c}$  to be the sum of terms fully within the collared region, then

$$\left\| \prod_{k=1} e^{A_k} X \prod_{k'=1} e^{-A_{k'}} - \prod_{k=1} e^{A_{k,c}} X \prod_{k'=1} e^{-A_{k',c}} \right\| \leq O((Z\gamma/\epsilon)^c) \quad (\text{B.15})$$

note that for  $L_k > c$  there's no rotation:  $A_k = 0$ . The constant  $Z$  will be found below.

*Proof:*

We start from looking at individual rotation, that was discussed above:

$$U_k X U_k^\dagger = \sum_m X_m, \quad \text{Supp} X_m = 2m(L_{k+1} - 1), \quad \|X_m\| \leq (2\chi)^{mL_k} \quad (\text{B.16})$$

here we set  $\|X\| = 1$  and neglected its support, as it won't affect the bound. If there are two rotations, we get:

$$U_{k'} U_k X U_k^\dagger U_{k'}^\dagger = \sum_{m,m'} X_{m,m'}, \quad (\text{B.17})$$

$$\text{Supp} X_{m,m'} = 2m(L_{k+1} - 1) + 2m'(L_{k'+1} - 1), \quad \|X_{m,m'}\| \leq (2\chi)^{mL_k + m'L_{k'}} \quad (\text{B.18})$$

we see that the order of unitaries indeed does not matter for the form of the bound. For an infinite product, the components of evolved  $X$  are indexed by a string of integers  $\{m_k\}$  for all  $k = 1, 2, 3 \dots$ :

$$\prod_{k=1} e^{A_k} X \prod_{k'=1} e^{-A_{k'}} = \sum_{\{m_k\}} X_{\{m_k\}}, \quad (\text{B.19})$$

$$\text{Supp} X_{\{m_k\}} = \sum_{\{m_k\}} 2m_k(L_{k+1} - 1), \quad \|X_{m,m'}\| \leq (2\chi)^{\sum_{\{m_k\}} m_k L_k} \quad (\text{B.20})$$

Terms  $X_{\{m_k\},a,b}$  contributing to supports  $\text{Supp} X_{\{m_k\}} = 2n$  ( $n \in \mathbb{Z}$ ) are bounded as  $\|X_{\{m_k\},n}\| \leq (2\chi)^{\sum_{\{m_k\}} m_k L_k}$ , where

$$\sum_{\{m_k\}} m_k L_k \geq \min(L_k/2(L_{k+1} - 1)) \sum_{\{m_k\}} 2m_k(L_{k+1} - 1) \geq \frac{8}{15}n \quad (\text{B.21})$$

we have used explicit choice  $L_k = (15/8)^k$  made by Imbrie. So the terms within  $\text{Supp} X_{\{m_k\}} = 2n$  are bounded as

$$\|X_{\{m_k\},a,b}\| \leq \left( (2\chi)^{8/15} \right)^n \quad (\text{B.22})$$

We need to estimate the number of terms with such support that are generated in our telescopic sums  $\sum_{\{m_k\}} X_{\{m_k\}}$ . First note that terms with  $m_k \neq 0$  for at least one  $k$  such that  $2(L_{k+1} - 1) > 2n$  do not contribute. Let  $k^*$  be the biggest  $k$  such that  $2(L_{k+1} - 1) < 2n$ :

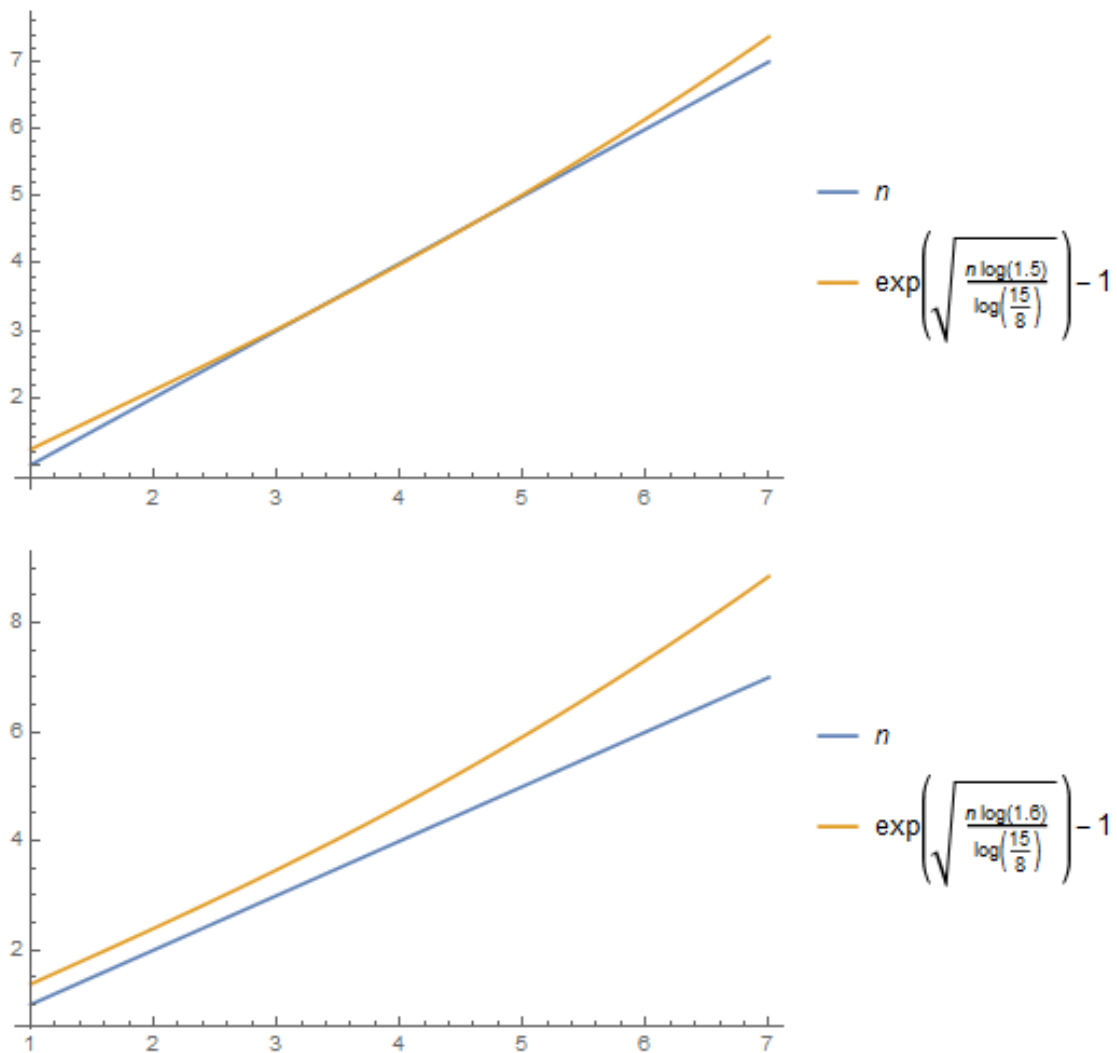
$$k^* = \lfloor \ln(n+1)/\ln(15/8) \rfloor - 1 \quad (\text{B.23})$$

The terms we are interested in have some  $m_k$  nonzero for  $k \leq k^*$ . For simplicity, let's overcount, and allow every  $m_k = 1 \dots n$  (it should be at least  $m_k = 1 \dots n/((L_{k+1} - 1))$ , but we overcount). Then the total number of terms contributing is bounded as

$$\leq n^{k^*} \text{ where } k^* = \lfloor \ln(n+1)/\ln(15/8) \rfloor - 1 \quad (\text{B.24})$$

we get the bound on terms in  $\sum_{\{m_k\}} X_{\{m_k\}}$  with that contribute to the  $2n$  supports:

$$\sum_{\{m_k\}} X_{\{m_k\}} \leq n^{k^*} \left( (2\chi)^{8/15} \right)^n \quad (\text{B.25})$$

Figure B.1: We see how the right-hand side is always bigger for  $Z = 1.6$ 

Let's simplify the  $n^{k^*}$  by weakening the bound a little bit:

$$n^{k^*} = \exp(\ln(n+1) - 1) \leq \exp(\ln^2(n+1)/\ln(15/8)) \quad (\text{B.26})$$

Now we use it to rewrite

$$n^{k^*} \left( (2\chi)^{8/15} \right)^n \leq \exp(\ln^2(n+1)/\ln(15/8)) \left( (2\chi)^{8/15} \right)^n \quad (\text{B.27})$$

We want to prove that

$$\exp(\ln^2(n+1)/\ln(15/8)) \left( (2\chi)^{8/15} \right)^n \leq \left( Z(2\chi)^{8/15} \right)^n \quad (\text{B.28})$$

for some constant  $Z > 1$  and all  $n \geq 1$ . Denote  $(2\chi)^{8/15} = \alpha$ . Observe that  $\alpha$  cancels immediately:

$$\exp(\ln^2(n+1)/\ln(15/8))(\alpha)^n \leq (Z\alpha)^n \quad (\text{B.29})$$

$$\ln^2(n+1)/\ln(15/8) \leq n\ln Z \quad (\text{B.30})$$

Here we can see that the right-hand side has slope  $\ln Z$ , while the left hand side never really grows that fast. The maximum slope of  $\ln^2(n+1)$  is achieved at  $n = e - 1$  and is  $2/e$ . We should demand  $2/e\ln(15/8) \leq \ln Z$  as well as the value of the left hand side to be smaller than the right hand side at the beginning ( $n = 1$ ):  $\ln^2 2/\ln(15/8) \leq \ln Z$ . The two inequalities give the following values of  $Z$ :

$$Z \geq e^{2/e\ln(15/8)} \approx 3.2 \quad (\text{B.31})$$

$$Z \geq e^{\ln^2 2/\ln(15/8)} \approx 2 \quad (\text{B.32})$$

So the analytically proven value for which the inequalities start working is  $Z = 3.2$ . We can strengthen it numerically as our proof was not tight:

$$\ln^2(n+1)/\ln(15/8) \leq n\ln Z \quad (\text{B.33})$$

$$n+1 \leq \sqrt{n\ln Z/\ln(15/8)} \quad (\text{B.34})$$

$$n \leq \sqrt{n\ln Z/\ln(15/8)} - 1 \quad (\text{B.35})$$

We compare the two sides numerically in Fig. B.1 and find that for  $Z = 1.6$  it works. Note that the bounds imply that  $Z\alpha < 1$ , which means  $(2\chi)^{8/15} < 1/Z = 0.6$ ,  $\chi < 0.2$ . Now we can use it in the telescopic sum that we had:

$$\prod_{k=1}^n e^{A_k} X \prod_{k'=1}^n e^{-A_{k'}} = \sum_n X_n, \text{ where } \text{Supp} X_n = 2n, \text{ and } \|X_n\| \leq n^{k^*} \left( (2\chi)^{8/15} \right)^n \quad (\text{B.36})$$

For  $\chi < 0.2$ , this bound can be simplified to

$$\prod_{k=1}^n e^{A_k} X \prod_{k'=1}^n e^{-A_{k'}} = \sum_n X_n, \text{ where } \text{Supp} X_n = n, \text{ and } \|X_n\| \leq \left( Z(2\chi)^{8/15} \right)^n \quad (\text{B.37})$$

where  $Z = 1.6$ . We also get a bound on collared neighborhoods

$$\|e^A X e^{-A} - \tilde{X}\| \leq 4 \left( Z(2\chi)^{8/15} \right)^n \text{ where } \tilde{X} = e^{A_c} X e^{-A_c} \text{ and } \text{Supp} A_c = 2n \quad (\text{B.38})$$

The error of the first step is already found above (for  $k=1$ ):

$$\|e^{A_1} X e^{-A_1} - \tilde{X}\| \leq 4L_2^c(\gamma/\epsilon)^{cL_1} \|X\| \quad (\text{B.39})$$

$L_1 = 1$  here. We just assume the scaling for the  $k$ 'th step  $\tilde{X}_k = \prod_{q=1}^k e^{A_q, c} X \prod_{q'=1}^k e^{-A_{q', c}}$ :

$$\left\| \prod_{q=1}^k e^{A_q} X \prod_{q'=1}^k e^{-A_{q'}} - \tilde{X}_k \right\| \leq f(k, c)(\gamma/\epsilon)^c \|X\| \quad (\text{B.40})$$

and set out to find  $f(k, c)$ . The construction of  $\tilde{X}$  also showed the telescopic sum structure:

$$\tilde{X} = \sum_{j=0}^c X_j, \quad \|X_j\| \leq L_2^j (\gamma/\epsilon)^j \|X\| \quad (\text{B.41})$$

We assume on the  $k$ 'th step that

$$\tilde{X}_k = \sum_{j=0}^c X_{j,k}, \quad \|X_{j,k}\| \leq f(j, k)(\gamma/\epsilon)^j \|X\| \quad (\text{B.42})$$

On the  $k + 1$ 'th step we get contributions to  $X_{j,k+1}$  from  $m$ 'th order terms of  $e^{A_{k+1}} X_{j-mL_{k+2}, k} e^{-A_{k+1}}$ . There will be at most  $j/L_{k+2}$  such contributions, all with the same factors in the norm. So the recursion relation will read:

$$f(j, k+1) = \sum_{m=0}^{j/L_{k+2}} f(j - mL_{k+2}, k) L_{k+2}^m \quad (\text{B.43})$$

$f(j, k)$  grows with  $j$ . If we bound

$$f(j, k+1) \leq f(j, k) \sum_{m=0}^{j/L_{k+2}} L_{k+2}^m \approx f(j, k) L_{k+2}^{j/L_{k+2}} \quad (\text{B.44})$$

Applying it recursively, we get

$$f(j, k') \leq \left( \prod_{k=1}^{k'} L_{k+1}^{1/L_{k+1}} \right)^j \quad (\text{B.45})$$

The product converges as can be seen by its logarithm:

$$\ln \prod_{k=1}^{k'} L_{k+1}^{1/L_{k+1}} = \left( \ln \frac{15}{8} \right) \sum_{k=1}^{k'} (k+1) \left( \frac{15}{8} \right)^{-k-1} \leq \left( \ln \frac{15}{8} \right)^{-1} \quad (\text{B.46})$$

Thus we find the bound

$$f(j, k') \leq \left( e^{(\ln \frac{15}{8})^{-1}} \right)^j \quad (\text{B.47})$$

and the constant  $Z = e^{(\ln \frac{15}{8})^{-1}} \approx 4.9$  in the

$$\tilde{X}_k = \sum_{j=0}^c X_{j,k}, \quad \|X_{j,k}\| \leq (Z\gamma/\epsilon)^j \|X\| \quad (\text{B.48})$$

Note that the bound on the norm doesn't depend on  $k$ . The error is given by

$$\left\| \prod_{k=1}^{\infty} e^{A_k} X \prod_{k'=1}^{\infty} e^{-A_{k'}} - \prod_{k=1}^{\infty} e^{A_{k,c}} X \prod_{k'=1}^{\infty} e^{-A_{k',c}} \right\| \leq \sum_{j=c+1}^{\infty} \|X_{j,\infty}\| \leq O((Z\gamma/\epsilon)^c) \quad (\text{B.49})$$

◀

## B.2 Circuit approximation

We would like to have a FDL circuit approximation of a unitary  $e^A$ . Consider a simple case of  $L_k = 2$  first:  $A = \sum_i A_{i,i+1}$ . The Trotter approximation in  $N$  steps is defined as:

$$U_T = (e^{\frac{1}{N}A_{\text{even}}} e^{\frac{1}{N}A_{\text{odd}}})^N \quad (\text{B.50})$$

where  $A_{\text{even}} = \sum_{i \text{ even}} A_{i,i+1}$ . The error is given by BCH formula while it remains small:

$$e^A = U_T + O(\|[A_{\text{even}}, A_{\text{odd}}]\|/N) = U_T + O(L\|A_{i,i+1}\|^2/N) \quad (\text{B.51})$$

Note that the error over whole macroscopic system diverges with size. However, over a small patch the error is small. Specifically, let's prove that for an operator  $X$  supported over  $m$  sites the conjugation with  $e^A$  is simulated by:

$$e^A X e^{-A} = U_T X U_T^\dagger + O\left(\|X\| \frac{(m+16N)}{N} \|A_{i,i+1}\|^2\right) \quad (\text{B.52})$$

We see that the system size dependence drops, also  $U_T X U_T^\dagger$  is an operator supported on  $m+2N$ , and expressed by a tensor network of size  $(m+2N) \times N$ . The terms outside the causal cone of  $X$  just cancel.

First we use the bound approximation by collared evolution (from now on we keep general  $L_k$ , so our arguments will also apply to  $A$  with bigger support of local terms):

$$\|e^A X e^{-A} - e^{A_c} X e^{-A_c}\| \leq 4L_{k+1}^c (\gamma/\epsilon)^{cL_k} \|X\| \quad (\text{B.53})$$

Here  $c$  is the number of sites we are to include in the "collar" of  $X$ .  $A_c$  are the terms in  $A$  supported inside the collared region. Taking a collar  $c \sim \ln\delta/L_k \ln(\gamma/\epsilon)$  we get

$$e^A X e^{-A} = e^{A_c} X e^{-A_c} + O(\|X\|\delta) \quad (\text{B.54})$$

The problem reduced to finding an FDL approximation to  $e^{A_c}$  supported on  $M = m+2c$  - a finite number of spins. For that purpose, Trotter approximation is used.

For general  $L_k$ , we group the terms  $A_{even} = \sum_{i/L_k \text{ even}} A_i$ . The Trotter approximation is then:

$$e^{A_c} \approx (e^{\frac{1}{N}A_{even}} e^{\frac{1}{N}A_{odd}})^N + O((\gamma/\epsilon)^{2L_k} L_k^2 M/N) \quad (\text{B.55})$$

is such a scheme with total depth  $D_0 = 2O(2^{2L_k})N$  and even and odd sites repeated  $N$  times. We have used that each  $2L_k$ -qubit gate from Trotter formula is written as  $\exp(2L_k)$  2-qubit gates. Note that the Lieb-Robinson velocity gets only a multiplicative adjustment  $v \rightarrow 2L_k v$ . So even though apparent causal cone of the circuit we get is  $2L_k v$ , the true causal structure of the circuit has tighter bound. The final circuit for  $e^{A_r}$  has "effective" depth  $4L_k N$  (the one that reflects the causal structure). The total precision defined as:

$$\|e^{A_k} X e^{-A_k} - U_T X U_T^\dagger\| \leq \|X\| \epsilon_{tot}(D_0, k, \gamma/\epsilon) \quad (\text{B.56})$$

is found to be

$$\epsilon_{tot}(D_0, k, \gamma/\epsilon) = O((2\gamma/\epsilon)^{2L_k} L_k^2 M/D_0) + O(L_{k+1}^c (\gamma/\epsilon)^{cL_k}) \quad (\text{B.57})$$

Note that if we were Trotter approximating  $e^A$  instead of the collared one, we still get the same result  $e_T^A X e_T^{-A} = e_T^{A_c} X e_T^{-A_c}$  by cancellations of the spare terms as long as  $c = 4L_k N$ . So there exists an FDL circuit  $e_T^A$  over the whole system that approximates  $e^A$  locally in every patch.

Plugging in  $c = 4L_k N$ , we find second term  $\sim (\gamma/\epsilon)^{4L_k^2 N}$  to be negligible. The error is now:

$$\epsilon_{tot}(D_0, k, \gamma/\epsilon) = O((\gamma/\epsilon)^{2L_k} L_k^2 (m + 8L_k N)/N) \quad (\text{B.58})$$

To conclude, let us study the state  $e^A|0\rangle\langle 0|e^{-A}$ . Any observable  $X$  on  $m$  sites is approximated by measuring it with  $e_T^A|0\rangle\langle 0|e_T^{-A}$  with error as in Eq. (B.57). The latter measurement is represented by a system-size independent tensor network due to the cancellations. So the difference in density matrices over  $m$  sites elementwise is bounded:

$$|(\rho - \rho_{appr})_{\alpha\beta}| \leq \epsilon_{tot}(D_0, k, t) \quad (\text{B.59})$$

We can also show the operator norm bound:

$$\|\rho - \rho_{appr}\| \leq \epsilon_{tot}(D_0, k, t) \quad (\text{B.60})$$

here  $\rho = \text{tr}_{\bar{m}} e^A|0\rangle\langle 0|e^{-A}$  and  $\rho_{appr} = \text{tr}_{\bar{m}} e_T^A|0\rangle\langle 0|e_T^{-A}$ . To see this, consider the eigenbasis of  $\rho - \rho_{appr}$ . We can make  $X$  to be measuring matrix elements in this

basis. In particular, the maximum eigenvalue of  $\rho - \rho_{appr}$  will not be bigger than the difference  $|\langle X \rangle - \langle X \rangle_{appr}| \leq \epsilon_{tot}(D_0, k, t)$ .

To approximate the Imbrie circuit, note that neglecting  $e^{A_c}$  in  $e^{A_c} X e^{-A_c}$  altogether leads to an error

$$\|e^{A_c} X e^{-A_c} - X\| \leq \|X\| \|A_c\| \quad (\text{B.61})$$

$$\|\rho - \rho_{appr}\| \leq \|X\| \|A_c\| \quad (\text{B.62})$$

by summing the result of the Taylor expansion, which converges because it is controlled by  $1/n!$ . This allows us to drop higher-order terms altogether. For instance, we can use the collared bounds from above to establish the bound on just using the first order  $L_1 = 2$  of the circuit (keeping the leading contributions):

$$\left\| \prod_{k=1} e^{A_k} X \prod_{k'=1} e^{-A_{k'}} - U_T X U_T^\dagger \right\| \leq \|X\| \left( O\left(\frac{(m+16N)}{N}(\gamma/\epsilon)^2\right) + O((m+8N)(\gamma/\epsilon)^{L_2}) \right) \quad (\text{B.63})$$

In Imbrie's construction,  $L_2 = 4$ .

### B.3 Area law

We will prove the following:

**Proposition** The state  $\prod_{k=1} e^{A_k} |prod\rangle$  obeys the area law: for  $B$  - the half of the system, the entanglement entropy  $S(\rho_A) \sim \xi$ . Here  $|prod\rangle$  is a product state in the  $z$ -basis.

We also discuss the tail of the distribution of entanglement entropies in the presence of resonances.

We turn to the paper Bravyi, M. B. Hastings, and Verstraete, 2006 which derives the entanglement production  $\delta S \leq c_0 + c_1 t$  under the evolution  $e^{iHt}$ . In our case, we apply the bound for every step using  $H_{(k)}t = A_k$ . We set  $t = 1$ .

We use the tightest bound on  $c_1$  that is given on the last page of Bravyi, M. B. Hastings, and Verstraete, 2006. The interaction between two parts can be written as a Shmidt decomposition  $H_{LR}^{(k)} = \sum_i r_i J_L^i \otimes J_R^i$ , where we have freedom to set  $\|J_L\| = 1$ ,  $\|J_R\| = 1$ . The  $H_{LR}$  is bounded by  $L_k(\gamma/\epsilon)^{L_k}$ , thus each  $\|r_i\| \leq L_k(2\gamma/\epsilon)^{L_k}$ . The entanglement produced over time  $t = 1$  will be

$$\delta S \leq c^* \sum_i \|r_i\| \leq c^*(4\gamma/\epsilon)^{L_k} \quad (\text{B.64})$$

The coefficient  $c^* \approx 1.9$  is universal and is found in Childs, Leung, and Vidal, 2004. The total entanglement is the sum of entanglement produced by each order  $k$  of the circuit. The total bound on entanglement is converging:

$$\delta S_{tot} \leq \sum_k c^* (4\gamma/\epsilon)^{L^k} \leq 16\gamma/\epsilon \quad (\text{B.65})$$

Thus the Imbrie states without resonances satisfy area law.

Every resonance is an extra local rotation over region of size  $n_r$  that does not have to be small. If it happens that our cut passes through the resonance, we need to add the entanglement created by this rotation to the total entanglement bound. A rotation over  $n_r$  sites can create  $\Delta S(n_r) \leq n_r$  entanglement. Naive expectation is  $\leq n_r/2$  which is true for a unitary acting on a whole system of size  $n_r$ . But in fact having a bigger system we can create two times more entanglement with the rotation on  $n_r$  sites! Indeed, the bound is saturated by a swap gate, that turns a state with  $n_r/2$  Bell pairs on every side of the cut into a state where every Bell pair crosses the cut.

After  $k_1$  when the first resonance appears across the cut, there may be other, bigger resonances containing the first one. Since a cut is placed randomly in the system, denote the probability that the biggest resonance across the cut has size  $n_r$  by  $P(n_r)$ . It is exactly the same quantity as the probability of a site to be a part of a connected cluster of resonances of size  $n_r$ . Imbrie shows that this probability decays faster than any polynomial. Thus the expectation value

$$\sum_{n_r} n_r P(n_r) \leq \text{const} \quad (\text{B.66})$$

Moreover, we know that first few terms go as  $\epsilon^{n_r}$  and then it keeps decaying faster than any polynomial, so the leading contribution to the expectation value is the first term:

$$\sum_{n_r} n_r P(n_r) \leq 4\epsilon \quad (\text{B.67})$$

Thus the total bound on the expectation value of the entanglement entropy is:

$$\overline{S_{tot}} \leq 16\gamma/\epsilon + 4\epsilon \quad (\text{B.68})$$

We note that the first term is smaller for the parameters used by Imbrie - so the main contribution to entanglement is from rare distributions of disorder when resonances cross the cut. We also note that in full construction by Imbrie, the perturbative parts of the circuit  $e^{A_k}$  get adjusted in the presence of resonances as the resonant spins are

grouped into metaspins. The entanglement produced by resulting unitaries is still bounded, so we dropped this complication from our simplified circuit.

Consider rare cuts that may have entanglement bigger than  $n_r = 2$ , by passing near the big resonant regions. Assuming for simplicity exponential distribution of entanglement as a random variable  $P(S = 2x) = \epsilon^x$  for  $x$  the half of the size of the resonance, with the biggest entanglement across the cut in a given system determined by:

$$LP(S_{max}) = L\epsilon^{-S_{max}} \approx 1 \quad (\text{B.69})$$

$$S_{max} \approx \ln L / (-\ln \epsilon) \quad (\text{B.70})$$

To derive maximal entanglement more carefully one needs to use the true statistics of resonances from Imbrie's paper: a superpolynomially decaying  $P(S)$  anyway. That only adjusts  $\ln L \rightarrow e^{\sqrt{\ln L}}$  - a difference between the two will be almost impossible to detect.

#### B.4 LRB

First we would like to derive a Lieb-Robinson bound (a bound on  $[A(t), B]$ ) for a diagonal local Hamiltonian with exponential tails:  $H = H(\sigma_z)$ ,  $H = \sum_{i,r} H_{i,r}$  such that  $\|H_{i,r}\| < e^{-cr}$ . The operator  $H$  has only diagonal matrix elements. The operators  $A$  and  $B$  can have arbitrary nonzero matrix elements, but  $A$  is local in the region  $\text{supp}(A)$  and  $B$  is local in the region  $\text{supp}(B)$ . Distance between regions  $A$  and  $B$  is the length of the shortest path connecting a point in  $A$  to a point in  $B$ , denoted  $d_{A,B}$ . In the commutator  $A(t) = e^{iHt} A e^{-iHt}$ . For  $H = H(\sigma_z)$ ,  $e^{iHt} = e^{i \sum_{ij} H_{ij} t} = \prod_{ij} e^{iH_{ij} t}$ . We immediately see that terms not supported on  $\text{supp}(A)$  in the Hamiltonian commute through and cancel each other:  $A(t) = e^{iH_A t} A e^{-iH_A t}$ . Then, since we are trying to bound a norm  $\|[A(t), B]\|$  and it's invariant under unitaries, we conjugate with  $e^{iH_A t}$  and get  $\|[A(t), B]\| = \|[A, e^{-iH_A t} B e^{iH_A t}]\|$ . Here we can commute through the terms in  $H_A$  that don't have support on  $B$ , to get  $\|[A(t), B]\| = \|[e^{iH_{AB} t} A e^{-iH_{AB} t}, B]\|$ . Now note that the locality condition enforces  $\|H_{AB}\| < e^{-cd_{A,B}}$ . We also note that the individual matrix elements over basis on  $\text{supp}(AB)$  are bounded by the same bound. So in fact we need to solve for Lieb-Robinson bound of small Hamiltonian, and then we get our LRB for diagonal local  $H$  with exponential tails as a trivial corollary.

Now, drop the  $A, B$  notation, just think that  $A = A \otimes 1$ ,  $B = 1 \otimes B$  (they act on different degrees of freedom  $\mathcal{H}_A \otimes \mathcal{H}_B$  we always suppress the extra degrees of

freedom of the rest of the system... we can't). And  $\|H\|$  is small as explained above. We consider matrix element of  $[A(t), B]$  in the basis of eigenstates of  $H$  (we need this basis to respect  $\mathcal{H}_A \otimes \mathcal{H}_B$ , so this bound won't work for general small Hamiltonian, only for ones diagonal in z-basis) :

$$[A(t), B]_{\alpha\beta, \alpha'\beta'} = (e^{iHt} A \otimes 1 e^{-iHt} \cdot 1 \otimes B)_{\alpha\beta, \alpha'\beta'} - (1 \otimes B \cdot e^{iHt} A \otimes 1 e^{-iHt})_{\alpha\beta, \alpha'\beta'} \quad (\text{B.71})$$

We label the eigenstates in  $\mathcal{H}_A$  by  $\alpha$ , and in  $\mathcal{H}_B$  by  $\beta$ . The Hamiltonian is diagonal so we write it as  $H_{\alpha\beta}$  - the diagonal element:

$$[A(t), B]_{\alpha\beta, \alpha'\beta'} = e^{iH_{\alpha\beta}t} A_{\alpha\alpha'} e^{-iH_{\alpha'\beta'}t} B_{\beta\beta'} - B_{\beta\beta'} e^{iH_{\beta'\alpha'}t} A_{\alpha\alpha'} e^{-iH_{\alpha'\beta'}t} \quad (\text{B.72})$$

We can pull the matrix elements of  $A$  and  $B$  in front:

$$[A(t), B]_{\alpha\beta, \alpha'\beta'} = A_{\alpha\alpha'} B_{\beta\beta'} (e^{iH_{\alpha\beta}t} e^{-iH_{\alpha'\beta'}t} - e^{iH_{\beta'\alpha'}t} e^{-iH_{\alpha'\beta'}t}) \quad (\text{B.73})$$

Let's bound the expression in the brackets:

$$e^{i(H_{\alpha\beta} - H_{\alpha'\beta'})t} - e^{i(H_{\beta'\alpha'} - H_{\alpha'\beta'})t} = e^{i\epsilon_1} - e^{i\epsilon_2} = \sum_{n=1}^{\infty} \frac{(i)^n (\epsilon_1^n - \epsilon_2^n)}{n!} \quad (\text{B.74})$$

Up to this point  $\epsilon_{1,2}$  are operators on the rest of the system. We bound the norm as

$$\|e^{i(H_{\alpha\beta} - H_{\alpha'\beta'})t} - e^{i(H_{\beta'\alpha'} - H_{\alpha'\beta'})t}\| \leq 2 \sum_{n=1}^{\infty} \frac{\|\epsilon\|^n}{n!} = \quad (\text{B.75})$$

$$= 2(e^{\|\epsilon\|} - 1) < 2(e - 1)\|\epsilon\| = 4(e - 1)t e^{-cd_{A,B}} \quad (\text{B.76})$$

Here we used the bound  $\|H_{AB, \alpha\beta}\| < e^{-cd_{A,B}}$ . So every matrix element of  $[A(t), B]$  is bounded as in Eqn. B.76 times the matrix elements of  $A$  and  $B$ , so we can bound the matrix as a whole:

$$\|[A(t), B]\| \leq \|A\| \|B\| 2^{\text{supp}(AB)} 4(e - 1)e^{-cd_{A,B}t} \quad (\text{B.77})$$

Now how do we apply this to the quantum Hamiltonian of Imbrie chain? Note that it can be reduced to the diagonal Hamiltonian by the rotation with the Imbrie circuit  $UHU^\dagger$ . The decay of long-range terms is governed by  $e^{-c} = \gamma/\epsilon$ . The local operators  $A, B$  are then rotated to  $UAU^\dagger, UBU^\dagger$ . The resulting operators have exponential tails and be replaced by ones strictly within a collar:

$$\|[A(t), B] - [A_c(t), B_c(t)]\| \leq c' \|A\| \|B\| (Z\gamma/\epsilon)^c \quad (\text{B.78})$$

The Lieb-Robinson bound acquires a constant term:

$$\|[A(t), B]\| \leq \|A\| \|B\| (2^{\text{supp}(AB)} 4(e-1)(\gamma/\epsilon)^{d_{A,B}-2c} t + c'(Z\gamma/\epsilon)^c) \quad (\text{B.79})$$

optimizing  $c$  gives (only for  $t > (\gamma/\epsilon)^{d_{A,B}/2}$ )

$$\|[A(t), B]\| \leq \|A\| \|B\| c''(\gamma/\epsilon)^{d_{A,B}/3} \sqrt[3]{t 2^{\text{supp}(AB)}} \quad (\text{B.80})$$

We believe that the bound should be  $t(\gamma/\epsilon)^{d_{A,B}}$  for all times, with no constant contribution. Either way, the light cone is given by  $t(\gamma/\epsilon)^{d_{A,B}} = 1$ ,  $d \sim \ln t$ .

Here's a sketch of a derivation that can give a better bound. Consider

$$A(t) = e^{iHt} A e^{-iHt} = U^\dagger e^{iH_z t} U A U^\dagger e^{-iH_z t} U = \sum_r U^\dagger e^{iH_z t} A_r e^{-iH_z t} U \quad (\text{B.81})$$

where  $A_r$  is supported on  $r$  sites and is bounded by  $\|A\|(Z\gamma/\epsilon)^r$ . Now the terms in  $e^{iH_z t}$  that do not overlap with  $r$  commute through, so

$$e^{iH_z t} A_r e^{-iH_z t} = e^{iH_z^r t} A_r e^{-iH_z^r t} \quad (\text{B.82})$$

where  $H_z^r = \sum_m H_z^{r+m}$  and this sum is bounded as  $(Z\gamma/\epsilon)^m$ . Now we find  $m^*$  such that  $(Z\gamma/\epsilon)^{m^*} t = 1$ . Our intuition is that the telescopic sum for  $e^{iH_z^r t} A_r e^{-iH_z^r t}$  should have the form

$$e^{iH_z^r t} A_r e^{-iH_z^r t} = \sum_p Q_{r+m^*+p}, \quad \|Q_{r+m^*+p}\| \leq \|A\|(Z\gamma/\epsilon)^p \quad (\text{B.83})$$

After plugging in and resumming all the telescopic sums, we get:

$$\|[A(t), B]\| \leq \|A\| \|B\| c''(Z\gamma/\epsilon)^{d_{A,B}-m^*} = \|A\| \|B\| c''(Z\gamma/\epsilon)^{d_{A,B}} t \quad (\text{B.84})$$

The validity of this approach rests on our ability to prove (B.83). It is very simple, since  $e^{iH_z^r t}$  is diagonal, we can extract terms  $m^* + p$  away:

$$e^{iH_z^r t} = e^{iH_z^{r+m^*} t} \prod e^{iH_z^{r+m^*+p} t} \quad (\text{B.85})$$

and the latter each has bounded support and bounded correction:

$$e^{iH_z^{r+m^*+p} t} = 1 + O((\gamma/\epsilon)^p) \quad (\text{B.86})$$

That concludes the proof.

## Appendix C

### INTERPRETATION OF IMBRIE'S PROOF

#### C.1 Bound on generators

Here we discuss the bound on the local generator  $A_{k,i}$  of the perturbative step  $e^{\sum_i A_{k,i}}$  of Imbrie circuit. Here  $i$  is the spatial index labeling sites of the chain, and  $k$  is the order of the perturbation theory. Each  $A_{k,i}$  is acting on  $L_k$  spins, where the radius of locality  $L_k = (1\frac{7}{8})^k \approx 2^k$  is growing with  $k$ . We have presented a bound

$$\|A_{k,i}\| \leq \chi^{L_k} \quad (\text{C.1})$$

Let's demonstrate how such bound can result from Imbrie's construction. First let's define the path formalism used by Imbrie on the following toy example.

**Toy example 1.** Consider an operator  $J$  defined as:

$$J = \sum_g J(g) \quad (\text{C.2})$$

The sum is over paths  $g = \{i_1 \dots i_{|g|}\}$  in the space of spin flips. Each  $i_n$  is a site on a lattice, and the length of the string of those sites  $g$  is denoted  $|g|$ . In the  $\sum_g$ , it is implied that  $|g| > 1$ . There's one condition on the string  $g$ : each new spin flip has to be within 1 lattice spacing from one of the old ones:

$$\forall n > 1 \exists n' < n : |i_n - i_{n'}| \leq 1 \quad (\text{C.3})$$

The operators  $J(g)$  are supported on the smallest consecutive region containing all spin flips in  $g$  plus a 1 spin collar on the left and on the right. Consider the following way to bound the terms in  $J$ :

$$|J_{\sigma\sigma'}(g)| \leq \frac{\gamma^{|g|}}{C(|g|)} \quad (\text{C.4})$$

where  $C(x)$  is a combinatorial factor to be determined and  $\gamma \ll 1$ . We'd like to see what  $C(x)$  do we need to be able to translate this bound to a more traditional norm bound. Consider a decomposition of  $J$  into "local" terms centered around sites of the lattice:

$$J = \sum_i J_i, \quad J_i = \sum_{g|i_1=i} J(g) \quad (\text{C.5})$$

where  $J_i$  contains only graphs starting at  $i_1$ . Let's show that a norm bound on  $J_i$  follows from a bound on  $J_{\sigma\sigma'}(g)$ :

$$\|J_i\| \leq \sum_{g|i_1=i} \|J(g)\| \quad (\text{C.6})$$

Note that any operator  $J(g)$  supported on  $\cup g \cup c$  where  $c$  is a 1-spin collar can be written in an operator basis with one basis vector per matrix element :

$$J(g) = \sum_{\sigma\sigma'} J_{\sigma\sigma'}(g) |\sigma\rangle\langle\sigma'| \quad (\text{C.7})$$

and since  $J(g)$  acts as an identity outside  $\cup g \cup c$ , and doesn't flip  $c$ , the number of terms in the sum is  $4^{|\cup g|} 2^{|c|} \leq 2^{2|g|+c}$ :

$$\sum_{g|i_1=i} \|J(g)\| \leq \sum_{g|i_1=i} \sum_{\sigma\sigma'} J_{\sigma\sigma'}(g) \leq \sum_{g|i_1=i} 2^{2|g|+c} \frac{\gamma^{|g|}}{C(|g|)} \quad (\text{C.8})$$

We can now split the sum into terms corresponding to each  $|g|$ :

$$\|J_i\| \leq \sum_{x=1}^{\infty} 2^{2x+c} \frac{\gamma^x}{C(x)} \sum_{g|i_1=i, |g|=x} 1 \quad (\text{C.9})$$

A simple upper bound on the number of elements in the sum  $\sum_{g|i_1=i, |g|=x} 1$  is if a flip  $i_n$  can be chosen from  $2n - 1$  sites centered at  $i_1$ . For  $|g| = x$  flips, it gives  $(2x - 1)!! = (2x - 1)(2x - 3) \dots$

$$\|J_i\| \leq \sum_{x=1}^{\infty} 2^{2x+c} \gamma^x \frac{(2x - 1)!!}{C(x)} \quad (\text{C.10})$$

So a choice of  $C(x) = (2x - 1)!!$  will cancel this factor. What remains is a geometric series which is bounded for  $4\gamma < 1/2$ :

$$\|J_i\| \leq 2^{C+1} (4\gamma) \quad (\text{C.11})$$

we have arrived at a desired bound.

**Toy example 2.** We will repeat the above construction with a minor modification: in the

$$J = \sum_g J(g) \quad (\text{C.12})$$

the  $\sum_g$  is now taken over  $g$  such that  $|g| > L_1$ . The bound on  $J_{\sigma\sigma'}(g)$  and  $C(x) = (2x - 1)!!$  are the chosen the same. All the steps go through in exactly the same way, until we arrive to:

$$\|J_i\| \leq \sum_{x=L_1}^{\infty} 2^{2x+c} \gamma^x \frac{(2x - 1)!!}{C(x)} = \sum_{x=L_1}^{\infty} 2^{2x+c} \gamma^x \leq 2^{C+1} (4\gamma)^{L_1} \quad (\text{C.13})$$

we see that any level is bounded by the smallest allowed flip.

**Toy example 3.** We will now introduce an extra layer of structure to match Imbrie's construction. Consider

$$J = \sum_G J(G) \quad (\text{C.14})$$

where  $G = \{g_1, g_2 \dots g_{|G|}\}$  a string of spin flip paths  $g_n$  defined in examples before. The constraint on the paths in  $G$  is now:

$$\forall n > 1 \exists n' < n : d(g_n, g_{n'}) \leq 1 \quad (\text{C.15})$$

where  $d(g_1, g_2)$  is the distance in lattice spacings between the two nearest spins in  $g_1, g_2$ .

The support of  $J(G)$  is in the smallest consecutive region containing all spin flips of underlying paths of  $G$  plus some constant collar  $c$ . Surprisingly, it is enough to bound

$$|J_{\sigma\sigma'}(G)| \leq \frac{1}{C(|G|)} \prod_{g \in G} \frac{\gamma^{|g|}}{C(|g|)} \quad (\text{C.16})$$

where  $C(x) = (2x - 1)!!$  again. Indeed, for a "local" term

$$J_i = \sum_{G|i=i_1 \in g_1 \in G} J(G) \quad (\text{C.17})$$

the norm bound

$$\|J_i\| \leq \sum_{G|i=i_1 \in g_1 \in G} \|J(G)\| \leq \sum_{G|i=i_1 \in g_1 \in G} \frac{4^{\sum |g|} 2^c}{C(|G|)} \prod_{g \in G} \frac{\gamma^{|g|}}{C(|g|)} \quad (\text{C.18})$$

The sum over  $G$  can be split into sums over paths with fixed values of  $|G|$  and all  $|g_m|$ :

$$\|J_i\| \leq \sum_{|G|, |g_m|} \frac{4^{\sum |g_m|} 2^c}{C(|G|)} \prod_m \frac{\gamma^{|g_m|}}{C(|g_m|)} \sum_{G|i=i_1 \in g_1 \in G, |G|, |g_m|} 1 \quad (\text{C.19})$$

so we need to do the counting again. We first count the small graphs as before, and then count how many ways are there to place  $|G|$  small graphs of sizes  $|g_m|$  so that each new one is a neighbor to one of the old ones. We get the following bound:

$$\sum_{G|i=i_1 \in g_1 \in G, |G|, |g_m|} 1 \leq \quad (\text{C.20})$$

$$\leq \prod_m C(|g_m|) |g_1| (|g_1| + 2|g_2|) (|g_1| + 2|g_2| + 2|g_3|) \dots (2 \sum_m |g_m| - |g_1|) \quad (\text{C.21})$$

or if we plug it in:

$$\|J_i\| \leq$$

$$(C.22)$$

$$\leq \sum_{|G|, |g_m|} 4^{\sum |g_m|} 2^c \gamma^{\sum_m |g_m|} \frac{|g_1|(|g_1| + 2|g_2|)(|g_1| + 2|g_2| + 2|g_3|) \dots (2 \sum_m |g_m| - |g_1|)}{C(|G|)}$$

$$(C.23)$$

Or if we separate sums over  $|G|, \sum_m |g_m| = X, |g_m| = x_m$ :

$$\|J_i\| \leq \sum_{|G|} \sum_{X \geq |G|} 4^X 2^c \gamma^X \sum_{x_m | \sum_m x_m = X} \frac{x_1(x_1 + 2x_2)(x_1 + 2x_2 + 2x_3) \dots (2X - x_1)}{C(|G|)}$$

$$(C.24)$$

We see that the smallest power of  $\gamma$  is given by  $\sum_m |g_m| = |G|$ , in which case the  $C(|G|)$  exactly cancels its numerator:

$$\|J_i\| \leq \sum_{|G|} 4^{|G|} 2^c \gamma^{|G|} F(|G|, \gamma)$$

$$(C.25)$$

where

$$F(|G|, \gamma) = 1 +$$

$$(C.26)$$

$$+ \sum_{X > |G|} 4^{X-|G|} \gamma^{X-|G|} \sum_{x_m | \sum_m x_m = X} \frac{x_1(x_1 + 2x_2)(x_1 + 2x_2 + 2x_3) \dots (2X - x_1)}{C(|G|)}$$

$$(C.27)$$

we want to show that  $f(|G|, \gamma)$  can be bounded by a constant for sufficiently small  $\gamma$ . It is a series in terms of  $n = X - |G|$ .  $F = \sum_{n=0}^{\infty} F_n$  and:

$$F_n = (4\gamma)^n \sum_{x_m | \sum_m x_m = |G|+n} \frac{x_1(x_1 + 2x_2)(x_1 + 2x_2 + 2x_3) \dots (2(|G| + n) - x_1)}{C(|G|)}$$

$$(C.28)$$

There are always  $|G|$  terms  $x_m$ . One can already see that

$$\sum_{x_m | \sum_m x_m = |G|+n} \frac{x_1(x_1 + 2x_2)(x_1 + 2x_2 + 2x_3) \dots (2(|G| + n) - x_1)}{C(|G|)} \leq (|G| + n)^{2|G|}$$

$$(C.29)$$

so we only get a polynomial prefactor in front of  $\gamma^n$  and the series converges. What we want to show is that it converges to something that goes to  $\infty$  only exponentially

in  $|G|$ , so we can suppress it by  $(4\gamma)^{|G|}$ . Clearly the naive bound  $(|G| + n)^{2|G|}$  where dropped  $C(|G|)$  altogether gives a factorial-like scaling even for the first term in the sum that we know is 1. We know that number of terms in the sum for each  $n$  is in fact given by  $C_{|G|+n}^{|G|} < 2^{|G|+n}$ , so what's left is to bound a single term in the sum:

$$\frac{x_1(x_1 + 2x_2)(x_1 + 2x_2 + 2x_3) \dots (2(|G| + n) - x_1)}{C(|G|)} \leq \quad (\text{C.30})$$

$$\leq \left( \frac{(2(|G| + n) - 1)}{2|G| - 1} \right)^{|G|} = \left( 1 + \frac{2n}{2|G| - 1} \right)^{|G|} \quad (\text{C.31})$$

these terms summed with  $4\gamma^n$  can only lead to logarithmic corrections  $(1/(-\ln\gamma))^{|G|}$  to the  $F(|G|, \gamma)$ . Putting it all together:

$$F_n \leq (4\gamma)^n 2^{|G|+n} \left( 1 + \frac{2n}{2|G| - 1} \right)^{|G|} \quad (\text{C.32})$$

There is no factorial in  $|G|$ , so:

$$F(|G|, \gamma) = \sum_{n=0}^{\infty} F_n \leq c' = O(1) \quad (\text{C.33})$$

dropping the logarithmic corrections, and

$$\|J_i\| \leq \sum_{|G|} c' 2^c (4\gamma)^{|G|} \leq c' 2^{c+1} (4\gamma) \quad (\text{C.34})$$

Each term in the sum is bounded by our choice of  $C(|G|)$ . We can also consider long paths of  $|G| > L_2$  like in the toy example 2 and get  $c' 2^{c+1} (4\gamma)^{L_2}$ .

The structure that we described is present in the generators  $A_i$  of steps 1 and 2 of Imbrie's construction, and then one can proceed in this manner inductively to prove the norm bound on the following steps. One difference is that in the original bound on  $A_{\sigma\sigma'}(g)$  the  $\gamma/\epsilon$  stands in place of  $\gamma$  that we used here. Another difference with  $J_i$  is that the paths for  $A$  are bounded in length from above by a growing scale  $L_{k+1}$ , which gives truly local generators, but does not in any way affect the derivation above.

## C.2 Effective Hamiltonian of an avoided crossing

We have already formulated this result in Chapter 2, but now we want to derive it carefully. From Imbrie's construction we know that the energy of level  $\sigma$  (labeled by a string that's the corresponding configuration at  $\gamma = 0$ ) is:

$$E_\sigma = E_\sigma^0 + \gamma^2 P_\sigma^{(2)} + \gamma^3 P_\sigma^{(3)} + \dots + R_\sigma \quad (\text{C.35})$$

Here  $E_\sigma^0$  is the energy with respect to  $\gamma = 0$  Hamiltonian,  $P_\sigma^{(i)}$  are  $O(1)$  results of a partial summation of the corresponding order in perturbation theory, and  $R_\sigma$  is the correction due to the presence of resonances.

If the start points  $E_\sigma^0, E_\mu^0$  and slopes  $P_\sigma^{(2)}, P_\mu^{(2)}$  are such that two levels intersect at some  $\gamma$ , we expect a contribution to appear in  $R_\sigma$  corresponding to their avoidance.  $R_\sigma$  is discontinuous at that value of  $\gamma$ : if it was continuous, the level  $\sigma$  would follow the crossing adiabatically thus transitioning to a different line with a different underlying spin configuration  $\mu$ . By notation, we want  $\sigma$  to always correspond to this particular string of spins in  $z$ -basis.

The discontinuity comes entirely from the nonperturbative rotation present at the resonance, and it is our freedom to choose the value  $\gamma^*$  at which the discontinuity takes place. Let's note that the circuit that produces eigenstates from the product states is also discontinuous. This rotation acts locally in a neighborhood of spins that need to be flipped. It is a very specific type of discontinuity such that the product states with the specific spin configurations as  $\sigma$  and  $\mu$  in the neighborhood of the resonance will be mapped into something that depends on  $\gamma$  in a discontinuous way.

We will use the above understanding to try and come up with an approximation to the Hamiltonian around  $\gamma^*$ . We will see that in a very generic case the avoidance happens. Let's restrict our attention to a system of size  $n$  such that this resonance is the only one that happens while  $\gamma$  is tuned in the interval  $[\gamma^* - \delta\gamma, \gamma^* + \delta\gamma]$ . At the ends of the interval the resonance is gone and there's no resonances in the system.

Now let's describe the dependence on  $\gamma$  in the regions near points  $\gamma^* - \delta\gamma, \gamma^* + \delta\gamma$  where the resonance is not yet present. The benefit of doing that is that states are given by a circuit  $U(\gamma)$  that is purely perturbative and depends on  $\gamma$  continuously, containing the terms that we understand.

Let's look at the eigenbasis at each  $\gamma$  in the perturbative regime. The Hamiltonian is a diagonal matrix, with energies given by the perturbation expansion as in Eq. (C.35), but without resonant terms. The would-be resonances are the ones that contain the denominator  $E_\sigma - E_\mu$  and its powers.

Looking at the ordinary perturbation theory for corrections to energies up to 5th order, we already note a peculiar property: even though we need to flip there and back from  $\sigma$  to  $\mu$  to obtain correction to  $E_\sigma$ , the difference  $E_\sigma - E_\mu$  appears only once in the denominator. That is because the energy correction is obtained by averaging  $H$ , so there's an extra energy in the numerator, which turns out to cancel one of the

denominators. The Imbrie's perturbation theory retains this property. Unfortunately, this is the only similarity, otherwise Imbrie's construction is very different from the ordinary perturbation theory. In particular, in the ordinary perturbation theory higher orders allow large powers of  $E_\sigma - E_\mu$  per given number of spin flips. Indeed, we can reach  $\mu$ , and then keep flipping one spin back and forth. Asymptotically, it will lead to the contribution

$$\delta E = O\left(\frac{\gamma^{2k}}{(E_\sigma - E_\mu)^k}\right) \quad (\text{C.36})$$

which is too big for our purposes - there's just two spin flips, not enough to suppress the blowup of the denominator. So we need to get the terms from Imbrie's perturbation theory as they don't have this problem.

The corrections to the energies from Imbrie's construction in the no-resonance case are

$$H_{diag} = H_0 + \sum_{\sigma} \sum_k \sum_{g_k} J_{\sigma\sigma}(g_k) |\sigma\rangle \langle \sigma| \quad (\text{C.37})$$

Here  $k$  is the order of perturbation theory,  $g_k$  are  $k$ 'th order graphs in the space of spin flips, and  $J_{\sigma\sigma}(g_k)$  appears after  $k$  products are taken in the expansion of

$$H_{diag} = \prod_k e^{\sum_{g_k} A(g_k)} H \prod_k e^{\sum_{g_k} A(g_k)} \quad (\text{C.38})$$

The construction is inductive:  $g_k$  is defined as a composition of flips from several  $g_{k-1}$ , and  $A(g_k)$  is constructed from  $J(g_k)$  by adding the appropriate denominator:

$$A(g_k) = \sum_{\sigma} \frac{J_{\sigma g_k(\sigma)}(g_k)}{E_\sigma - E_{g_k(\sigma)}} \quad (\text{C.39})$$

Note that the graphs  $g_k$  in the definition of  $A(g_k)$  have to flip at least one spin, whereas the graphs  $g_k$  in  $J_{\sigma\sigma}(g_k)$  always loop back to the original configuration. After the combinatoric factors are taken into account  $J_{\sigma\sigma}(g_k) \sim (\gamma/\epsilon)_k^L$ .

We see that for a specific denominator to appear, the corresponding graph  $g_k$  has to be present. So there will be a numerator  $(\gamma/\epsilon)^{L_k}$  for every problematic denominator of size  $L_k$ . In our case, in the vicinity of the potential resonance  $E_\sigma - E_\mu$  of size  $x$ , every term with a power  $p$  of such denominator will have at least  $(\gamma/\epsilon)^{px}$  in the numerator. We call these terms problematic and see which ones dominate the corrections.

There's something to note: consider the flip back and forth in  $J_{\sigma\sigma}(g_k)$ . That is,  $g_k$  contains two graphs -  $g_{k-1}^{(1)}$  flipping spins from  $\sigma$  to  $\mu$ , and  $g_{k-1}^{(2)}$  - back. Each

graph had to come from corresponding  $A(g_{k-1})$  and have the denominator  $E_\sigma - E_\mu$ . However, there's also  $H$  that stands in the middle of the rotations in Eq. (C.38). This  $H$  will take value of either  $E_\sigma$  or  $E_\mu$  depending on where the  $A$ 's are. We are looking at the expression that looks like:

$$[[H, A]A] \quad (C.40)$$

where  $A$  flips  $\sigma$  to  $\mu$  and back and otherwise zero. It is easy to see that the above is proportional to  $E_\sigma - E_\mu$ , which cancels one of the problematic denominators! In general, every problematic denominator either that appears twice will have

$$[\dots [H, \dots A] \dots A] \quad (C.41)$$

term in  $H_{diag}$ , so one of the two cancels.

Every energy contains problematic terms as well as smooth terms with respect to  $\gamma - \gamma^*$ . The energies  $E_\sigma$  and  $E_\mu$  themselves have the biggest problematic terms, as for each problematic denominator the suppression is  $\gamma^{2x}$ , while it's  $\gamma^{2x+a}$  for other levels. Here  $x$  is the number of flips required to go from  $\sigma$  to  $\mu$ , and  $a \geq 0$ . Let's consider  $\sigma$  and  $\mu$  first. We've already considered the flip back and forth. A single problematic denominator will just have  $\gamma^{2x}$  suppression. A triple problematic denominator will have  $\gamma^{4x}$  suppression and two powers remaining. A fifth power problematic denominator will have  $\gamma^{6x}$  suppression and three powers remaining. You can see the pattern.

For other states  $\nu$ , the denominator will not appear unless we go through both of  $\sigma$  and  $\mu$  and return to  $\nu$ , which requires  $a \geq 0$  additional flips.

$$E_\sigma = E_\sigma^p + O\left(\frac{\gamma^{2x}}{E_\sigma - E_\mu}\right) \quad (C.42)$$

$$E_\mu = E_\mu^p + O\left(\frac{\gamma^{2x}}{E_\sigma - E_\mu}\right) \quad (C.43)$$

$$E_\nu = E_\nu^p + O\left(\frac{\gamma^{2x+a}}{E_\sigma - E_\mu}\right) \quad (C.44)$$

We will first neglect the problematic term in the last line. This will allow us to show that  $|E_\sigma - E_\mu| \geq O(\gamma^{2x})$  from what we understand about perturbative circuit. This justifies neglecting the problematic term for  $\nu$  - it's always suppressed by at least extra  $x$  powers of  $\gamma$ , which is sufficiently small compared to the average level distance at this number of flips. Moreover, we assume that we are looking at an isolated crossing separated by  $\geq \epsilon^x$  from other levels, which is  $\gg \gamma^x$ .

What we have left are the corrections that enter with a different sign:

$$E_\sigma = E_\sigma^p + a \left( \frac{\gamma^{2x}}{E_\sigma - E_\mu} \right) + o \left( \frac{\gamma^x}{E_\sigma - E_\mu} \right) \quad (\text{C.45})$$

$$E_\mu = E_\mu^p - a \left( \frac{\gamma^{2x}}{E_\sigma - E_\mu} \right) + o \left( \frac{\gamma^x}{E_\sigma - E_\mu} \right) \quad (\text{C.46})$$

The remaining terms are always small, since exactly at  $\gamma^*$  we will show that  $|E_\sigma - E_\mu| = O(\gamma^x)$ . So the remaining terms will have higher powers of  $\gamma$ . But we are going to look at the avoidance away from  $\gamma^*$ , prove that  $|E_\sigma - E_\mu| \geq \sqrt{a}\gamma^x$ , and then make a generalization. Away from  $\gamma^*$ , we are left with just two terms in approximation:

$$E_\sigma = E_\sigma^p + a \left( \frac{\gamma^{2x}}{E_\sigma - E_\mu} \right) \quad (\text{C.47})$$

$$E_\mu = E_\mu^p - a \left( \frac{\gamma^{2x}}{E_\sigma - E_\mu} \right) \quad (\text{C.48})$$

Then we come up with a basis where instead of  $\sigma, \mu$  we take their linear combinations such that the expected value of energy is  $E_\sigma^p, E_\mu^p$  correspondingly. The general form of such basis is

$$|\psi\rangle = \alpha|\sigma\rangle + e^{i\phi}\sqrt{1-\alpha^2}|\mu\rangle \quad (\text{C.49})$$

The condition on energies leads to

$$\alpha^2 = \frac{a}{E_\sigma^p - E_\mu^p} \left( \frac{\gamma^{2x}}{E_\sigma - E_\mu} \right) \quad (\text{C.50})$$

and the orthogonality of the basis relates  $\phi$  of two basis vectors. The offdiagonal element of the Hamiltonian between them is

$$\alpha e^{i\phi}(E_\sigma - E_\mu) = \sqrt{\frac{a(E_\sigma - E_\mu)}{E_\sigma^p - E_\mu^p}} \gamma^x \quad (\text{C.51})$$

We cancel the energy differences to the leading order, which results in a Hamiltonian

$$H'_{\sigma\mu} = \begin{pmatrix} E_\sigma^p & \sqrt{a}\gamma^x \\ \sqrt{a}\gamma^x & E_\mu^p \end{pmatrix} \quad (\text{C.52})$$

This is a Hamiltonian written in a very specific basis, designed by combining only two levels, and staying diagonal in the rest. What we observe, however, is that this Hamiltonian is very different from diagonal Hamiltonian in a sense that it is fully continuous in these two levels, if we continue it to  $\gamma^*$ . It also gives a very specific avoidance behavior - at  $E_\sigma^p = E_\mu^p$  the gap is  $2\sqrt{a}\gamma^x$ . Which is great - the  $|E_\sigma - E_\mu| = O(\gamma^x)$  and everything works out as we thought!

Our demonstration of avoidance behavior is restricted to an isolated crossing in a small system. In a bigger system, there may be levels in the background corresponding to spin flips far away. These form cases of triple crossing and provide extra complications for the use of logic of this section..

### C.3 Level repulsion is generic

If the continuation argument does not seem very convincing, there's also a more general logic coming from the random matrix theory. Consider two hermitean matrices  $H$  and  $V$  that are made by choosing a complex matrix with i.i.d. random elements  $C$ , and then taking  $C + C^\dagger$ . The distribution of elements is taken to be rectangular or normal. There was recently a proof for discrete ( $\pm 1$ ) random elements. Anyways we get a semicircle of eigenvalues that have level repulsion for each of them - it is less likely to find eigenvalues close to each other than what would be expected if they were scattered independently on the energy axis (Poissonian distribution).

Now consider  $H + \lambda V$ . This will result in level crossing as  $\lambda$  is varied. How often is it that two levels of  $H$  coincide? This condition forms a hypersurface in the space of elements of the matrix  $H$ . Depending on the dimension of this hypersurface, we can either see avoidance, crossing or sticking together in the  $(E, \lambda)$  picture.  $H + \lambda V$  is a line in matrix element space. For a given two levels, This line will have intervals of  $\delta E = 0$  if the set  $(\delta E = 0)$  is codimension 0 (level sticking), frequent points of  $\delta E = 0$  if the set  $(\delta E = 0)$  is codimension 1 (level crossing), and almost never have  $\delta E = 0$  if the set  $(\delta E = 0)$  is codimension 2 or greater (level repulsion). It is the same as with drawing a line in a random direction in a 3-dimensional space that has a ball, a sphere and another line. It will almost always have an interval intersection (if any) with the ball, 2 points of intersection with the sphere, and it requires fine tuning to have it intersect the other line.

Let's try to find the codimension of  $(\delta E = 0)$  surface for  $H + \lambda V$ . To find the dimension, we sit at a point in matrix elements where  $(\delta E = 0)$ , and try to move away from this point. Let's first consider the two given levels and the matrix elements of  $H + \lambda V$  between them:

$$H + \lambda V = \begin{pmatrix} E_1 & 0 \\ 0 & E_1 \end{pmatrix} + \begin{pmatrix} \delta_1 & \delta_3 + i\delta_4 \\ \delta_3 - i\delta_4 & \delta_2 \end{pmatrix} \quad (\text{C.53})$$

If only this four parameters are moving, then we note that the first correction to energy should be the same for both levels on  $(\delta E = 0)$  surface:

$$\delta_1 = \delta_2 \quad (\text{C.54})$$

is the only constraint.  $\delta_3$  and  $\delta_4$  can be chosen arbitrarily, and we still stay in  $(\delta E = 0)$  surface to the first order. So it seems that we have codimension 1 surface  $(\delta E = 0)$ . However, we know from eigenvalues of 2x2 matrix that  $\delta_3 = \delta_4 = 0$  is also required. It's just that in the direction of  $\delta_3$  and  $\delta_4$  the dependence of  $\delta E$  on  $\delta$  is quadratic, thus only seen in second order of perturbation theory. So we have a codimension 3 surface set by the following conditions:

$$\delta_1 = \delta_2; \quad \delta_3 = \delta_4 = 0 \quad (\text{C.55})$$

This condition stemmed from solving

$$\delta E = \sqrt{(\delta_1 - \delta_2)^2 + 4\delta_1^2 + 4\delta_2^2} = 0 \quad (\text{C.56})$$

Now for a system of bigger dimension, only two levels are degenerate. So one can apply perturbation theory to find corrections from others. Let  $E_{1,2} = \frac{\delta_1 + \delta_2 \pm \delta E}{2}$ . The correction from level  $E_3$  that's sufficiently far is given by orders of perturbation theory:

$$\delta E_1 = \frac{|\langle 1|V|3 \rangle|^2}{E_1 - E_3} + \dots \quad (\text{C.57})$$

all the shifts like that can be incorporated by the choice of  $\delta$  that does not exactly satisfy Eqns. (C.55). We can use the correction above neglecting the dependence of  $E_1$  on  $\delta$ . Then we can approximately cancel the effect of the third level by choosing:

$$\delta_1 - \delta_2 = \frac{|\langle 2|V|3 \rangle|^2}{E_1 - E_3} - \frac{|\langle 1|V|3 \rangle|^2}{E_1 - E_3} \quad (\text{C.58})$$

A more precise choice of those two  $\delta$ 's may be required to cancel subsequent corrections of the presence of the third (and other) levels. But since the other levels are separated by a constant difference from  $E_1$ , and the perturbations  $\delta$  and  $V$  can be chosen arbitrarily small, there is always a perturbation theory type calculation that one can do for subsequent corrections, and find  $\delta$ 's to higher and higher accuracy. However, we will never need more than 3 equations to force  $\delta E = 0$ , so we find codimension to be 3 - it's very unlikely to find a level crossing in  $H(\lambda)$  eigenenergies plot, or even in a 3d plot of  $H(\lambda, \mu)$ .

The classic argument considers the unitary that diagonalizes the Hamiltonian, observes that the eigenstate coincidence leads to a freedom of choice of a 2x2 unitary matrix in that block, and counts the number of free parameters to arrive at the codimension 3 result.